

DISSERTATION

TRENDS IN SNOW WATER EQUIVALENT IN ROCKY MOUNTAIN NATIONAL PARK
AND THE NORTHERN FRONT RANGE OF COLORADO, USA

Submitted by

Glenn G. Patterson

Department of Geosciences

In partial fulfillment of the requirements

For the Degree of Doctor of Philosophy

Colorado State University

Fort Collins, Colorado

Fall 2016

Doctoral Committee:

Advisor: Steven R. Fassnacht

Melinda J. Laituri
William E. Sanford
James Pritchett

Copyright by Glenn Gilman Patterson 2016

All Rights Reserved

ABSTRACT

TRENDS IN SNOW WATER EQUIVALENT IN ROCKY MOUNTAIN NATIONAL PARK AND THE NORTHERN FRONT RANGE OF COLORADO, USA

The seasonal snowpack in Rocky Mountain National Park and the northern Front Range of Colorado, USA, within 50 km of the park, is undergoing changes that will pose challenges for water providers, natural resource managers, and winter recreation enthusiasts. Assessing long-term temporal trends in measures of the seasonal snowpack, and in the climatic factors that influence its annual accumulation and ablation, helps to characterize those challenges. In particular, evaluating the patterns of variation in those trends over different parts of the snow season provides new understanding as to their causes. This also helps to determine specific ramifications of the trends. In addition, placing the current 35-year trends in the longer context of longer-term observational records, and paleoclimate tree-ring reconstructions, provides useful comparisons of current and past trends. Finally, projections of future trends provided by linked climate and hydrologic models offer a sense of how these trends are likely to affect the snowpack of the future.

Some factors such as the high elevation of the study area help to preserve conditions favorable to development of the seasonal snowpack, and hence to limit trends toward greater warming-induced melt and less precipitation falling as snow. Nevertheless, traditional snowpack measures such as April 1 snow water equivalent (SWE) show consistent declining trends over the 35-year period of record for automated snow monitoring stations in the study area. The trends are not uniform throughout the snow season, but vary significantly by month. As a result,

November and March have warming and drying trends that delay the beginning of the winter snow season and reduce the traditional accumulation that formerly characterized the early spring. In contrast, the core winter months of December, January, and February have cooling and wetting trends that have been enhancing SWE during the heart of the winter. Mid-April to early May is another period during which cooling and wetting trends have been enhancing SWE, although these months also show more variability. This oscillating pattern helps to explain why there has not been a pervasive shift to earlier and lower annual peak SWE in the study area.

Paleo SWE reconstructions based on tree-ring chronologies show that at least some of the recent 35-year trends in observed SWE described in this study have comparable precedents during the preceding five centuries, but we do not yet know how long the recent trends will continue. Linked climate and hydrologic models project that the observed trends are likely to continue, and that by 2050 measures such as April 1 SWE in the study area are likely to decrease by 25 percent.

ACKNOWLEDGMENTS

I would like to thank my wife and soulmate, Dr. Margaret K. Patterson, for inspiring me to commence this project and supporting me through its challenges. I would also like to thank my father, Bradley Patterson, and the rest of my family for their love and support.

A special acknowledgment goes to my advisor, Dr. Steven R. Fassnacht, for agreeing to accept me as an unfunded non-traditional graduate student, and for providing exceptional guidance, advice, inspiration, and friendship. Similarly, the members of my Advisory Committee have been most helpful and generous with their time. Amanda Weber kindly provided assistance in compiling data for this project.

Partial funding for this project, for which I am grateful, was provided by the Continental Divide Science and Learning Center of Rocky Mountain National Park.

Appreciation is also expressed to the men and women of the U.S. Natural Resources Conservation Service, formerly the Soil Conservation Service, whose dedicated efforts to measure snowpack characteristics over the last 80 years have provided much of the information base for this dissertation.

Appreciation is extended to the National Weather Service for the use of their weather data for Grand Lake (National Oceanic and Atmospheric Administration, 2016), to Dr. William P. Rense for the use of his weather data for Allenspark, and to the U.S. Geological Survey and Colorado State University for the use of weather data from Loch Vale. The Loch Vale data were provided by the USGS supported Loch Vale Watershed Long-term Ecological Research and Monitoring program and Colorado State University (Colorado State University, 2016).

The author acknowledges the World Climate Research Programme's Working Group on Coupled Modelling, which is responsible for CMIP, and thanks the climate modeling groups for producing and making available their model output. For CMIP the U.S. Department of Energy's Program for Climate Model Diagnosis and Inter-comparison provides coordinating support and led development of software infrastructure in partnership with the Global Organization for Earth System Science Portals.

TABLE OF CONTENTS

ABSTRACTii
ACKNOWLEDGEMENTSiv
LIST OF TABLES	viii
LIST OF FIGURESix
LIST OF ABBREVIATIONSxiv
1. CHAPTER 1—INTRODUCTION1
1.1 THE SEASONAL SNOWPACK1
1.2 TRENDS IN SNOWPACK MEASURES3
1.3 PROBLEM STATEMENT5
1.4 STUDY AREA7
2. CHAPTER 2--DATA SOURCES11
2.1 SNOW COURSES11
2.2 SNOWPACK TELEMETRY STATIONS12
2.3 TEMPERATURE STATIONS14
2.4 ELEVATION OF FREEZING TEMPERATURE15
2.5 PALEOCLIMATE SWE RECONSTRUCTIONS16
2.6 PROJECTIONS OF FUTURE TEMPERATURE, PRECIPITATION, AND SWE17
3. CHAPTER 3--METHODS19
3.1 SNOW WATER EQUIVALENT19
3.2 ESTIMATION OF DAILY NIVEOGRAPHS FROM SNOW COURSE DATA20
3.3 TREND ANALYSIS23
3.4 PRECIPITATION25
3.5 TEMPERATURE26
3.6 FREEZING LEVEL27
3.7 PALEOCLIMATE SWE RECONSTRUCTIONS28
3.8 PROJECTIONS OF FUTURE TEMPERATURE, PRECIPITATION, AND SWE29
4. CHAPTER 4—RESULTS30
4.1 TRENDS IN SNOW WATER EQUIVALENT30
4.1.1 MONTHLY SWE30
4.1.2 TRENDS DERIVED FROM DAILY SWE40
4.2 ESTIMATION OF DAILY NIVEOGRAPHS FROM SNOW COURSE DATA49
4.3 TRENDS IN PRECIPITATION50
4.4 TRENDS IN TEMPERATURE52
4.5 TRENDS IN FREEZING LEVEL54
4.6 PALEOCLIMATE SWE RECONSTRUCTIONS57
4.7 PROJECTIONS OF FUTURE TEMPERATURE, PRECIPITATION, AND SWE60
5. CHAPTER 5—DISCUSSION65
5.1 TRENDS IN SNOW WATER EQUIVALENT65
5.1.1 VARIABILITY IN ANNUAL MEASURES OF SWE65
5.1.2 MONTHLY TRENDS IN SWE66
5.1.3 OTHER MEASURES OF SWE DERIVED FROM DAILY DATA68
5.1.4 PATTERNS IN SWE TRENDS70

5.1.5 TRENDS IN NUMBER OF DAYS PER YEAR WITH THRESHOLD ACCUMULATION AND ABLATION VALUES	72
5.2 NIVEOGRAPH INTERPOLATION FROM SNOW COURSE DATA	73
5.3 TRENDS IN PRECIPITATION	73
5.4 TRENDS IN TEMPERATURE	75
5.5 TRENDS IN FREEZING LEVEL AND MAXIMUM DAILY TEMPERATURES ABOVE ZERO	78
5.6 CLIMATIC INFLUENCE ON SWE TRENDS	79
5.7 TRENDS IN MAGNITUDE AND TIMING OF PEAK SWE VERSUS SWE CHANGE	80
5.8 ELEVATION DEPENDENT SWE LOSS	84
5.9 ALBEDO-FEEDBACK AND HUMIDITY EFFECTS	86
5.10 PALEOCLIMATE SWE RECONSTRUCTIONS	87
5.11 FUTURE PROJECTIONS OF SWE TRENDS	84
5.12 RAMIFICATIONS FOR NATURAL RESOURCE MANAGEMENT	90
6. CHAPTER 6—CONCLUSIONS	92
7. REFERENCES	97
8. APPENDIX	106

LIST OF TABLES

2.1 SNOW COURSE AND SNOTEL STATIONS INCLUDED IN THE INVESTIGATION	13
2.2 TEMPERATURE DATA COLLECTION STATIONS USED IN THIS INVESTIGATION	15
2.3 SNOW COURSES AND PERIODS FOR ASSOCIATED TREE-RING CHRONOLOGIES USED IN THIS INVESTIGATION	16
2.4 CLIMATE AND HYDROLOGIC MODELS FROM WHICH PROJECTIONS WERE USED IN THIS INVESTIGATION	18
4.1 PERFORMANCE MEASURES FOR NIVEOGRAPH ESTIMATION MODEL COMPARED TO ASSUMPTION OF ANNUAL PEAK SWE ON APRIL 1	49
4.2 TRENDS IN AVERAGE ANNUAL TEMPERATURE AT THREE WEATHER STATIONS	52
4.3 RESULTS OF TREND ANALYSIS OF PALEO-SWE RECONSTRUCTIONS BASED ON TREE RINGS	58
A.1 TREE-RING RECONSTRUCTIONS USED IN THIS INVESTIGATION (FROM WOODHOUSE, 2003)	106
A.2 HALF MATRIX OF APRIL 1ST SWE CORRELATIONS FOR THE STUDY PERIOD 1981-2015 WITH THREE LEVELS OF CORRELATION ($R^2 > 0.5, 0.7, 0.9$) HIGHLIGHTED	107
A.3 PERCENT DIFFERENCE BETWEEN OBSERVED PEAK SWE AND INDICATED STATISTIC, AS PERCENT OF PEAK SWE	114

LIST OF FIGURES

1.1 LOCATIONS OF STUDY AREA, DATA COLLECTION SITES, AND RETRIEVAL AREA FOR CLIMATE MODELS.	8
3.1 SAMPLE NIVEOGRAPH (LAKE IRENE, 2011), ILLUSTRATING EXAMPLES OF VARIOUS SWE MEASURES, AND SEPARATION OF NIVEOGRAPH INTO PHASES FOR ESTIMATION	22
4.1 EXAMPLE PLOT OF ANNUAL SERIES OF APRIL 1 SWE FOR A SNOW COURSE AND A SNOTEL STATION, SHOWING STRONG INTER-ANNUAL VARIABILITY.	31
4.2 EXAMPLE PLOT OF ANNUAL SERIES OF SWE MEASURES FOR LAKE IRENE SNOTEL STATION, INCLUDING 1981-2015 TRENDS.	31
4.3 MEDIAN ANNUAL PEAK SWE AT SNOTEL STATIONS, 1981-2015, IN RELATION TO ELEVATION.	33
4.4 MEDIAN DATE OF PEAK SWE AT SNOTEL STATIONS, 1981-2015, IN RELATION TO ELEVATION.	33
4.5 TRENDS IN FIRST-OF-MONTH SWE AT SNOW COURSES AND SNOTEL STATIONS, 1981-2015.	35
4.6 A) DISTRIBUTION OF MONTHLY TRENDS IN SWE ON THE FIRST OF EACH MONTH DURING THE SNOW SEASON FOR VARIOUS GROUPINGS OF SNOW COURSES AND SNOTEL STATIONS, 1981-2015, AND B) DISTRIBUTION OF TRENDS IN MONTHLY CHANGE IN SWE.	36
4.7 A) TRENDS IN FIRST-OF-MONTH SWE AT SNOW COURSES AND SNOTEL STATIONS, 1981-2015, IN RELATION TO ELEVATION. B) TRENDS IN MONTHLY CHANGE IN SWE AT SNOW COURSES AND SNOTEL STATIONS, 1981-2015, IN RELATION TO ELEVATION	38
4.8 A) MEDIAN SWE, 1981-2015, AND AVERAGE VALUES FOR 15-DAY CHANGES IN SWE, AVERAGED FROM 6 SNOTELS. (B) TRENDS IN 15-DAY CHANGES IN SWE, AVERAGED FROM 6 SNOTELS	42
4.9 DAILY SWE TRENDS FOR A) LAKE IRENE SNOTEL, AND B) COPELAND LAKE SNOTEL, IN RELATION TO MEDIAN DAILY SWE FOR ENTIRE PERIOD OF RECORD, AND FOR EARLY AND LATE SEGMENTS OF THE RECORD. ALSO SHOWS RASTER PLOTS OF DAILY SWE FOR EACH YEAR, 1981-2015. “ANNUAL” DOT DENOTES ANNUAL PEAK SWE	44
4.10 DAILY SWE TRENDS FOR A) JOE WRIGHT SNOTEL, AND B) PHANTOM VALLEY SNOTEL, IN RELATION TO MEDIAN DAILY SWE FOR ENTIRE PERIOD OF RECORD, AND FOR EARLY AND LATE SEGMENTS OF THE RECORD. ALSO SHOWS RASTER PLOTS OF DAILY SWE FOR EACH YEAR, 1981-2015. “ANNUAL” DOT DENOTES ANNUAL PEAK SWE	45
4.11 DAILY SWE TRENDS FOR A) WILLOW PARK SNOTEL, AND B) BEAR LAKE SNOTEL, IN RELATION TO MEDIAN DAILY SWE FOR ENTIRE PERIOD OF RECORD, AND FOR EARLY AND LATE SEGMENTS OF	

THE RECORD. ALSO SHOWS RASTER PLOTS OF DAILY SWE FOR EACH YEAR, 1981-2015. “ANNUAL” DOT DENOTES ANNUAL PEAK SWE	46
4.12 TRENDS IN MONTHLY PRECIPITATION, SNOWFALL EQUIVALENT (SFE), AND RATIO OF SFE TO PRECIPITATION, 1981-2015, AVERAGED FROM 6 SNOTEL STATIONS	51
4.13 A) AVERAGE MONTHLY TEMPERATURE AT 3 WEATHER STATIONS, AND B) TRENDS IN AVERAGE MONTHLY TEMPERATURE, 1981-2015	53
4.14 A) AVERAGE MONTHLY ELEVATION OF FREEZE LEVEL (ZERO-DEGREE ISOTHERM), 1981-2015, AND B) TRENDS IN ELEVATION OF FREEZE LEVEL	56
4.15 CORRELATION BETWEEN THE MODELED (TREE RING ESTIMATED) AND OBSERVED APRIL 1ST SWE FOR THE NORTH INLET OF GRAND LAKE SNOW COURSE. DATA WERE FOR THE PERIOD 1938 (START OF SNOW COURSE) TO 1999 (END OF TREE RING CHRONOLOGY)	58
4.16 NORTH INLET OF GRAND LAKE APRIL 1ST SWE RECONSTRUCTION FROM 1571 TO 1999	59
4.17 SLOPE OVER 35-YEAR TIME PERIOD FOR THE RECONSTRUCTED AND OBSERVED (HISTORICAL) APRIL 1ST SWE AT NORTH INLET OF GRAND LAKE SNOW COURSE	59
4.18 COMPARISON OF TRENDS IN APRIL 1 SWE BETWEEN OBSERVED LONGS PEAK SNOW COURSE DATA AND IPSL MODEL	62
4.19 TREND IN FIRST-OF-MONTH SWE, 1981-2015, SIMULATED BY IPSL MODEL AND OBSERVED AVERAGES AT SNOTELS AND SNOW COURSES	63
4.20 IPSL MODEL PROJECTIONS FOR TRENDS IN FIRST-OF-MONTH SWE, 2015-2099	64
5.1 AVERAGE TRENDS IN SWE, MONTHLY CHANGE IN SWE, SFE, AND TEMPERATURE, BY MONTH	71
5.2 FOUR-YEAR MOVING AVERAGE OF OCT-JUNE PRECIPITATION AT WILLOW PARK SNOTEL, 1981-2015, SUPERIMPOSED OVER TIME VS. SOLAR LATITUDE DIAGRAM OF THE RADIAL COMPONENT OF THE SOLAR MAGNETIC FIELD BASED ON THE 11-YEAR SUNSPOT CYCLE	74
5.3 MAGNITUDES AND TRENDS IN 15-DAY CHANGE IN SWE AT WILLOW PARK SNOTEL, 1981-2015, FOR SELECTED DAYS	81
5.4 MAGNITUDES AND TRENDS IN 15-DAY CHANGE IN SWE AT COPELAND LAKE SNOTEL, 1981-2015, FOR SELECTED DAYS	82
5.5 MAGNITUDES AND TRENDS IN 15-DAY CHANGE IN SWE AT PHANTOM VALLEY SNOTEL, 1981-2015, FOR SELECTED DAYS	83
5.6 RELATION BETWEEN TREND IN DATE OF PEAK SWE AND DATE OF PEAK SWE AT SNOTEL STATIONS. THE FITTED FUNCTION IS A SECOND-ORDER POLYNOMIAL	84
A.1 FITTING THE MEDIAN NIVEOGRAPH TO OBSERVED DATA FOR A	

GIVEN YEAR USING DIFFERENT TECHNIQUES FOR ACCUMULATION, PEAK, AND MELT PHASES.	108
A.2 NIVEOGRAPH ESTIMATION PROCEDURE SHOWING EXTENSION OF THE PEAK PHASE AND DELAYING THE MELT PHASE WHEN SWE IS STILL INCREASING ON MAY 1	109
A.3 APRIL 1 SWE FOR EACH SNOW YEAR, 1986-2015, AT PHANTOM VALLEY SNOTEL, IN RELATION TO ANNUAL VARIATIONS IN TOTAL OCTOBER-JUNE PRECIPITATION AND AVERAGE OCTOBER-JUNE TEMPERATURE AS RECORDED AT THE SNOTEL STATION.	110
A.4 REGRESSION ANALYSES OF MEDIAN APRIL 1 SWE, 1981-2015, ON OCTOBER-JUNE A) TEMPERATURE AND B) PRECIPITATION AT PHANTOM VALLEY SNOTEL	111
A.5.A) COMPARISON OF TRENDS IN SWE ON FIRST OF MONTH AT SNOW COURSES INSIDE AND OUTSIDE ROCKY MOUNTAIN NATIONAL PARK FOR TWO DIFFERENT PERIODS: 1981-2015, AND ENTIRE PERIOD OF RECORD. B) SAME COMPARISON FOR TRENDS IN MONTHLY CHANGE IN SWE	112
A.6 A) TRENDS IN ANNUAL PEAK SWE AT SNOTEL STATIONS IN RELATION TO ELEVATION. B) TRENDS IN DATE OF PEAK SWE AT SNOTEL STATIONS IN RELATION TO ELEVATION	113
A.7 RESULTS OF COMPARISON OF OBSERVED ANNUAL PEAK SWE WITH APRIL 1 SWE, AND WITH THE MAXIMUM OF FIRST-OF-MONTH SWE VALUES, IN RELATION TO ELEVATION	113
A.8 A) MEDIAN SWE, 1981-2015, AND AVERAGE VALUES FOR 15-DAY CHANGES IN SWE AT LAKE IRENE SNOTEL. B) TRENDS IN 15-DAY CHANGE IN SWE.	115
A.9 A) MEDIAN SWE, 1981-2015, AND AVERAGE VALUES FOR 15-DAY CHANGES IN SWE AT JOE WRIGHT SNOTEL. B) TRENDS IN 15-DAY CHANGE IN SWE.	116
A.10 A) MEDIAN SWE, 1981-2015, AND AVERAGE VALUES FOR 15-DAY CHANGES IN SWE AT WILLOW PARK SNOTEL. B) TRENDS IN 15-DAY CHANGE IN SWE.	117
A.11 A) MEDIAN SWE, 1981-2015, AND AVERAGE VALUES FOR 15-DAY CHANGES IN SWE AT BEAR LAKE SNOTEL. B) TRENDS IN 15-DAY CHANGE IN SWE.	118
A.12 A) MEDIAN SWE, 1981-2015, AND AVERAGE VALUES FOR 15-DAY CHANGES IN SWE AT PHANTOM VALLEY SNOTEL. B) TRENDS IN 15-DAY CHANGE IN SWE.	119
A.13 A) MEDIAN SWE, 1981-2015, AND AVERAGE VALUES FOR 15-DAY CHANGES IN SWE AT COPELAND LAKE SNOTEL. B) TRENDS IN 15-DAY CHANGE IN SWE.	120
A.14. TRENDS IN NUMBER OF DAYS PER YEAR WITH SWE >100 MM AT SNOTEL STATIONS, 1981-2015, IN RELATION TO ELEVATION	121

A.15 TRENDS IN NUMBER OF DAYS WITH A) SWE ACCUMULATION AND B) SWE ABLATION GREATER THAN 0, 5 AND 10 MM, 1981-2015, IN RELATION TO ELEVATION	121
A.16 ESTIMATED (SOLID) AND OBSERVED (DASHED) NIVEOGRAPHS FOR TWO SNOTEL STATIONS FOR LOW, MEDIUM, AND HIGH SWE YEARS	122
A.17 ANNUAL PEAK SWE FROM OBSERVED DATA, FROM THE ASSUMPTION OF APRIL 1 PEAK SWE, AND FROM THE ESTIMATED NIVEOGRAPHS	123
A.18 DATES OF PEAK SWE FROM OBSERVED DATA, FROM THE ASSUMPTION OF APRIL 1 PEAK SWE, AND FROM THE ESTIMATED NIVEOGRAPHS	124
A.19 AVERAGE, MAXIMUM, AND MINIMUM MONTHLY PRECIPITATION, 1981-2015, AT 6 SNOTEL STATIONS AND 3 WEATHER STATIONS	124
A.20 AVERAGE ANNUAL PRECIPITATION, 1981-2015, AT 6 SNOTEL AND 3 WEATHER STATIONS, IN RELATION TO ELEVATION	125
A.21 TRENDS IN TOTAL ANNUAL SNOWFALL EQUIVALENT (TOTAL OCTOBER-JUNE SWE ACCUMULATION), 1981-2015, AT 13 SNOTEL STATIONS, IN RELATION TO ELEVATION	125
A.22 TRENDS IN APRIL 1 SWE AT SNOTELS IN RELATION TO TRENDS IN PRECIPITATION AND TEMPERATURE AT THE SNOTELS	126
A.23 AVERAGE ANNUAL TEMPERATURE AT THREE WEATHER STATIONS, 1981-2013.	127
A.24 AVERAGE ANNUAL TEMPERATURE AT GRAND LAKE, 1949-2015, WITH TRENDS FOR ENTIRE AND SELECTED PARTIAL PERIODS	128
A.25 A) MONTHLY SUMS OF MAXIMUM DAILY TEMPERATURES WARMER THAN ZERO FOR LAKE IRENE AND COPELAND LAKE, AND B) TRENDS IN THESE SUMS	129
A.26 CAMERON PASS MAY 1 ST SWE RECONSTRUCTION FROM 1486 TO 2000	130
A.27 SLOPE OVER 35-YEAR TIME PERIOD FOR THE RECONSTRUCTED AND OBSERVED (HISTORICAL) MAY 1 ST SWE AT CAMERON PASS SNOW COURSE	130
A.28 LONGS PEAK MAY 1 ST SWE RECONSTRUCTION FROM 1571 TO 1999	131
A.29 SLOPE OVER 35-YEAR TIME PERIOD FOR THE RECONSTRUCTED AND OBSERVED (HISTORICAL) MAY 1 ST SWE AT LONGS PEAK SNOW COURSE	131
A.30 MEDIAN ELEVATIONS [M] FOR THE NINE 1/8 BY 1/8 DEGREE PIXELS OF THE CMIP5 CLIMATE MODEL RETRIEVAL	132
A.31 DISTRIBUTION OF ELEVATIONS WITHIN THE NINE PIXELS OF THE CMIP5 CLIMATE MODEL RETRIEVAL	133
A.32 ANNUAL PRECIPITATION SIMULATED BY THE CMIP5 MODEL ENSEMBLE, AND OBSERVED AT WILLOW PARK SNOTEL, 1981-2015	133

A.33 AVERAGE MONTHLY PRECIPITATION SIMULATED BY THE CMIP5 MODEL ENSEMBLE, AND OBSERVED AT WILLOW PARK SNOTEL, 1981-2015	134
A.34 TRENDS IN MONTHLY PRECIPITATION, 1981-2015, SIMULATED BY THE CMIP5 MODEL ENSEMBLE AND OBSERVED AT WILLOW PARK	134
A.35 TRENDS IN MONTHLY PRECIPITATION, 2015-2099, SIMULATED BY THE CMIP5 MODEL ENSEMBLE	135
A.36 AVERAGE FIRST OF MONTH SWE, 1981-2015, SIMULATED BY THE CMIP5 MODEL ENSEMBLE AND OBSERVED AT WILLOW PARK	135
A.37 431-YEAR SWE RECONSTRUCTION FOR THE GUNNISON REGION, COLORADO, SMOOTHED WITH A 5-WEIGHT BINOMIAL FILTER (HEAVY LINE), AND ERROR BARS (THIN LINES), 1571-1997	136

LIST OF ABBREVIATIONS

CMIP5	Coupled Model Inter-comparison Project, 5 th Phase
NRCS	Natural Resources Conservation Service
RMNP	Rocky Mountain National Park
SFE	Snowfall Equivalent
SNOTEL	Snowpack Telemetry
SWE	Snow Water Equivalent

CHAPTER 1. INTRODUCTION

1.1 The Seasonal Snowpack

The seasonal snowpack is defined as “snow that accumulates during one season and does not last for more than one year” (National Snow and Ice Data Center, 2008; Fierz *et al.*, 2009).

This occurs where average daily temperatures are mostly below freezing during the winter months and are mostly above freezing during the summer months.

The seasonal snowpack in mountainous regions is important to humans and to natural ecosystems for many reasons. Often known as “*nature’s water tower*” (Viviroli *et al.*, 2007), the snowpack provides seasonal storage for most of the annual precipitation in the mountains, releasing the stored winter precipitation during the spring and early summer when water demand for reservoir storage and irrigation is higher than in the winter (Bales *et al.*, 2006). Snowmelt runoff also produces most of the groundwater recharge that takes place in the mountains and nearby plains (Barnett *et al.*, 2008). In most river basins of the western United States, water storage in the snowpack exceeds the storage capacity of man-made reservoirs (Mote *et al.*, 2005). In Colorado, more than 60 percent of annual precipitation falls as winter and spring snow (Serreze *et al.*, 1999). Spring snowmelt runoff is said to generate 80 percent of streamflow in Colorado (Colorado Climate Center, 2016).

As in most of the west, Colorado’s economy is sensitive to changes in water availability, and hence to changes in the seasonal snowpack. One estimate of the marginal value of an acre-foot (1233 cubic meters) of water under conditions of changing streamflow is \$34-46 in 1985 dollars (Harding and Payton, 1990). This equates to \$75-102/acre-foot (6-8 cents/cubic meter) in 2016 dollars. Rocky Mountain National Park (RMNP) has an area of 265,761 acres (107,550

hectares), so a difference of 1 mm of snow water equivalent (SWE) over the whole park would equate to a marginal value for water of about \$77,000 per year.

In addition to providing water supply, the seasonal snowpack represents an important recreational resource. During the decade 2005-2015, the economic impact of the downhill ski industry in Colorado grew from \$2.5 billion to \$4.8 billion (Denver Post, 2015). During the same period recreational visits to Rocky Mountain National Park during March more than doubled, from about 60,000 to over 130,000 (National Park Service, 2016a). This is the season for snow-related recreation in the park, including snowshoeing, cross-country skiing, sledding, and back-country skiing. In 2011, 63 percent of winter visitors to Rocky Mountain National Park participated in recreation involving snow (Papadogiannaki *et al.*, 2011).

Like the water-supply industry, the winter recreation industry is sensitive to changes in the seasonal snowpack. Potential impacts on the ski industry include not only loss of skiable snow (Gilaberte-Burdalo *et al.*, 2014), but also increased risk of wet avalanches (Lazar and Williams, 2008). Measures of the number of days per year with sufficient snow for enjoyable winter recreation, in terms of both observed trends and future projections, provide important information for recreation planners. The difference in the economic value of Colorado's ski industry in a low snow year compared with a high snow year has been estimated at \$154 million (Burakowski and Magnusson, 2012). Assuming that the difference in April 1 SWE in the snow zone in a low snow year compared with a high snow year is typically about 500 mm, then a difference of 1 mm of April 1 SWE in Colorado's snow zone would equate to a marginal value, for recreation, of about \$308,000 statewide.

In addition to its value for humans, the seasonal snowpack provides important benefits for ecosystems. It is the source of most of the water used by plants and animals in the snow zone

and in riparian areas downstream. In addition to nourishing vegetation, it also enhances the ability of vegetation to resist wildfire (Westerling *et al.*, 2006). The snowpack also provides critical shelter and winter habitat for a variety of plants and animals (Jones *et al.*, 2001, chapters 5 and 6). Snow shelters tree branches from cold, desiccating winds that would otherwise kill the branch (Denver Botanical Garden, 2016). Similarly, snow shelters grass and forbs that provide food for elk, which are adapted to pawing through the snow to find sustenance. Animals such as ptarmigan, pikas, snowshoe hares, ermine, voles, shrews, and snow fleas are examples of animals that are adapted to seeking food and shelter in the snow (Jones *et al.*, 2001, chapter 5).

The seasonal snowpack also plays an important feedback role affecting winter climate. Snow has a much higher albedo than bare soil, rock, or vegetation. Once the seasonal snowpack forms, most of the incoming solar radiation is reflected back to the sky, leaving less to be absorbed by the land surface than when snow is not present. This helps to cool the terrain and the snowpack itself (Flanner *et al.*, 2011).

1.2 Trends in Snowpack Measures

In light of the importance of the seasonal snowpack and of changes in its patterns of accumulation and ablation, it is important to examine long-term trends in measures of the snowpack. A number of studies have found indications that the seasonal snowpack in the western United States is changing over time (mostly diminishing), and that these changes reflect underlying trends in climate.

Accumulation and ablation of snow are tightly linked with temperature and precipitation. Like most of the rest of the globe, Colorado has been experiencing a warming trend over the past century, and that warming trend has been accelerating since about 1970. The current rate of

warming in Colorado, in terms of average annual temperature, is about $0.37^{\circ}\text{C}/\text{decade}$ statewide (Lukas *et al.*, 2014). The warming trends are not uniform in space and time. Warming has been found to be more rapid in the northern central mountains of Colorado, while a few stations in the southern San Juan Mountains have shown cooling trends (Ray *et al.*, 2008; Mote *et al.*, 2005). The warming trends have also been shown to vary with elevation, with higher elevation sites showing more rapid warming trends (Diaz and Eischeid, 2007). Variation in time has also been noted for warming trends, with November and March, in particular, showing more rapid warming trends than other months (Rense, 2016; Ray *et al.*, 2008).

In contrast to temperature, researchers often report that there are no obvious trends in cold-season precipitation (Harpold *et al.*, 2012). As with temperature trends, however, precipitation trends are variable in space and time, reflecting the varying weather patterns that bring moisture to different parts of the state at different times (Ray *et al.*, 2008).

The most common measure of the seasonal snowpack is the snow water equivalent (SWE) on April 1. This measure has been declining in most of the western United States over the second half of the last century (Mote *et al.*, 2005). The period of snow cover was found to be declining in the highest elevations of the Colorado River Basin, with the caveat that significant spatial and temporal variability highlights the need for additional research into the mass and energy balance of the seasonal snowpack in the inter-mountain west (Harpold *et al.*, 2012). There is spatial and temporal variability of snowpack accumulation and ablation across the Mountains of the Colorado River Basin with different snowpack patterns in different parts of the state and in some locations changing with elevation (Fassnacht and Derry, 2010). Not only are accumulation patterns different, typically increasing with elevation (Fassnacht *et al.*, 2003), but melt rates are also highly variable (Fassnacht and Records, 2015). Trends in April 1 SWE in the

northern Front Range of Colorado, the area of this investigation, for the period 1978-2007 were found to be unchanging, as opposed to declining trends elsewhere in Colorado (Clow, 2010).

Trends in SWE in the mountains of Colorado have also been found to vary by month (Rasmussen *et al.*, 2014).

Earlier snowmelt has been found to be associated with earlier spring runoff in streams in the western United States (Stewart *et al.*, 2004; Stewart *et al.*, 2005; Fritze *et al.*, 2011) and in Colorado (Clow, 2010). In the latter study, while statewide trends toward earlier snowmelt runoff averaged about two weeks earlier in 2007 compared with 1978, the trends toward earlier snowmelt runoff for the area of this investigation were among the weaker trends noted in the state (Clow, 2010). In a more recent study using a different method to identify streamflow components, trends in snowmelt runoff timing in the Colorado Rockies during 1976-2015 were found to be mostly toward earlier runoff, but about one-quarter of the trends were toward later snowmelt runoff (Pfohl, 2016).

1.3 Problem Statement

The foregoing discussion suggests a need for additional research addressing trends in snowpack accumulation and ablation in specific areas using measures that take into account the variable nature of trends with time during the snow season. To characterize this intra-season variability in SWE trends, it is important to use measures that have annual time series that are based on more than one measurement per year, for example, more than just April 1st SWE. A more complete picture of these time-varying trends can emerge if the annual time series analyses are based on more frequent measurements during the year. Monthly SWE data, such as the measurements derived from snow courses (described in section 2.1 below), are often

used to provide a more detailed assessment of SWE variations and trends. However, even monthly SWE data are insufficient to characterize sub-monthly variations in SWE (Bohr and Aguado, 2001). These sub-monthly variations are best characterized by using daily SWE measurements, such as those provided by SNOTEL stations (described in section 2.2 below). These data can also be used to assess specific characteristics of the snow season, such as amount and timing of peak SWE, length of season, and trends in short-term changes in SWE. The purpose of this investigation is to examine such intra-season variability in trends of snowpack accumulation and ablation for Rocky Mountain National Park and the surrounding northern Front Range of Colorado, extending up to 50 km from the park. Daily SWE measurements will be used to evaluate patterns among snowpack trends. The trends will be examined in relation to corresponding trends in temperature, elevation of the average level of freezing temperatures, and precipitation, as well as terrain variables, such as elevation and location.

The time period of the trend analysis will encompass the 80-year period of snow-course measurements in the study area (1936-2015), with emphasis on the 35-year period of daily SNOTEL measurements (1981-2015). Information will be presented showing how observed daily SWE data from SNOTEL stations can be used to estimate daily SWE data for snow courses, thereby lengthening the period for which trends can be evaluated for measures, such as peak SWE, that depend on daily SWE data. The trends evaluated in the trend analysis will be examined in the context of the past, by using multi-century reconstructions of paleo SWE to determine whether the observed trends are unique over a longer term. The trends will also be examined in the context of the future, by using projections of future Temperature, Precipitation, and SWE based on climate models, to anticipate future changes in snowpack accumulation and

ablation. Finally, some ramifications of the results for managing park resources will be discussed.

1.4 Study Area

It is important to examine snowpack dynamics and trends across the northern Front Range within 50 km of Rocky Mountain National Park (Figure 1.1) for several reasons. The park and surrounding national forest lands are an important recreational resource and source of water. The high elevation, memorable scenery, abundant recreation opportunities, accessibility, and proximity to the Denver metropolitan area make this a popular tourist destination, with over 3,000,000 visitors per year to the park (National Park Service, 2016c), and over 6,000,000 recreational visits per year to Arapahoe-Roosevelt National Forest (U.S. Forest Service, 2016). Snowmelt runoff from the study area contributes significant portions of the flows of the Colorado, North Platte, Cache la Poudre, Big Thompson, and Little Thompson Rivers, and St. Vrain, Left Hand, and Boulder Creeks. These creeks and rivers provide water for irrigation, industry, municipal supply, recreation, and aquatic habitat for a large part of northern Colorado and adjacent states.

A unique aspect of the park is its emphasis on high-elevation mountain terrain. One-third of the park (about 36,000 hectares) is within the alpine tundra biome, above timberline which is about 3,505 m above sea level (National Park Service, 2016b). Another major portion of the park is within the subalpine biome (2,895-3,505 m), typically the zone of maximum seasonal snow accumulation.

The zone of seasonal snow accumulation in this part of Colorado has been defined in terms of intermittent, transitional, and persistent snow cover (Richer *et al.*, 2013). Also

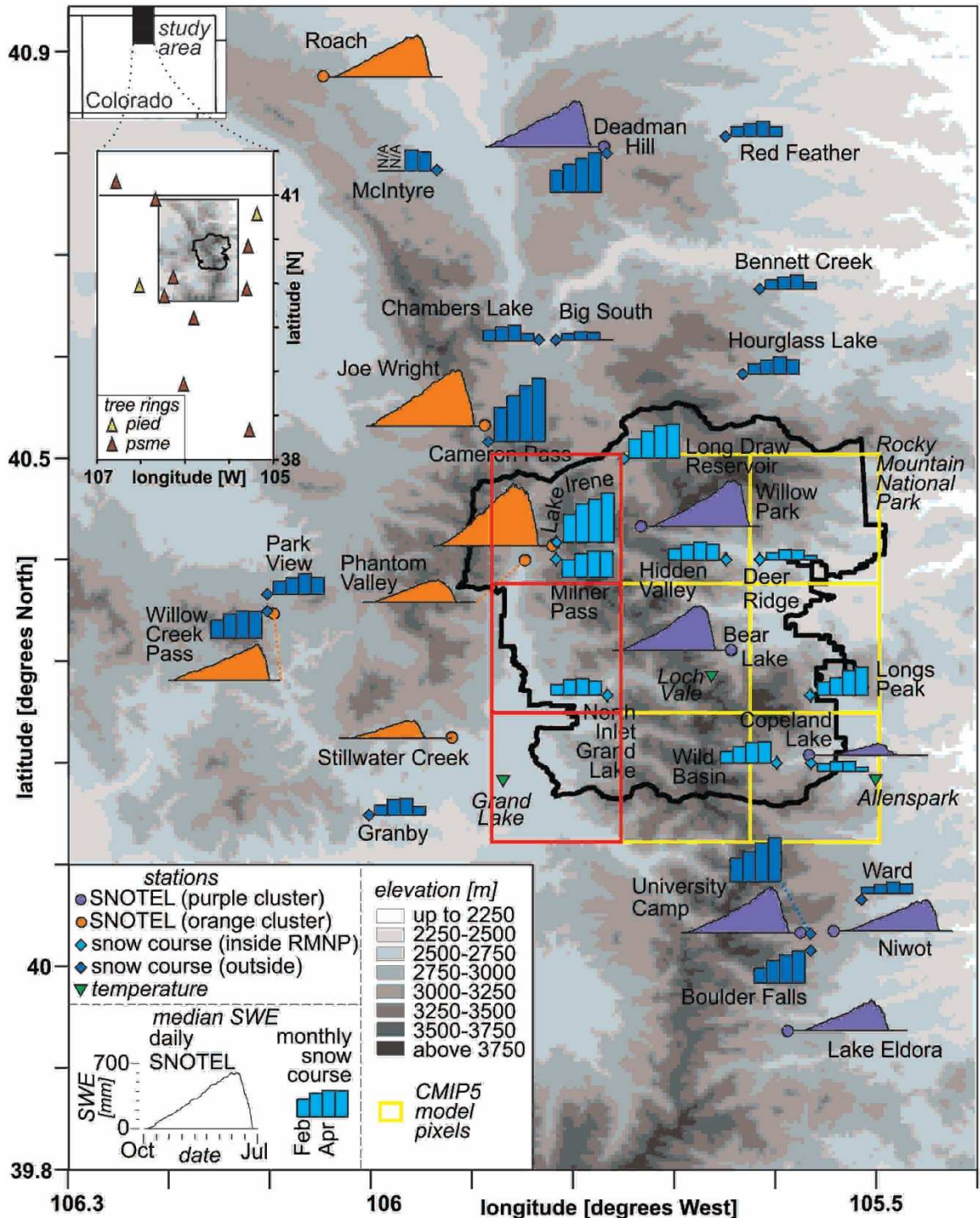


Figure 1.1. Locations of study area, data collection sites, and retrieval area for climate models. SNOTEL stations are designated by median niveographs scaled according to the example in the legend. SNOTEL purple and orange clusters refer to those used by Clow (2010). Snow courses are designated by bar graphs showing median monthly SWE, on the same scale. Snow courses within Rocky Mountain National Park are shown in light blue; those outside the park are in dark blue.

described in this paper is a Snow Cover Index (SCI), defined for a specific date during the snow year as the proportion of 8-day MODIS images over a 10-year period in which a particular pixel is snow-covered on that date. The zone of intermittent snow cover, generally between 2,000 and 2,550 m in elevation, has frequent snow during the winter months, but the snow cover often disappears between storms. The SCI is less than one for many dates during the snow season. This zone generally coincides with the montane life zone, with ponderosa pine as the predominant vegetation. Average annual temperature is greater than zero Celsius. The transitional snow zone, generally between 2,550 and 3,050 m, is more likely to have snow cover that persists through most of the winter, especially as elevation increases. The snow cover index is equal to one for more dates during the snow season. This zone is transitional between the montane and subalpine life zones, with lodgepole pine as the predominant vegetation. Average annual temperature is close to zero. The persistent snow zone, generally higher than 3,050 m, has dependable snow cover throughout the winter. The snow cover index is one or close to one throughout most of the snow season. This zone generally coincides with the subalpine life zone. Spruce and fir are the predominant vegetation. Average annual temperature is less than zero. In terms of these snow zones, the seasonal snowpack is said to occur in the transitional and persistent zones.

The high elevations in the study area keep temperatures cool. On the tundra, temperatures vary from lows of about -37°C in winter to highs of about 24°C in summer. At lower elevations in the park, temperatures are typically about 5°C warmer (National Park Service, 2016d).

Monthly variation in precipitation is relatively small, with lower monthly totals during the summer months of June through September, and highest monthly totals in April and May.

Precipitation occurs mostly as snow, which can fall during any month of the year. Most of the snowfall occurs during October through May. The snowpack typically develops in October, and peaks during March, April, or May with SWE ranging from about 100 to about 1400 mm (Dressler *et al.*, 2006, Patterson and Fassnacht, 2014). While snowmelt may continue to produce runoff in decreasing amounts throughout the summer, the bulk of snowmelt runoff is complete by mid-June. Snow tends to collect in depressions in the alpine zone that are protected from sun and wind, where it may persist from one year to the next. Snow accumulation in these depressions is augmented by wind redistribution of snow that may fall on the windward side of the ridge. These firn fields of multi-year snow that remain at the end of the summer, often referred to as glaciers, are not considered part of the seasonal snowpack.

CHAPTER 2. DATA SOURCES

Snowpack measurements have been made across the western United States for the past eight decades by the U.S. Natural Resources Conservation Service (NRCS), formerly known as the Soil Conservation Service (SCS). These data were collected to facilitate current-year forecasts of snowmelt runoff, underscoring the importance of year-to-year variations in snowpack accumulation and ablation as drivers of water-management decisions. The use of consistent locations and methods of data collection make the resulting multi-year datasets valuable for examining long-term temporal trends in snowpack accumulation and ablation.

2.1 Snow Courses

Snow courses are designated locations, operated by the NRCS, where repeated monthly manual measurements of snow depth and SWE are made; snow density is calculated from SWE and depth. Most snow courses have 5 to 20 sampling points at regularly spaced intervals along a transect. The interval between sampling points is typically in the range of 20-100 ft (6.1-30.5 m). Samples are taken using a coring device (Federal Sampler) to determine depth, and are weighed to determine SWE (Natural Resources Conservation Service, 2016a). While there is some variation in sampling schedules, at most snow courses, measurements are made four times per year, on or within 5 days prior to the first day of February, March, April, and May. Snow courses were established in the study area starting in the late 1930s. For this investigation, 23 snow courses in and near Rocky Mountain National Park were selected for analysis based on proximity to the park and on length and completeness of record (Figure 1.1, Table 2.1). Of these 23, nine lie within the park.

2.2 Snowpack Telemetry Stations

Snowpack Telemetry (SNOTEL) stations are instrumented, automated sites, also operated by the NRCS, that measure SWE and precipitation. More recently they measure temperature and snow depth, as well as other variables (e.g., soil moisture and temperature) at some stations. The frequency of measurement is hourly year-round, and meteor-burst communications technology is used to transmit the data to receiving stations and the Internet in near-real time. SWE is measured using a snow pillow and pressure transducer, precipitation is measured using a weighing storage gauge, snow depth is measured using a sonic sensor, and temperature is measured using a shielded thermistor (NRCS, 2016b). The longest SNOTEL records are for SWE and precipitation (more than 35 years at some stations); sensors for temperature (last 25 years) and snow depth (last 10 years) were added later.

The hourly data are compiled into daily statistics. Both snow-course and SNOTEL data are available on the world-wide web at <www.wcc.nrcs.usda.gov> (NRCS, 2016c). SNOTEL stations were initially established in the study area in 1979, with various other longer term stations in operation by 1981. For this investigation, 13 SNOTEL stations were selected for analysis based on proximity to the park and on length and completeness of record (Figure 1.1, Table 2.1). Of these 13, five lie within the park. These 13 SNOTEL stations are the same stations used by Clow (2010) in the orange and purple clusters in his analysis of snowmelt and streamflow timing. The orange cluster includes SNOTEL stations on the western side of the Front Range, while the purple cluster includes SNOTEL stations on the eastern side of the Front Range. In this investigation all 13 SNOTEL stations were used for snowpack analysis, and precipitation data were used from six stations (Phantom Valley, Joe Wright, Willow Park, Lake Irene, Bear Lake, and Copeland Lake).

Table 2.1. Snow course and SNOTEL stations included in the investigation. Data are available online at <<http://www.wcc.nrcs.usda.gov/snow/>>, accessed 7-9-16

Snow Courses	Elevation [m]	Station in/out of RMNP	SNOTEL stations	Elevation [m]	Cluster (Clow, 2010)
Lake Irene	3261	Inside	Lake Irene	3261	Orange
Longs Peak	3201	In	Willow Park	3261	Purple
University Camp	3140	Outside	University Camp	3140	Purple
Cameron Pass	3135	Out	Deadman Hill	3116	Purple
Deadman Hill	3116	Out	Joe Wright	3085	Orange
Boulder Falls	3049	Out	Niwot	3021	Purple
Long Draw Reservoir	3042	In	Roach	2957	Orange
Milner Pass	2973	In	Lake Eldora	2957	Purple
Wild Basin	2915	In	Willow Creek Pass	2909	Orange
Willow Creek Pass	2909	Out	Bear Lake	2896	Purple
Ward	2896	Out	Phantom Valley	2752	Orange
Hidden Valley	2890	In	Stillwater Creek	2659	Orange
Hourglass Lake	2854	Out	Copeland Lake	2621	Purple
Bennett Creek	2804	Out			
Park View	2793	Out			
North Inlet Grand Lake	2744	In			
Red Feather	2744	Out			
McIntyre	2744	Out			
Deer Ridge	2743	In			
Chambers Lake	2743	Out			
Granby	2622	Out			
Copeland Lake	2621	In			
Big South	2621	Out			

2.3 Temperature Stations

Although the SNOTEL stations collect temperature data, changes in sensor technology have complicated the evaluation of long-term temperature trends at these stations (Oyler *et al.*, 2015). As well, temperature data have been collected for shorter time periods, with many of the thermistors being installed around 1990. Consequently, temperature records for this investigation were obtained from three non-SNOTEL data collection sites in and near Rocky Mountain National Park (Figure 1.1, Table 2.2). The temperature records for the period 1983-2015 from Loch Vale represent an update of the Loch Vale temperature data previously reported for the period 1983-2007 (Clow, 2010). Although there are issues with SNOTEL temperature data, temperature records from SNOTEL stations were used for illustrative purposes when it was important for the temperature record to be associated with a co-located SWE record.

Table 2.2. Temperature data collection stations used in this investigation. Data are from the National Oceanic and Atmospheric Administration (2016a), William P. Rense (private monitoring), and U.S. Geological Survey (Colorado State University, 2016).

Station name (identification)	Data source	Elevation [m]	Latitude [N]	Longitude [W]	First year of record
Grand Lake 6SSW (USC00053500)	NWS (NOAA) Cooperative Weather Station	2526	40° 11' 06"	105° 52' 00"	1948
Allenspark	Private weather station operated by William P. Rense	2520	40° 11' 17"	105° 30' 05"	1960
Loch Vale Main and Remote Area Weather Stations	U.S. Geological Survey	3162	40° 17' 17"	105° 39' 46"	1983

2.4 Elevation of Freezing Temperature

Estimated monthly mean elevation of freezing temperatures (freezing level or 0-degree isotherm level) were obtained from the North American Freezing Level Tracker (Western Regional Climate Center, 2016). The definition of instantaneous freezing level for this application is:

“The elevation above sea level in the free atmosphere at which a temperature of 0° C (or 32° F) is first encountered. The mean daily temperature profile used for this process is formed from the four six-hour averages available from Global Reanalysis.” (WRCC, 2016).

The spatial discretization of the freezing level tracker is 2.5 degrees of latitude and longitude, or a rectangle of about 320 x 288 km. This rectangle is centered at 40.35° north latitude, 105.72° west longitude, just south of Trail Ridge Road in Rocky Mountain National Park, and covers the entire study area. The temporal discretization is monthly. As the freezing level determination is simulated for the free atmosphere, terrain effects are ignored.

2.5 Paleoclimate SWE Reconstructions

Estimates of multi-century patterns of SWE for locations near the study site were derived from tree-ring chronologies in the general vicinity of the study area (Figure 1.1, Table A.1). These chronologies are calculated based on relative ring-width indices, i.e., departures from normal, where the normal is assumed to be without a long-term trend. Therefore, the chronologies are not useful for determining the presence, direction, or magnitude of multi-century trends in SWE. However, reconstructions of estimated SWE based on the chronologies can be useful in examining trends over several decades. This investigation used three tree-ring-based SWE reconstructions for the evaluation of past trends (Table 2.3).

Table 2.3. Snow courses and periods for associated tree-ring chronologies used in this investigation

Snow course	Reconstruction date for SWE	Tree-ring chronology		SWE start
		Start	End	
North Inlet Grand Lake	April 1	1571	1999	1938
Cameron Pass	May 1	1486	2000	1936
Longs Peak	May 1	1571	1999	1951

2.6 Projections of Future Temperature, Precipitation, and SWE

Climate scientists have used various models to project future trends in climatic and hydrologic variables that affect the seasonal snowpack. This investigation examines results from several of these strategies to compare trends from the past few decades with trends that are likely to occur over the rest of the 21st century according to the models (Table 2.4). The primary group of model projections used are the multi-model ensemble projections made by the Coupled Model Inter-comparison Project-Phase 5 (CMIP5) (World Climate Research Programme, 2016). Regionally downscaled projections from these models offer estimates of future trends in temperature and precipitation on a monthly basis, for grid cells measuring 1/8 by 1/8 degree of latitude and longitude (Maurer *et al.*, 2007; <http://gdo-dcp.ucllnl.org/downscaled_cmip_projections/>).

The projections of monthly temperature and precipitation have been used to drive hydrologic models that provide projections of monthly values for hydrologic variables including SWE (U.S. Bureau of Reclamation, 2014, Milly *et al.*, 2005; Stahl *et al.*, 2008). For this investigation, regionally downscaled projections of climate and SWE for the remainder of the 21st century, averaged from an ensemble of 31 CMIP5 climate models, were examined and compared with the observed trends (Maurer *et al.*, 2007, Brekke *et al.*, 2014). The selected representative concentration pathway was RCP4.5, representing an assumption for a low-to-moderate greenhouse-gas emissions scenario (Clarke *et al.*, 2007). The area selected for regionally downscaled results is a rectangle of 3/8 degree of latitude and 3/8 degree of longitude, roughly centered on Rocky Mountain National Park (Figure 1.1). In addition to examining the ensemble model projections, individual CMIP5 models were evaluated to select one that, when linked to the Variable Infiltration Capacity (VIC) hydrologic model (Brekke *et al.*, 2014), most

closely matched observed SWE data in the study area. One model that matched the observed trend fairly well was the Institut Pierre Simon Laplace (IPSL) model from the IPSL Climate Modelling Centre (Dufresne *et al.*, 2013). Projections made using this model, linked to the VIC hydrologic model, were also examined and compared with observed trends in SWE.

Table 2.4. Climate and hydrologic models from which projections were used in this investigation.

Name of model(s)	Description	Representative Concentration Pathway	Period of projection	Spatial resolution	Reference
CMIP5 Ensemble	Averaged results of 31 regionally downscaled global climate models, linked to hydrologic models	RCP 4.5	1951-2099	12 km	Maurer <i>et al.</i> , 2007
IPSL	Single model from the CMIP5 ensemble, linked to hydrologic model	RCP 4.5	1951-2099	12 km	Dufresne <i>et al.</i> , 2013
WRF-Hydro	High-resolution climate and hydrologic model (Mentioned in discussion)	AR4 scenario A1B; equivalent to RCP 6.0	2006-2050	4 km	Rasmussen, 2011, Rasmussen 2014, Skamarock <i>et al.</i> , 2005

CHAPTER 3. METHODS

3.1 Snow Water Equivalent

Monthly records of SWE were tabulated for the 23 snow courses for their periods of record, covering up to eight decades (as early as 1936 through 2015). Daily records of SWE were tabulated for the 13 SNOTEL stations, covering the period 1981 to 2015. The 13 SNOTEL stations were considered as two groups based on proximity, according to the orange and purple groupings used by Clow (2010) (Figure 1.1). First of each month SWE (typically occurring within 3 days of the first of the month (Pagano, 2012)) for the snow season for snow courses (available over the long term from February 1 to May 1) and SNOTEL stations (October 1 to June 1) were compiled, and monthly change in SWE was computed.

A correlation matrix was constructed for median April 1 SWE, 1981-2015, for all 13 SNOTEL stations and all 22 snow courses. This matrix illustrates the degree to which April 1 SWE is correlated among all the data collection sites.

Traditionally, the most commonly used measure of snowpack condition is April 1 SWE (for example, Mote *et al.*, 2005), based on the assumption that of the four monthly SWE measurements at most snow courses, April 1 SWE best approximates the annual peak SWE. In this study area, on average, peak SWE occurs any time from mid-March through mid-May, but it can be earlier (1981, 2002, or 2012) or later (1995, 2011), depending on location, elevation, and the amount of winter precipitation in a given year. Using the assumption that peak SWE occurs on April 1 can yield an under-estimation of peak SWE by as much as 12 percent (Bohr and Aguado, 2001). In this study, this underestimation is evaluated for the 13 study SNOTEL stations. The daily SWE records provided by SNOTEL stations facilitate computation of

additional measures to help characterize snowpack accumulation and ablation in greater detail. In this investigation these included measures such as annual peak SWE, difference between annual peak and first-of-month SWE values, date of peak SWE, number of days per year with accumulation greater than 5 mm and greater than 10 mm, and the total accumulation of SWE during a given period such as a month or a season (Figure 3.1). This last measure is roughly equivalent to “snowfall equivalent” as defined by Knowles *et al.* (2006): “*precipitation totals on days for which newly fallen snow was recorded*”. Another measure of SWE that can be calculated using daily SNOTEL data is the change in SWE over a 15-day period. Evaluating the change in SWE over a specified period, such as a month or 15 days, and trends in the change in SWE, rather than just the amount of SWE present over the ground, can be an instructive way to emphasize the changes that are occurring to the pattern of snowpack accumulation and ablation. For example, if there is a trend toward more SWE during February, followed by a trend toward less SWE in March, then the negative change in SWE from February to March grows at a rate that may be greater than either of the monthly SWE trends. As stated in Chapter 1, winter recreation is increasingly popular in the study area. A reasonable index of sufficient snow depth for enjoyable winter recreation is a minimum of 100 mm of SWE. Therefore, the SWE measures analyzed also included number of days each year with SWE greater than 100 mm.

3.2 Estimation of Daily Niveographs from Snow Course Data

A niveograph is a plot of SWE versus time (Fassnacht and Patterson, 2013), usually for a full snow season. As mentioned above, the daily SWE records provided by SNOTEL stations provide significant added value for analysis of snowpack accumulation and ablation, compared with the four monthly SWE values provided by snow courses. However, snow courses have the

advantage of a longer period of record compared with SNOTEL stations. Accordingly, it would be helpful to have a method for estimating daily niveographs based on monthly snow course data. Simply interpolating between the four monthly SWE values from the snow course often results in a poor estimate for the daily niveograph, as the annual peak frequently occurs after the final SWE measurement on May 1. Even for those cases when the annual peak SWE occurs prior to May 1, simple interpolation misses the peak (Bohr and Aguado, 2001).

Median values for daily SWE data from co-located or nearby SNOTEL stations can be used to help construct simulated niveographs for specific years at a snow course. Further, these simulated daily niveographs can be used to estimate the magnitude and timing of the annual peak, and other measures, such as short-term changes in SWE, that depend on the daily niveograph. This enhanced niveograph interpolation method was tested using data from two sites in Rocky Mountain National Park (Lake Irene and Willow Park SNOTEL stations used as snow courses), for three snow years representing low, medium, and high SWE accumulation (Patterson and Fassnacht, 2014). The estimated niveographs were then compared with the actual observed niveographs to evaluate the performance of the estimation approach.

Several characteristics of annual niveographs from Rocky Mountain National Park SNOTEL stations became apparent during the study, suggesting a scheme for dividing the niveograph into five components based on the geometric appearance of the niveograph and the underlying physical snowpack processes (Figure 3.1). From September 1 through October 20, and from late June through August 31, daily SWE values typically were zero. In most, but not all years, SWE was also zero from early June through late June. From October 20 through March 1, the accumulation phase, daily SWE values increased at rates that were somewhat irregular, reflecting the dominant process of precipitation driven by weather patterns. From

March 2 through mid-May, the peak phase, SWE reached the annual peak, reflecting the transition from precipitation-driven accumulation to melt driven by solar radiation. The geometric appearance of the niveograph during the peak phase approximated a second-order polynomial function. In most years peak SWE occurred prior to 1 May, but in some years peak SWE occurred as late as late May. Following the peak phase, SWE values declined at an increasing rate, reflecting the increasing melt rates driven by increasing solar radiation. The shape of the melt phase approximated a declining second-order polynomial function.

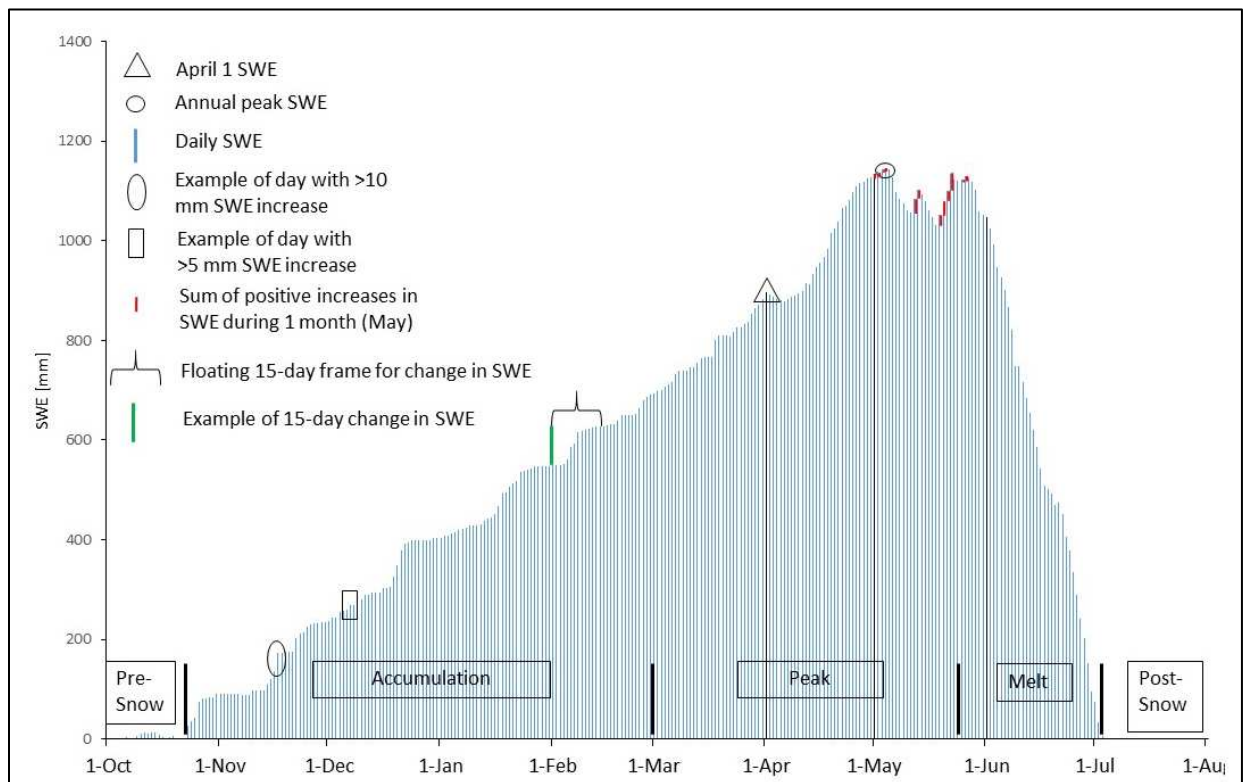


Figure 3.1. Sample niveograph (Lake Irene, 2011), illustrating examples of various SWE measures, and separation of niveograph into phases for estimation.

These characteristics of the niveographs were used to devise separate approaches for estimating the accumulation, peak, and melt phases of the niveograph (Figure A.1). Prior to the accumulation phase, SWE values were held to zero until October 20, the typical date for the start of accumulation. For the accumulation phase from then until March 1, the median niveograph

was fitted to zero on October 20, and the observed SWE values on February 1 and March 1, using time-prorated multipliers based on the ratio of these observed values to the values for the same day on the median niveograph. For the peak phase from March 1 through May 1, the three observed values, March 1, April 1, and May 1, were used to define a second-order polynomial function passing through these three points. For the melt phase, a generic second-order polynomial function was defined that approximated the melt phase of the median niveograph, and this function was fitted to the data using a scaled multiplier. In most years, SWE was declining by May 1 (May 1 SWE < April 1 SWE), and so the scaled multiplier for the melt function was applied on May 2. This brought SWE values back to zero by early June.

For the minority of years when SWE was still increasing on May 1 (May 1 SWE > April 1 SWE), the peak phase was extended to make the peak fall on May 15, midway between May 1, the final date of observed rising SWE, and June 1, after which the peak never occurred (Figure A.2).

The estimated daily niveographs were plotted along with the observed daily niveographs for comparison purposes. The estimation model was also compared with the traditional assumption of peak SWE on April 1, in terms of the ability to estimate the magnitude of the peak SWE and the date of the peak SWE.

3.3 Trend Analysis

The primary goal of this investigation is to evaluate long-term trends in snowpack accumulation and ablation in the study area. Many of the SWE measures described above provide annual time series suitable for trend analysis. In this investigation trend analysis

involves testing a time series of annual values to determine the likely presence of a long-term trend, and further estimation of the slope and statistical significance level of the trend, if present. Trend analysis of snow course SWE data covered two different periods: the entire period of record for the snow course starting in the 1930s to 1950s through 2015, and the 35-year period for SNOTEL data from 1981 to 2015. Trend analyses of SWE on early and late halves of the period of record for snow courses has shown varying patterns of sequential trends in northern Colorado (Fassnacht and Hultstrand, 2015). This variability in trends suggests that a reasonable period for trend analysis in the study area is the 35-year period, 1981-2015, which is long enough for trend analysis but also short enough to represent a consistent trend. This also corresponds with the period of record for most of the SNOTEL stations.

Some trend statistics are computed using one value per year, such as April 1 SWE or annual peak SWE. Since sub-seasonal variations in SWE and other variables are an important part of the pattern of snowpack accumulation and ablation, many of the trend statistics are computed for annual series of monthly values, such as SWE on the first of each month during the snow season. Some trend statistics are computed for annual series on a shorter, sub-monthly time step, such as 15-day change in SWE, or even shorter, such as daily for the snow season. The month-to-month trends exhibited irregular variability that could not be characterized as a seasonal cycle, hence, the Seasonal Kendall test (Helsel and Hirsch, 1995) was not used.

The SWE trends were further analyzed in relation to station characteristics such as location and elevation, and to other variables such as temperature, freezing level, and precipitation. For location, stations were grouped according to Clow's orange and purple clusters (Clow, 2010), representing locations on the western and eastern sides of the Front Range in north-central Colorado. For elevation, SWE trends were presented as a function of elevation.

For temperature, freezing level, and precipitation, monthly SWE trends were compared with monthly trends in temperature and precipitation.

Given the large amount of natural inter-annual variability in many of the annual series of SWE data, occasional missing values, and the likelihood that the data are not normally distributed, a non-parametric approach was used for the trend analysis method. The method used here is the Mann-Kendall test for monotonic trend (Mann, 1945; Kendall, 1975; Gilbert, 1987), supplemented by the Theil-Sen estimate of slope of the linear trend (Theil, 1950; Sen, 1968; Gilbert, 1987; Helsel and Hirsch, 1995). Application of the combined method was made using the “MAKESENS” Excel macro (Salmi *et al.*, 2002).

3.4 Precipitation

Monthly precipitation values from the SNOTEL stations for the cold season (October-June) were used in two analyses. The first was a comparison of total monthly precipitation, total monthly SWE accumulation, and the fraction of total precipitation represented by the SWE accumulation. This comparison was made using precipitation records from six SNOTEL stations representing the range of station elevation, temperature, SWE, and precipitation totals for the study area. The stations were Joe Wright, Willow Park, Phantom Valley, Lake Irene, Bear Lake, and Copeland Lake (Figure 1.1). Joe Wright, Lake Irene, and Phantom Valley are in the orange cluster, and Willow Park, Bear Lake, and Copeland Lake are in the purple cluster. As mentioned above, the value for total SWE accumulation is roughly equivalent to “snowfall equivalent” (Knowles *et al.*, 2006). The second analysis, which used monthly precipitation and temperature data from all of the SNOTEL stations, was a three-way comparison of trends in total

cold-season precipitation, average cold-season temperature, and April 1 SWE, to evaluate associations between SWE trends and precipitation or temperature trends.

3.5 Temperature

Although SNOTEL stations have temperature sensors, there are several reasons why the temperature records from SNOTEL stations are not the preferred records to use for studies of long-term temperature trends. The first reason is the shorter length of record; while the first SNOTEL stations were installed in 1979 across the study area, and temperature was not recorded until the late 1980s or thereafter. The second reason is inconsistency in the collection of temperature data at SNOTEL stations. During the early to mid-2000s the SNOTEL program switched to an extended range temperature sensor, installed a new radiation shield, instituted a new data collection protocol, and moved all temperature sensors to a new location so that each was above the snow pillow. These changes resulted in records with uncertainty about consistency over the long term (Oyler *et al.*, 2015). For this reason, most of the temperature data used in this investigation are from three stations (Allenspark, Grand Lake, and Loch Vale) that are not part of the SNOTEL network. Average monthly temperature data from the three weather stations were analyzed for magnitudes and trends for the period 1981-2015 (1983-2015 for Loch Vale).

This investigation did make use of temperature data from SNOTEL stations for analyses in which the association with particular SNOTEL stations was important. Two SNOTEL stations, the highest, Lake Irene and the lowest, Copeland Lake, were selected for an analysis of temperature records to characterize the amount of warmer-than-freezing weather at the station during a given month. Daily maximum temperature records were examined to identify days on

which the maximum daily temperature was warmer than zero degrees C. The data homogenization method developed by Oyler *et al.* (2015) was applied, in an effort to improve data homogeneity. The quantity included in the comparison was the number of degrees Celsius, if any, warmer than zero, reported for the daily maximum temperature each day, accumulated for each month. As a measure of total monthly duration of warmer-than-freezing weather that can help to melt snow, this quantity involves an assumption that the duration of warmer-than-freezing weather, on each day when it occurs, is similar from day to day, or that the variations over a month average out to the same durations from month to month. Without examining at the hourly records (some issues with the hourly data are summarized in Avanzi *et al.*, 2014), this assumption, and the use of these melt-degree days, represents a reasonable approach to quantifying the amount of warmer-than-freezing weather in a month.

Temperature data from SNOTEL stations were also used in an analysis of trends and variability in SWE and in October-June temperature and precipitation at SNOTEL stations, similar to an analysis presented for the Pacific Northwest (Mote, 2003). For this analysis the patterns of trends in average October-June temperature and total October-June precipitation at each SNOTEL station were evaluated with respect to trends in SWE in order to assess influences of temperature and precipitation trends on SWE trends.

3.6 Freezing level

The monthly freezing-level estimates from the North American Freezing Level Tracker <www.wrcc.dri.edu/cwd/products/> (Chapter 2) were compared with the elevation range of the SNOTEL stations at times when SWE decreases were occurring. Trends in monthly freezing

level were also evaluated, to identify months with strong upward or downward trends over time. These trends were compared with those for temperature and SWE.

3.7 Paleoclimate SWE Reconstructions

A question that arises in a trend study is: Have there been other periods of similar duration during recent centuries, with indications of similar trends? This question can be addressed using tree-ring reconstructions. Tree rings can be used to reconstruct snow water equivalent (SWE) from historical snow course data (Woodhouse, 2003). With such reconstructions it can be difficult or impossible to identify multi-century trends, because growth trends and autocorrelation have been removed from the record (Woodhouse and Lukas, 2006), and because the algorithms used to produce the reconstructions mute extreme values. As a result, “*reconstructions are usually a conservative estimate of past variability*” (Woodhouse, 2016). However, these reconstructions can be used to examine trends with durations of several decades. Accordingly, multi-variate linear regression was used to develop relations between tree rings and snow course SWE. First the monthly SWE data from the 23 snow courses were examined to identify, for each snow course, the month with the highest median SWE (closest to the annual peak). The monthly SWE data were also used to identify months with large trend values to facilitate comparison of reconstructed trends during paleo time periods and observed trends during the recent (35-year) period. Next, multi-variate regressions were developed between observed SWE for the highest-SWE month for each year of record at each snow course, and tree-ring width index for the same months for each of 26 tree-ring chronologies from the northern Colorado Rockies (Woodhouse and Lukas, 2006). The three relations with the highest coefficients of determination were selected for analysis of past SWE trends.

The selected relations were used to estimate SWE for the period of record of the chronologies. The reconstructions were then used to compute 35-year linear trends to identify possible large increases or decreases in SWE over the reconstructed time period. To compute the 35-year linear trends, a moving 35-year time frame was centered around each year of the reconstructed record, and a 35-year trend was computed for each year.

3.8 Projections of Future Temperature, Precipitation, and SWE

The terrain of the nine 1/8 by 1/8 degree pixels for which CMIP5 climate model projections were retrieved was analyzed hypsometrically using a geographic information system to determine the distribution of elevations within each pixel.

The primary question addressed in the evaluation of climate model projections was whether the trends observed in the study are likely to continue in the future. To address this question, the climate model projections of temperature, precipitation, and SWE described in Chapter 2, section 2.6, were compared with observed trends. The comparison included overall trend on an annual basis, as well as trends for each month of the snow season.

CHAPTER 4. RESULTS

4.1 Trends in Snow Water Equivalent

The correlation matrix for April 1 SWE for all 35 data collection sites showed a wide range of correlation among sites. Coefficients of determination ranged from 0.04 to 0.95 (Table A.2). The highest correlations were between co-located snow courses and SNOTEL stations, such as University Camp (0.9). But other co-located snow courses and SNOTEL stations were less well correlated, such as Copeland Lake (0.6) and Willow Creek Pass (0.6). Some other high correlations were geographically close, such as Milner Pass and Lake Irene snow courses (0.9). But some other high correlations are not close, such as Boulder Falls and University Camp (0.9). The snow courses in the park tended to be well correlated with each other, but otherwise the pattern of correlations is well distributed throughout the matrix.

4.1.1 Monthly SWE

SWE measures, such as first-of-month SWE at snow courses and SNOTEL stations, (Figure 4.1) and peak annual SWE (Figure 4.2), exhibit strong inter-annual variability. This variability is related to variations in weather patterns from year to year. Hence, a very high year for April 1 SWE and peak SWE (2011) can be followed by a very low year (2012), even with decreasing trend in a 35-year period. Inter-annual variations in measures of SWE, such as April 1 SWE, are more closely related to variations in precipitation than to variations in temperature (Figure A.3). Regression analyses of April 1 SWE at a representative SNOTEL station, Phantom Valley, on average October-June temperature as recorded at the SNOTEL station, and

on total October-June precipitation, showed a much stronger correlation with precipitation ($R^2 = 0.50$, with a strong positive slope) than with temperature ($R^2 = 0.04$, with a slight negative slope) (Figure A.4).

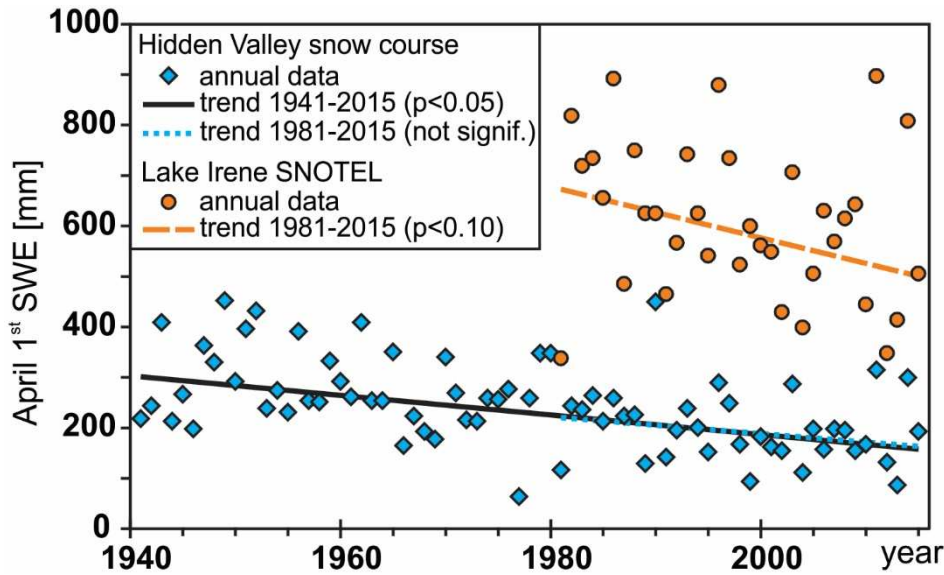


Figure 4.1. Example plot of annual series of April 1 SWE for a snow course and a SNOTEL station, showing strong inter-annual variability. Lines are linear best-fit trend lines.

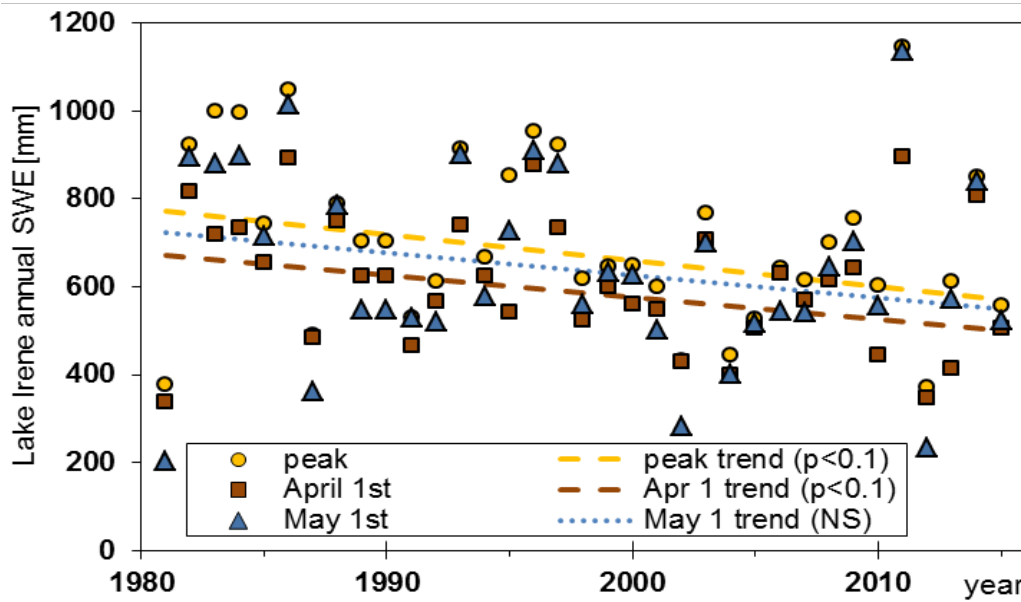


Figure 4.2. Example plot of annual series of SWE measures for Lake Irene SNOTEL station, including 1981-2015 trends.

Median SWE values computed over the 35-year analysis period illustrate the range of measures of snowpack accumulation and ablation in the study area (Figure 1.1). Median April 1 and May 1 SWE values ranged from just over 100 mm at low-elevation snow courses on the eastern slope, such as Copeland Lake, Deer Ridge, Bennett Creek, Chambers Lake, Big South, and Red Feather, to 500 to 600 mm at higher elevation snow courses near the summit of the Front Range, such as Lake Irene and Cameron Pass. Several of the higher-elevation snow courses, such as Deadman Hill, Cameron Pass, Long Draw Reservoir, Lake Irene, Longs Peak, University Camp, and Boulder Falls, had median May 1 SWE values that exceeded those on April 1, indicating annual peaks that typically occurred after April 1. Median values for annual peak SWE at SNOTEL stations reflect similar variability, from 149 mm at Copeland Lake to 668 mm at Lake Irene (Figure 4.3). The median date of peak SWE at SNOTEL stations ranged from March 6 at Lake Eldora to May 6 at Joe Wright (Figure 4.4). Three SNOTEL stations had median dates of peak SWE prior to April 1 and one, Copeland Lake, had a date more than three weeks prior to April 1. Ten SNOTEL stations had median dates of peak SWE after April 1 and eight of these were more than three weeks after April 1 (Figure 4.4).

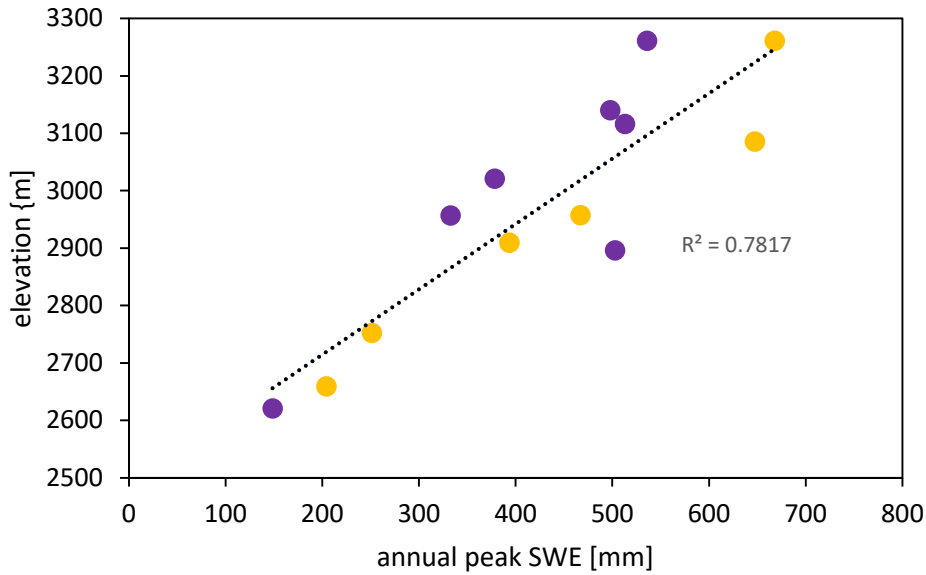


Figure 4.3. Median annual peak SWE at SNOTEL stations, 1981-2015, in relation to elevation. Orange and purple circles refer to Clow's clusters (2010).

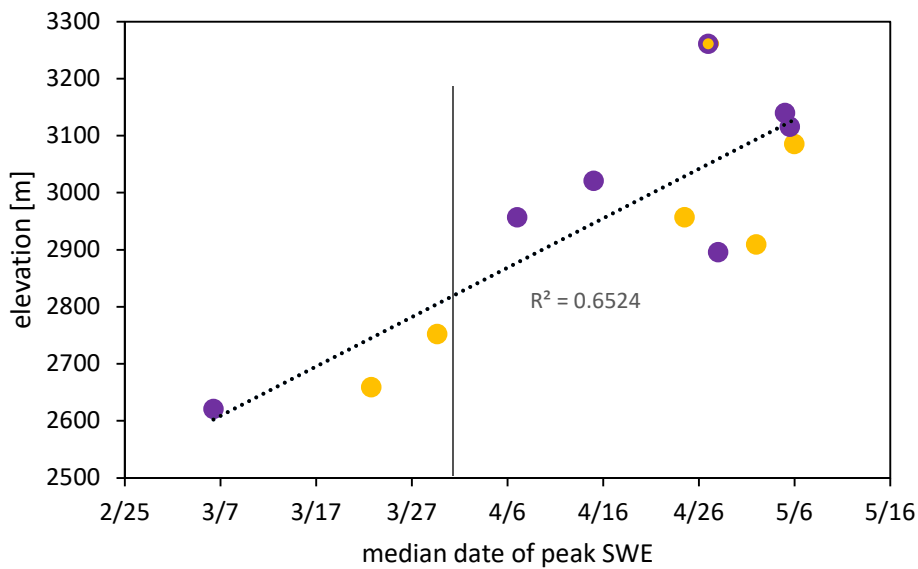


Figure 4.4. Median date of peak SWE at SNOTEL stations, 1981-2015, in relation to elevation.

Across the study area, there was a preponderance of decreasing trends in SWE on the first of the month, meaning a trend toward less SWE with time (Figure 4.5). For example, the trend at the Lake Irene SNOTEL station for the period 1981-2015 was generally downward at a rate of

about 31 mm/decade (Figure 4.1). These decreasing trends were not universal, but were pervasive. Magnitudes of the SWE trends varied from zero to gains of as much as 30 mm/decade during February, and losses of as much as 50 mm/decade during March (Figures 4.5 and 4.6a). Of the 159 monthly trend values for the period 1981-2015, computed based on data from snow courses and SNOTEL stations, 94 (59 percent) were negative, while 65 (41 percent) were positive (Figures 4.5 and 4.6a). Four of the increasing trends and none of the decreasing trends were statistically significant at the $p < 0.05$ level; six of the increasing trends and four of the decreasing trends were statistically significant at the $p < 0.10$ level. When sorted according to Clow's orange and purple clusters, the orange cluster (western side of the Front Range) had 80 percent decreasing trends, and the purple cluster (eastern side of the Front Range) had 52 percent decreasing trends.

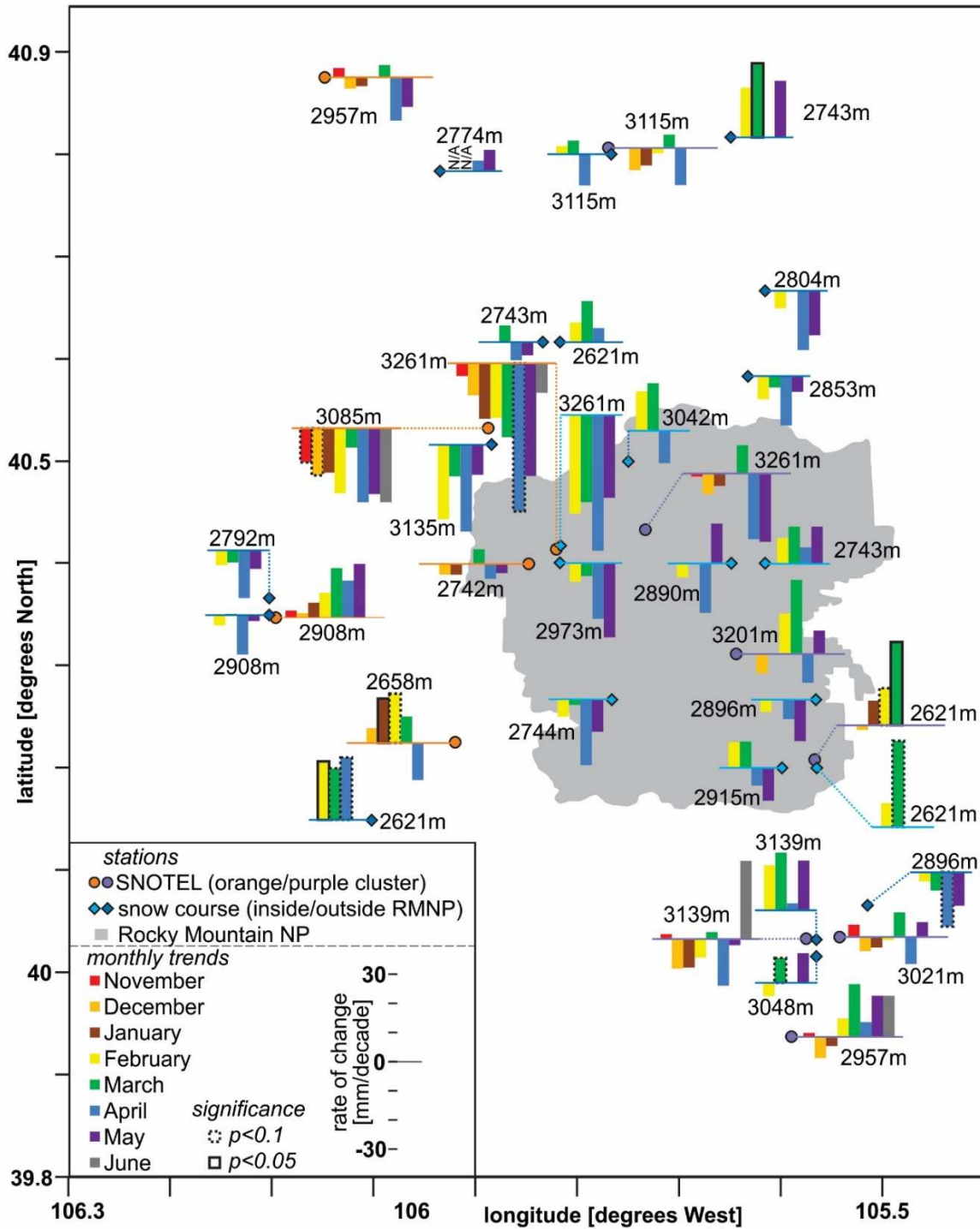


Figure 4.5. Trends in first-of-month SWE at snow courses and SNOTEL stations, 1981-2015. Orange and purple clusters refer to Clow's clusters (2010).

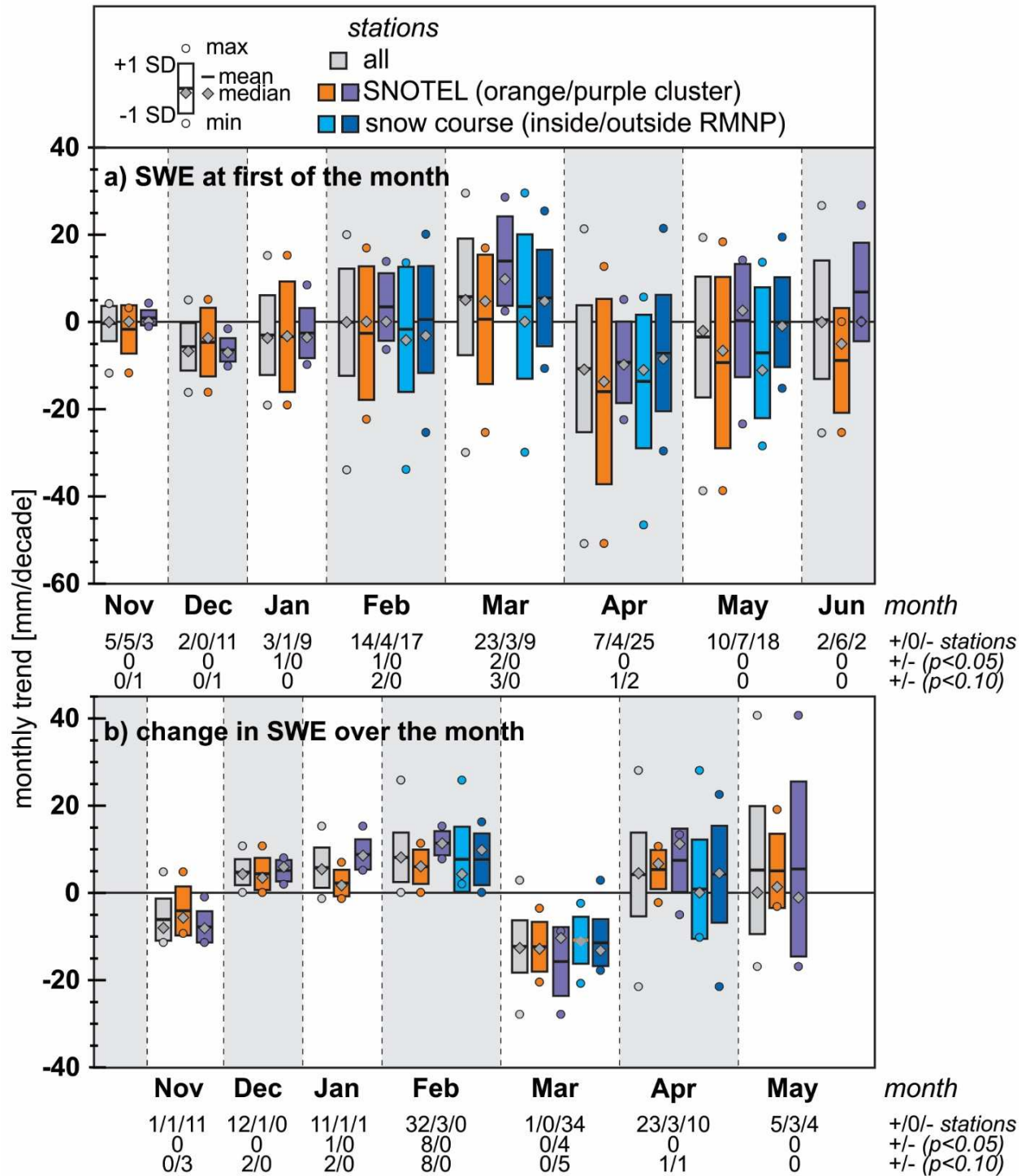


Figure 4.6. a) Distribution of monthly trends in SWE on the first of each month during the snow season for various groupings of snow courses and SNOTEL stations, 1981–2015, and b) distribution of trends in monthly change in SWE. Designation such as 23/3/9 means 23 trends were positive, 3 were level, and 9 were negative. Designation such as 2/0 means 2 positive trends and 0 negative trends were statistically significant.

When the SWE trends are sorted by month, the difference between upward trends in February and downward trends in March is again highlighted. The monthly SWE value with the most increasing trends (more SWE) was March 1, representing conditions during February (Figure 4.6a). The following month, April 1, representing conditions during March; as well as December, representing conditions during November, had the most decreasing trends. Comparing the monthly SWE values for the orange and purple SNOTEL clusters on the western and eastern sides, respectively, of the Front Range, shows that on March 1 and June 1, reflecting conditions during February and May, the purple cluster had more increasing trends than the orange cluster (Figure 4.6a).

Nearly all of the trends in monthly change in SWE during December, January, and February were positive, meaning a trend toward greater gain in SWE during those months (Figure 4.6b). Nearly all of the trends during November and March were negative, meaning a trend toward less gain (or greater loss) in SWE during those months. April and May had mixed trends in monthly change in SWE.

Higher-elevation sites tended to have more decreasing trends in SWE, while lower-elevation sites tended to have more increasing trends in SWE (Figure 4.7a). This pattern holds for all months, as indicated by the slopes of the colored best-fit lines in Figure 4.7a. The positions of these best-fit lines indicates that the March 1 SWE trend, representing conditions during February, has the highest preponderance of increasing trends, while the April 1 SWE trend, representing conditions during March, has the highest preponderance of decreasing trends. This is a pattern that will recur throughout the results and discussion of this investigation. As indicated by the values for R^2 in Figure 4.7a, the correlation between elevation and SWE trend tended to be stronger during November and December (on December 1 $R^2=0.52$ and on January

1 $R^2=0.66$), moderate during January to March (on February 1 $R^2=0.31$, on March 1 $R^2=0.27$, and on April 1 $R^2=0.32$), and weaker during April (on May 1 $R^2=0.16$).

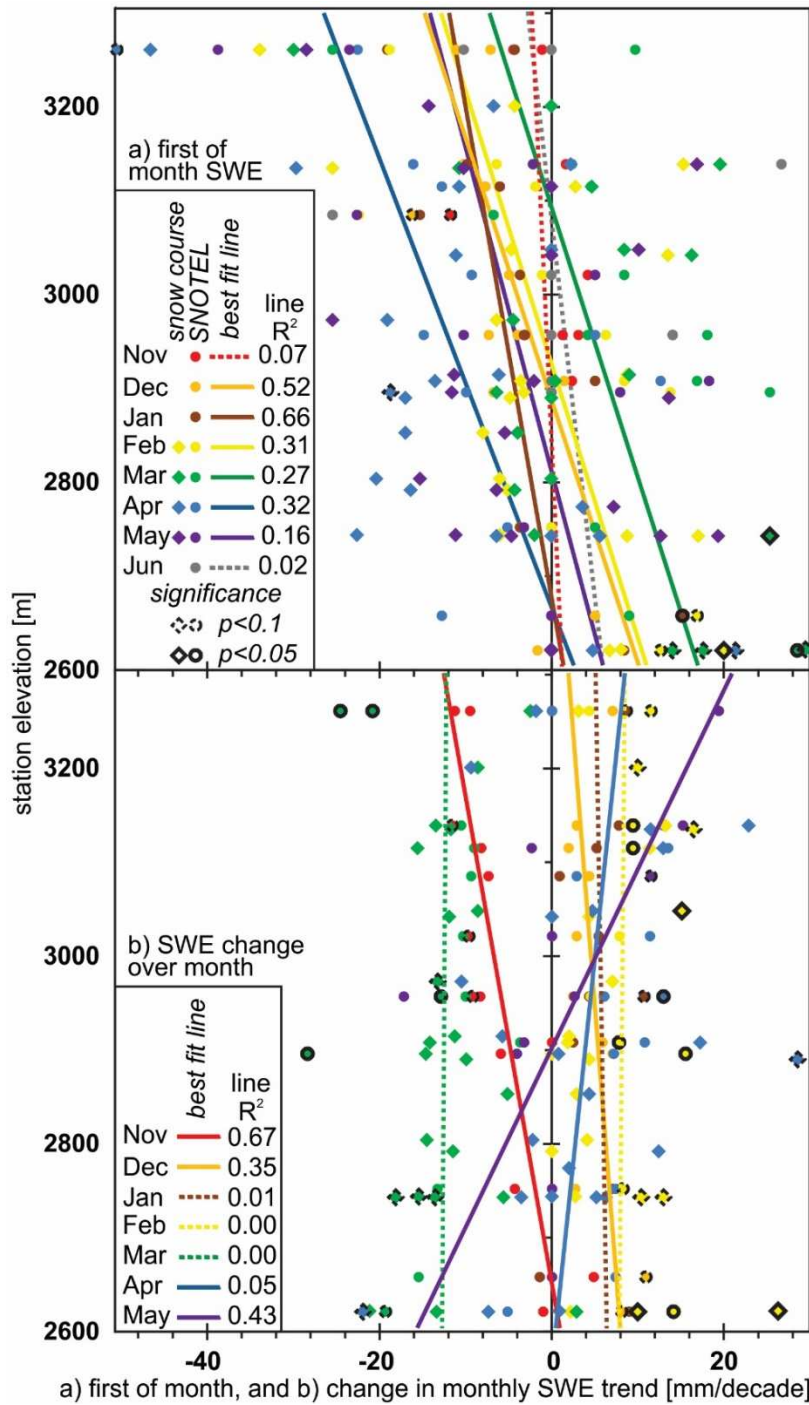


Figure 4.7. a) Trends in first-of-month SWE at snow courses and SNOTEL stations, 1981-2015, in relation to elevation. b) Trends in monthly change in SWE at snow courses and SNOTEL stations, 1981-2015, in relation to elevation.

Trends in monthly change in SWE showed little relation with elevation, except for November and May (Figure 4.7b). In November higher elevation sites had more negative trends in monthly change in SWE than lower elevation sites. In May the relation with elevation was reversed, with higher elevation sites having more positive trends. Although the other months had trends in SWE change with little relation to elevation.

While this investigation focuses on the 35-year period (1981-2015), some trends in SWE measures from snow courses were analyzed for longer periods. Most (66) of monthly SWE trends for the 23 snow courses over the entire period of record were decreasing, especially on April 1 and May 1, reflecting conditions during March and April (Figure A.5a). Twelve of the trends for February 1 and March 1st SWE outside the park (6 stations) were increasing, while only two stations inside the park had an increase on March 1st (Figure A.5a). In comparison to monthly SWE trends over the 35-year period 1981-2015, trends over the longer period tended to be more negative. Only two stations with decreasing trends over the short term had increasing trends over the long term (upper left quadrant in Figure A.5a). However, 25 stations with increasing trends over the short term had decreasing trends over the long term (lower right quadrant in Figure A.5a). This is especially true for SWE trends on February 1 and March 1. Trends in monthly change in SWE at snow courses were negative during March for both periods, with stronger negative values in the shorter period (Figure A.5b). This reflects the largely decreasing trends for April 1 SWE in Figure A.5a. Trends in monthly change in SWE during April were mostly positive for both periods, especially the shorter period. This reflects the largely increasing trends for May 1 SWE in Figure A.5a. Trends during February were mixed and close to zero for the longer period, and were mostly positive for the shorter period.

4.1.2 Trends Derived from Daily SWE

Trends in annual peak SWE at the 13 SNOTEL stations were mixed, with 7 declining trends, 5 increasing trends, and one station with no trend. When plotted in relation to elevation, there was again a tendency for higher elevation stations to have trends that are more negative, and lower elevation stations to have trends that are more positive (Figure A.6a). When grouped by cluster, the orange (west) cluster had more decreasing trends (4 down, 1 up, 1 zero), while the purple (east) cluster had slightly more increasing trends (3 down, 4 up).

Trends in date of annual peak SWE at the 13 SNOTEL stations were also mixed, with 4 trends toward earlier date of peak, 8 trends toward later date of peak, and one station with no trend. There was a slight tendency for higher elevation stations to have trends toward later date of peak, and for lower elevation stations to have trends toward earlier date of peak (Figure A.6b). When grouped by cluster, the orange cluster had a relatively even mix, with 3 trends toward later peak, 2 trends toward earlier, and one zero trend. The purple cluster had more trends toward later peak, with 5 trends toward later peak, and 2 trends toward earlier peak.

A comparison was made between observed annual peak SWE, based on the SNOTEL daily SWE records, and first-of-month SWE from monthly records (Figure A.7, Table A.3). Results showed that the median difference over the period 1981-2015 between observed annual peak SWE and April 1 SWE averaged 20 percent. In this comparison, Copeland Lake, the station with a median date of peak SWE of March 6, was an outlier, with a median difference of 75 percent. The remaining 12 SNOTEL stations had median differences ranging from 9 to 22 percent. Ignoring Copeland Lake, the remaining 12 SNOTEL stations had a weak ($R^2=0.14$) correlation with elevation, with higher elevation stations tending to have a higher percent difference (Figure A.7). The median difference between observed annual peak SWE and the

maximum of the first-of-month SWE values averaged 6 percent, with no outliers. This relation had a strong ($R^2=0.53$) correlation with elevation, with a slight tendency for higher elevation stations to have a lower percent difference (Figure A.7).

Accumulation, loss, and net change in SWE during a moving 15-day period were calculated on a daily basis for six representative SNOTEL stations spanning the range of SNOTEL elevations: Lake Irene, Willow Park, Joe Wright, Bear Lake, Phantom Valley, and Copeland Lake. Willow Park, Bear Lake, and Copeland Lake are in the purple cluster, and Lake Irene, Joe Wright, and Phantom Valley are in the orange cluster (Clow, 2010). All six SNOTEL stations showed similar patterns of accumulation, loss, and net change, with progressively lower SWE values at lower elevations (Figures 4.8 and A.8 – A.13). Fifteen-day accumulation was relatively consistent from October through May, with a slight increase in accumulation rate during late April to early May at Willow Park. SWE loss occurred in October and November when weather suitable for melting typically occurred. Then during December, January, February, and (at Willow Park and Phantom Valley) early March, 15-day SWE loss was virtually zero, as very little melt occurred during that period. From late March (early March at Copeland Lake) through the end of the melt season, 15-day SWE loss accelerated, and reached its greatest (negative) values. Combining accumulation and loss into a 15-day net change in SWE, a typical pattern emerges of positive 15-day net change in SWE during the accumulation season, and negative 15-day net change in SWE during the melt season.

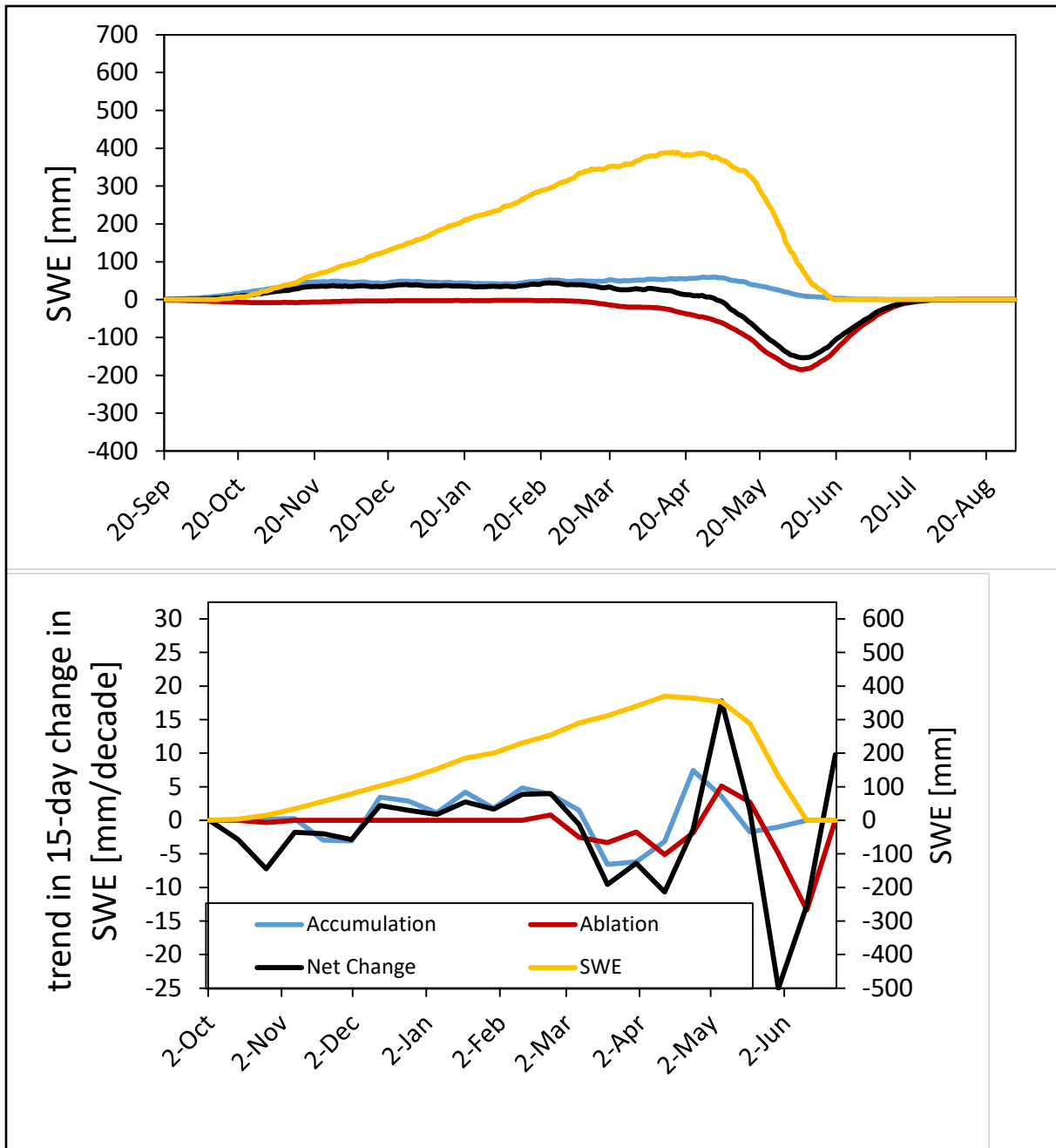


Figure 4.8. a) Median SWE, 1981-2015, and average values for 15-day changes in SWE, averaged from 6 SNOTELs. (b) Trends in 15-day changes in SWE, averaged from 6 SNOTELs.

Trends in these 15-day SWE changes for the period 1981-2015 were computed for every 20th day during the snow season. All six SNOTEL stations showed similar trends (Figures 4.8

and A.8 – A.13). During November the trend was toward greater net loss of SWE. November also had a trend toward less accumulation. From December through early March, the trend was toward greater net gain in SWE. This period also had a trend toward greater accumulation. During mid-March through early April, the trend shifted abruptly to greater net loss in SWE. This period also had a trend toward greater ablation, and to some extent a trend toward less accumulation. During mid-April through mid to late May, the trend in net SWE change was again positive (or zero for Copeland Lake). This period also had a trend toward greater accumulation, and less ablation. Finally, at the five out of six SNOTEL stations (all except Copeland Lake) where the snow season is sufficiently long, in late May through early June, the trend in net change in SWE shifted one more time to greater net loss. At these stations this period also had a trend toward greater loss through ablation.

Trends in SWE for each day of the snow year were computed for the same six SNOTEL stations (Figures 4.9 – 4.11). For the Lake Irene SNOTEL station, all of the daily SWE trends were negative, varying from zero to -75 mm/decade, while they were all positive for Copeland Lake (Figures 4.9 a and b). The greatest negative trends at Lake Irene, while not statistically significant, occurred in mid to late May. The least negative late-season trends at Lake Irene occurred during mid-May. The greatest increasing trends (about 30 mm/decade) at Copeland Lake occurred during early March, with trends that were significant at the $p < 0.05$ or $p < 0.10$ level. The most significant trends occurred around the time of the median annual peak SWE. Significant trends also occurred early in the season at Lake Irene (decreasing for 3 days in early January), as well as at Copeland Lake (increasing for 9 days in late December).

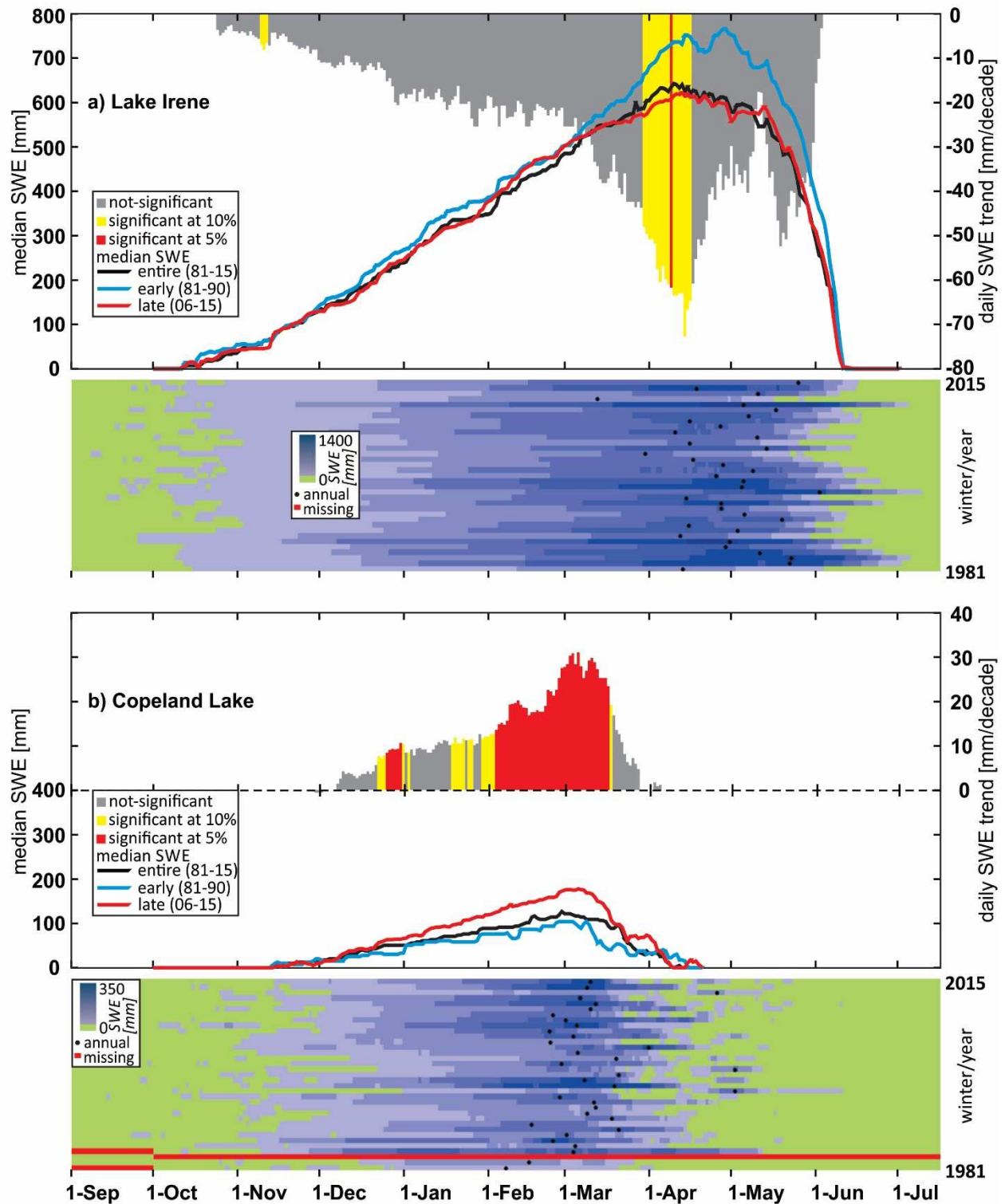


Figure 4.9. Daily SWE trends for a) Lake Irene SNOTEL, and b) Copeland Lake SNOTEL, in relation to median daily SWE for entire period of record, and for early and late segments of the record. Also shows raster plots of daily SWE for each year, 1981-2015. “Annual” dot denotes annual peak SWE.

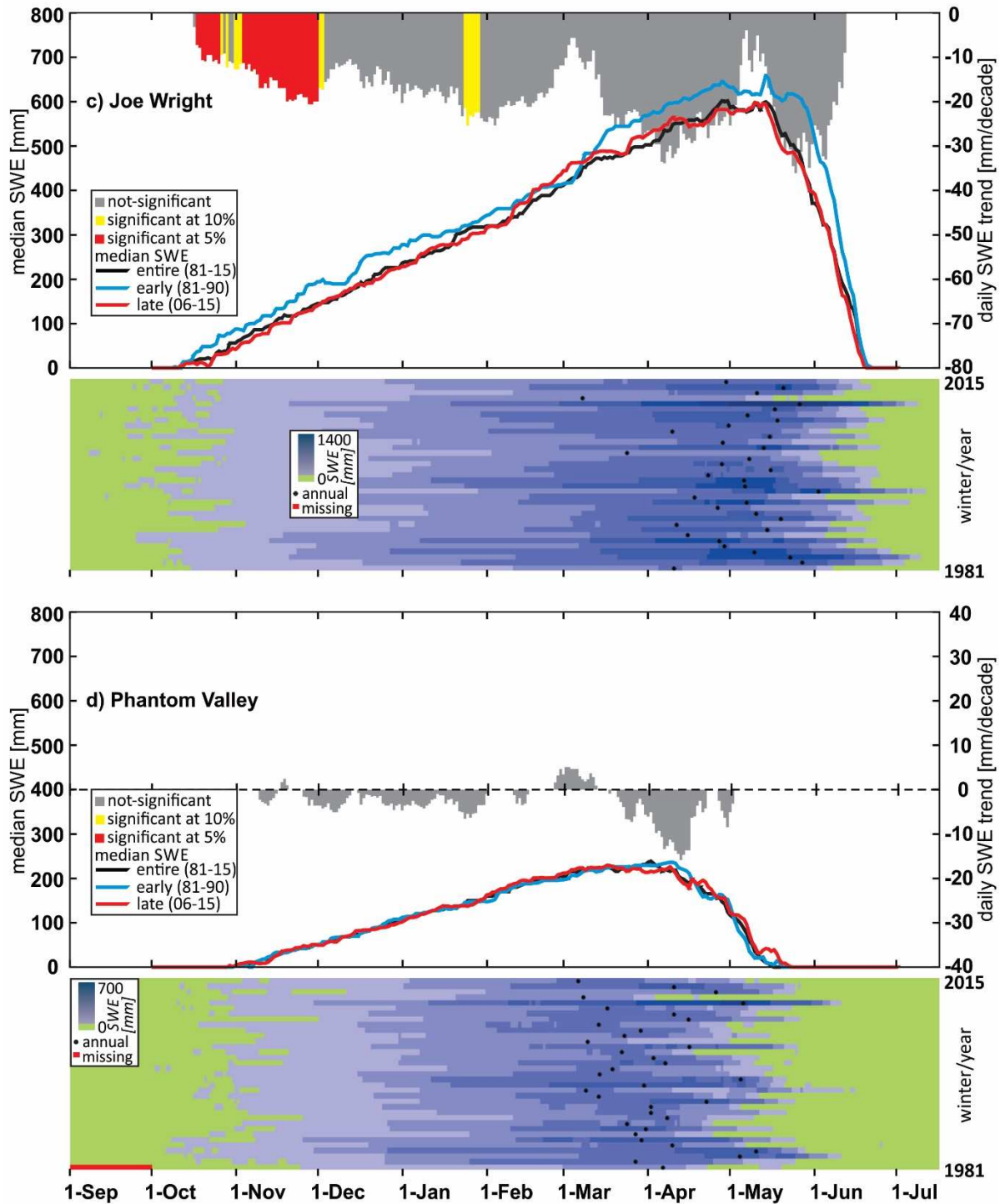


Figure 4.10. Daily SWE trends for a) Joe Wright SNOTEL, and b) Phantom Valley SNOTEL, in relation to median daily SWE for entire period of record, and for early and late segments of the record. Also shows raster plots of daily SWE for each year, 1981-2015. “Annual” dot denotes annual peak SWE.

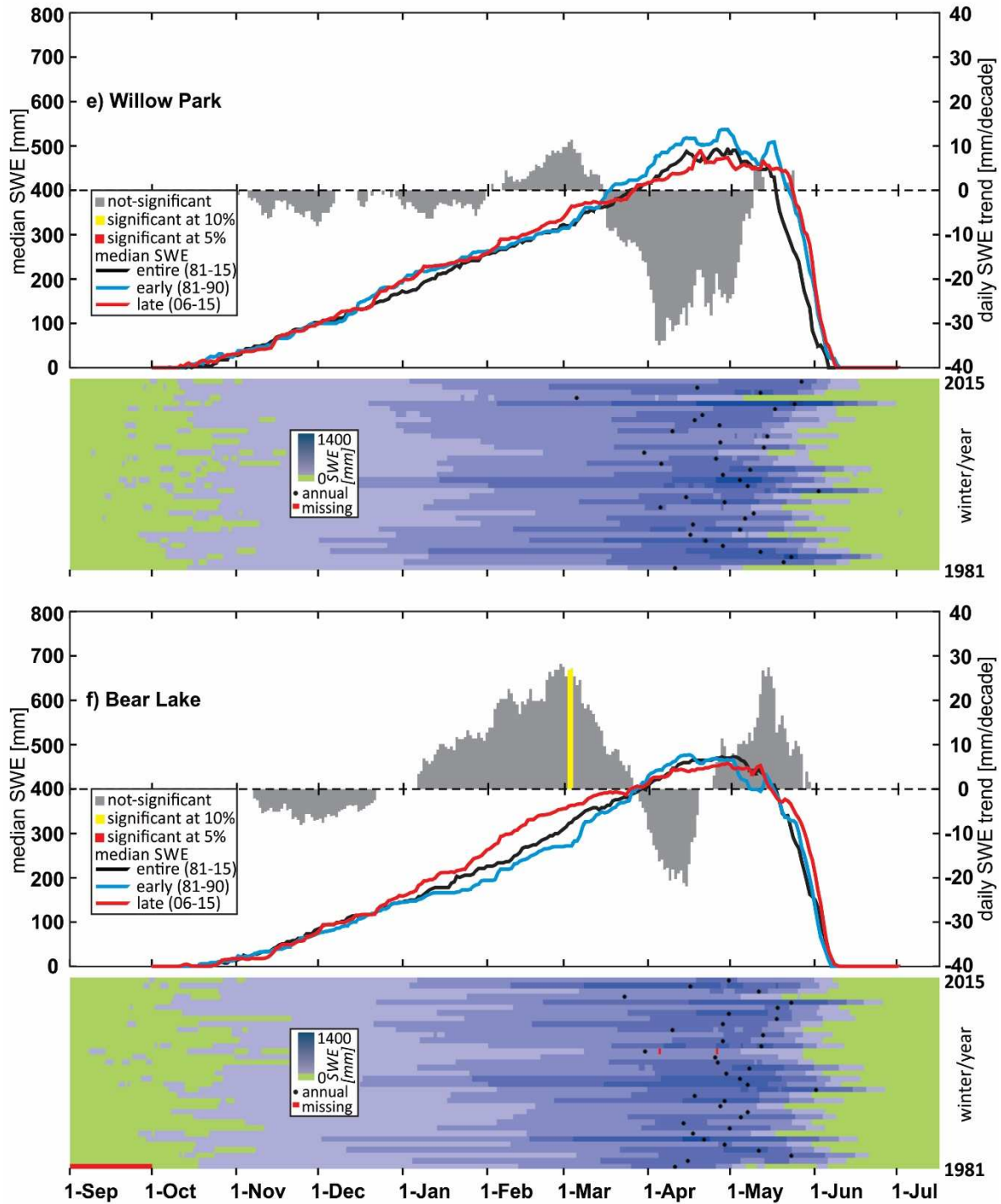


Figure 4.11. Daily SWE trends for e) Willow Park SNOTEL, and b) Bear lake SNOTEL, in relation to median daily SWE for entire period of record, and for early and late segments of the record. Also shows raster plots of daily SWE for each year, 1981-2015. “Annual” dot denotes annual peak SWE.

As at Lake Irene, at Joe Wright all of the daily SWE trends were negative, varying from 0 to -35 mm/decade (Figure 4.10a). The pattern was similar to Lake Irene, with the greatest negative trends during early April and late May, and the least negative trends during early March and early May. Significant decreasing trends occurred during October, November, and January at Joe Wright.

At Phantom Valley daily SWE trends had lesser magnitudes and fluctuated between negative and positive (-15 to +5 mm/decade) (Figure 4.10b). The pattern was similar to the other stations, with greatest positive trends in early March, and greatest negative trends in early April. None of these trends were statistically significant.

At Willow Park trends fluctuated in a similar pattern to Phantom Valley, but reached greater negative values (about -35 mm/decade) during early April (Figure 4.11a). None were significant.

At Bear Lake the trends, which were not significantly significant, fluctuated in a similar pattern, with a greater range, from about -35 to about +35 mm/decade (Figure 4.11b). Trends were negative in November and early December, positive from early January to late March, negative from late March to late April, then positive again for the rest of the snow season.

The variability in these daily trends often occurred on time scales of a few days or weeks, creating patterns of variability that could not be discerned using monthly SWE data. Reversals in sign of daily SWE trends frequently took place over a few days, and peaks and valleys in the patterns were sharp, often of just a few days' duration. At all six stations, whether the trends were negative or positive, they decreased from late February through early April, becoming less positive or more negative. At the five stations with niveographs extending later than early April,

the trends increased again through early May, followed by a final decrease at the end of the snow season.

The niveographs in Figures 4.9 – 4.11 illustrate changes in patterns of SWE accumulation and ablation that reflect the above-mentioned daily trends. Each graph has three niveographs, one for the entire 35-year period, one for the first ten years (1981-90), and one for the most recent ten years (2006-15). At all stations except for Copeland Lake, the early-period niveograph exceeded the late-period niveograph beginning around early to mid-March and lasting through mid-April or later.

Trends in number of days per year with over 100 mm of SWE at SNOTEL stations during the period 1981-2015 were mostly negative, with 9 decreasing trends, 3 increasing trends, and one zero trend (Figure A.14). Higher elevation stations had uniformly decreasing trends, while lower elevation stations had mostly increasing trends. The orange and purple clusters had similar trends, mostly negative but one or two trends that were zero or positive.

Trends in the number of days per year with SWE accumulation or ablation in excess of 10, 5, and 0 mm were also mixed (Figure A.15). The higher elevation stations tended to have trends toward fewer days with accumulation in excess of 5 and 10 mm, while the lower elevation stations tended to have trends toward more days with such accumulation. Stations at all elevations tended to have trends toward more days with ablation exceeding 0 and 10 mm. The trends in number of days with accumulation and ablation in excess of the lowest amount (0 mm) were the most statistically significant. When grouped by cluster, the orange cluster had slightly more increasing trends in days with both accumulation and ablation exceeding the thresholds. The purple cluster had a strong preponderance of increasing trends, especially for ablation.

4.2 Estimation of Daily Niveographs from Snow Course Data

Testing of the niveograph estimation technique described in Chapter 3, Section 3.2, resulted in interpolated niveographs for Willow Park and Lake Irene for the period 1981-2012. The niveograph estimation model performed adequately in approximating the observed daily niveographs at the two sites selected for the tests (Table 4.1, Figure A.16). In all six tests (low, medium, and high SWE years at the two sites), the shape of the estimated niveograph gave a close approximation to the shape of the observed niveograph. Also, the magnitude and timing of the peaks of the estimated niveographs matched fairly closely the observed values. Extending the peak phase and delaying the melt phase for the two high-SWE years when SWE was still increasing on 1 May helped to match the estimated niveographs to the observed ones for those years.

Table 4.1. Performance measures for niveograph estimation model compared to assumption of annual peak SWE on April 1.

Measure of Model Performance	Peak SWE		Date of Peak	
	Model	1-Apr	Model	1-Apr
NSCE of Model	0.922	0.1	0.589	-1.113
Mean absolute value of % diff, model-observed [%]	6.34	21.86	10.00	23.87

In comparison to the assumption that 1 April SWE represents the annual peak, these estimated niveographs were more accurate in simulating the magnitude and timing of the annual peak. The estimated niveographs underestimated the peak by an average of 4.2 percent, while the 1 April assumption underestimated the peak by 19.6 percent (Figure A.17). The estimated niveographs averaged 1.7 days early for the timing of the peak, while the 1 April assumption averaged 19.5 days early for the peak (Figure A.18). The mean differences between modeled

and observed peak SWE, date of peak SWE, and total SWE accumulation during the year, were -4.8 percent, -1.4 percent, and -22.0 percent, respectively.

4.3 Trends in Precipitation

Precipitation in the study area is well distributed throughout the year, yet April and May typically have higher monthly precipitation (Figure A.19). There is a strong elevation dependency to the distribution of precipitation, with higher sites receiving more than twice as much precipitation as lower sites (Figure A.20). Precipitation trends, however, had a different relation with elevation. For example, trends in total cold-season snowfall equivalent (sum of accumulation of SWE) tended to be negative at higher elevation sites, and positive at lower elevation sites (Figure A.21).

Monthly trends in precipitation at the six SNOTEL stations have the same general pattern (Figure 4.12). October tended to have weak trends for precipitation, snowfall equivalent (SFE), and fraction of precipitation represented by SFE. November had significant decreasing trends in precipitation and SFE, indicating trends toward warmer and drier conditions. December, January, and February had moderate to strong increasing trends in precipitation, SFE, and fraction of precipitation represented by SFE, indicating trends toward colder and wetter conditions. March had strong decreasing trends in precipitation, indicating a trend toward drier conditions, and no trend or decreasing trends in SFE. March had increasing trends in fraction of precipitation represented by SFE at three of the four stations, and a slight decreasing trend in this fraction at Willow Park. During April trends again became positive for precipitation (except at Phantom Valley), and for SFE, and were mixed for fraction, indicating a trend toward wetter conditions. During May trends were mixed with generally small trends.

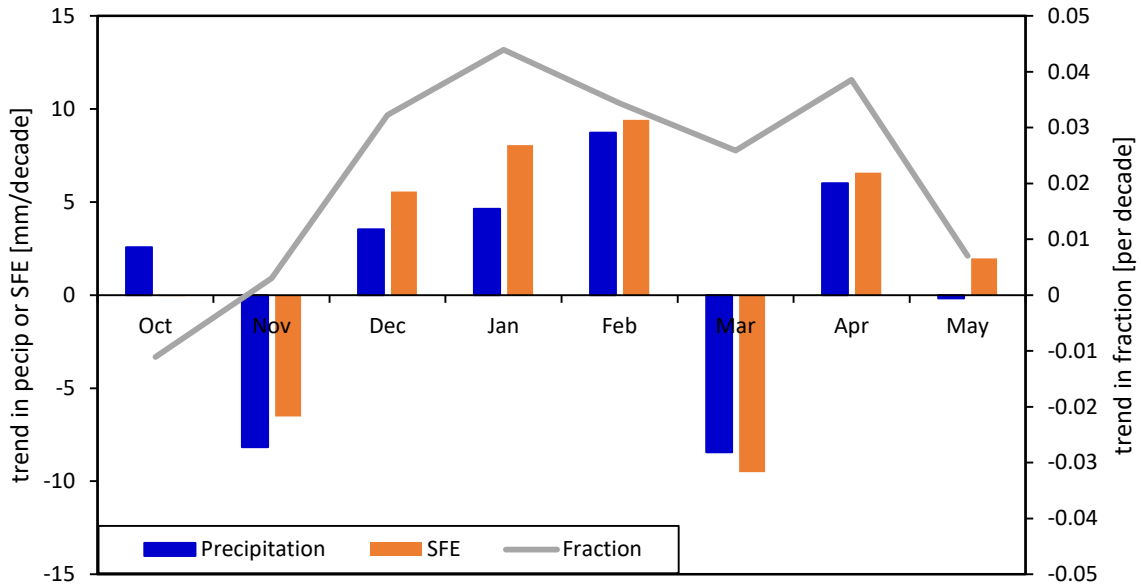


Figure 4.12. Trends in monthly precipitation, snowfall equivalent (SFE), and ratio of SFE to precipitation, 1981-2015, averaged from 6 SNOTEL stations.

Based on the technique used by Mote *et al.* (2003), trends in April 1 SWE at the SNOTELS were plotted as circles with diameters proportional to the SWE trends, along a pair of axes representing trends in total October-June precipitation and average October-June temperature at the SNOTEL stations (Figure A.22). Results showed that variations in precipitation trends had a stronger influence on trends in April 1 SWE than did variations in temperature.

4.4 Trends in Temperature

The three temperature stations exhibited a normal pattern of seasonal variation in average monthly temperature (Figure 4.13a). They also exhibited a normal pattern of cooler temperatures at higher elevation, as seen at Loch Vale. For the period 1981-2015 (1983-2015 at Loch Vale), the three temperature stations showed warming trends ranging from 0 to 0.28°C/decade (Table 4.2, Figure A.23). The annual time series showed typical inter-annual variations, but the general warming trend appeared to be relatively consistent throughout the 35 (33)-year period (Figure A.23).

Table 4.2. Trends in average annual temperature at three weather stations.

	Trend in average annual temperature [degrees C/decade]		Level of significance if any
	Linear	Theil-Sen	
Allenspark	0.17	0.20	
Grand Lake	0.23	0.28	p<0.01
Loch Vale	0.06	0.00	

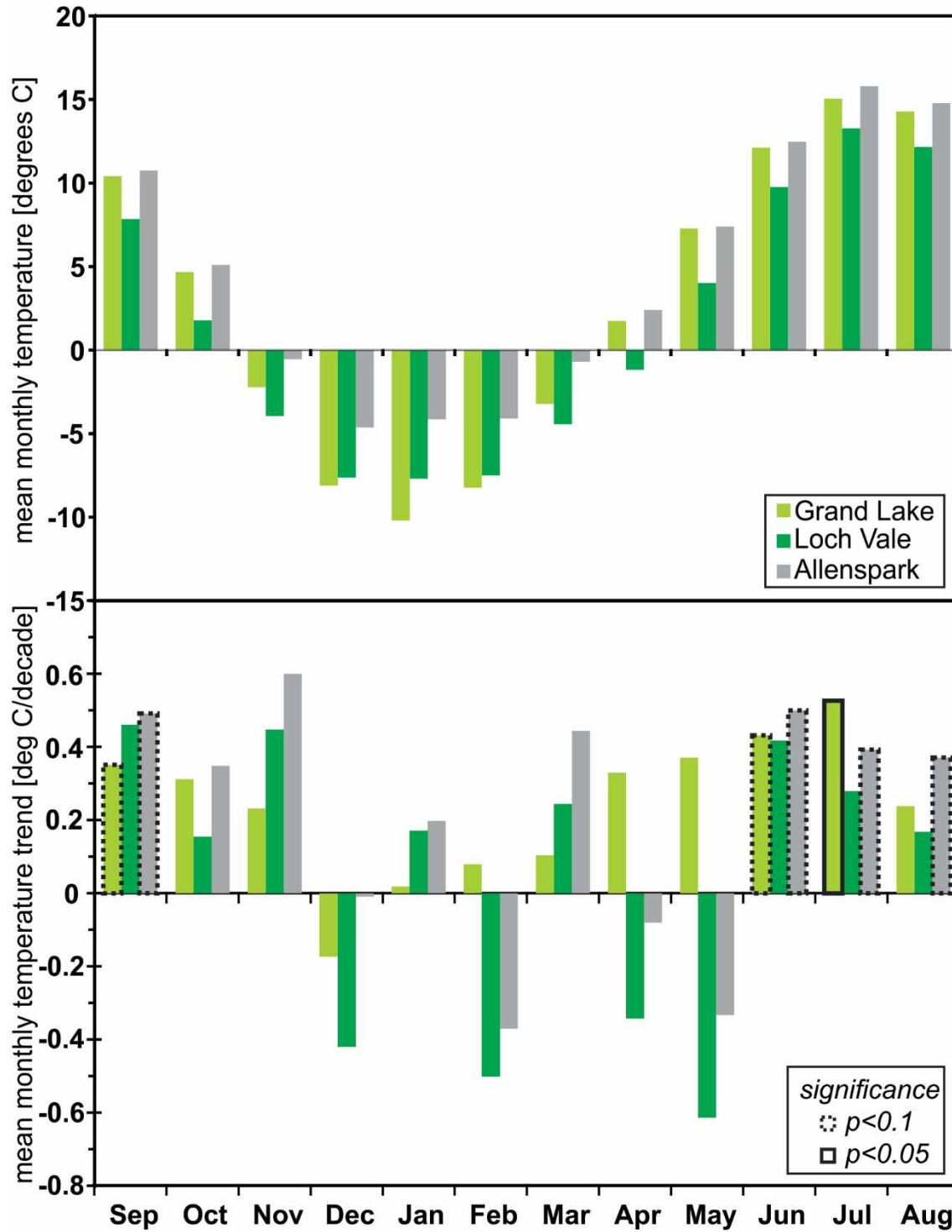


Figure 4.13. a) Average monthly temperature at 3 weather stations, and b) trends in average monthly temperature, 1981-2015.

The longer temperature record at Grand Lake enables us to evaluate the temperature trend at that station over a longer period from 1949 to 2015 (Figure A.24). While a single trend over the entire period is increasing, the declining, then increasing pattern of the data suggest that it would be appropriate to separate the longer period into two distinct shorter periods. The trend during the period 1949 to 1975 was decreasing, showing a cooling trend, and the trend during the period 1981 to 2015 was increasing, showing a warming trend (Figure A.24).

Trends in monthly average temperature at these three stations over the period 1981-2015 show substantial variability among months (Figure 4.13b). Consistent warming trends at all three stations were noted during eight months: September, October, November, January, March, June, July, and August. Rates were as high as $0.60^{\circ}\text{C}/\text{decade}$ in November at Allenspark. Grand Lake had warming trends in every month, although those for December and February were the smallest, around $0.10^{\circ}\text{C}/\text{decade}$. Seven of the monthly warming trends were statistically significant. At Allenspark and Loch Vale, cooling trends were present during December, February, April, and May, with rates as high as $-0.60^{\circ}\text{C}/\text{decade}$ in May at Loch Vale. The decreasing trend in May at Loch Vale was statistically significant.

4.5 Trends in Freezing Level

Simulated free-atmosphere average monthly freezing-level elevations were retrieved from the North American Freezing Level Tracker for the seven coldest months of the year (November through May) for each year during the 35-year study period (1981-2015). The averages of these monthly simulated freezing levels showed a typical seasonal trend of decreasing early in the winter, then increasing freezing level later in the snow season (Figure 4.14a). The average freezing levels for November and March both were about 500-600 m

below the bottom of the elevation zone containing the SNOTEL stations. Freezing levels for December, January, and February were well below this level, and freezing levels for April and May were above this level. Trends in monthly freezing level (Figure 4.14b) were upward (warming) in all months except February, which had a slight downward (cooling) trend. The strongest upward trends, about 160-170 m/decade, were in November and March.

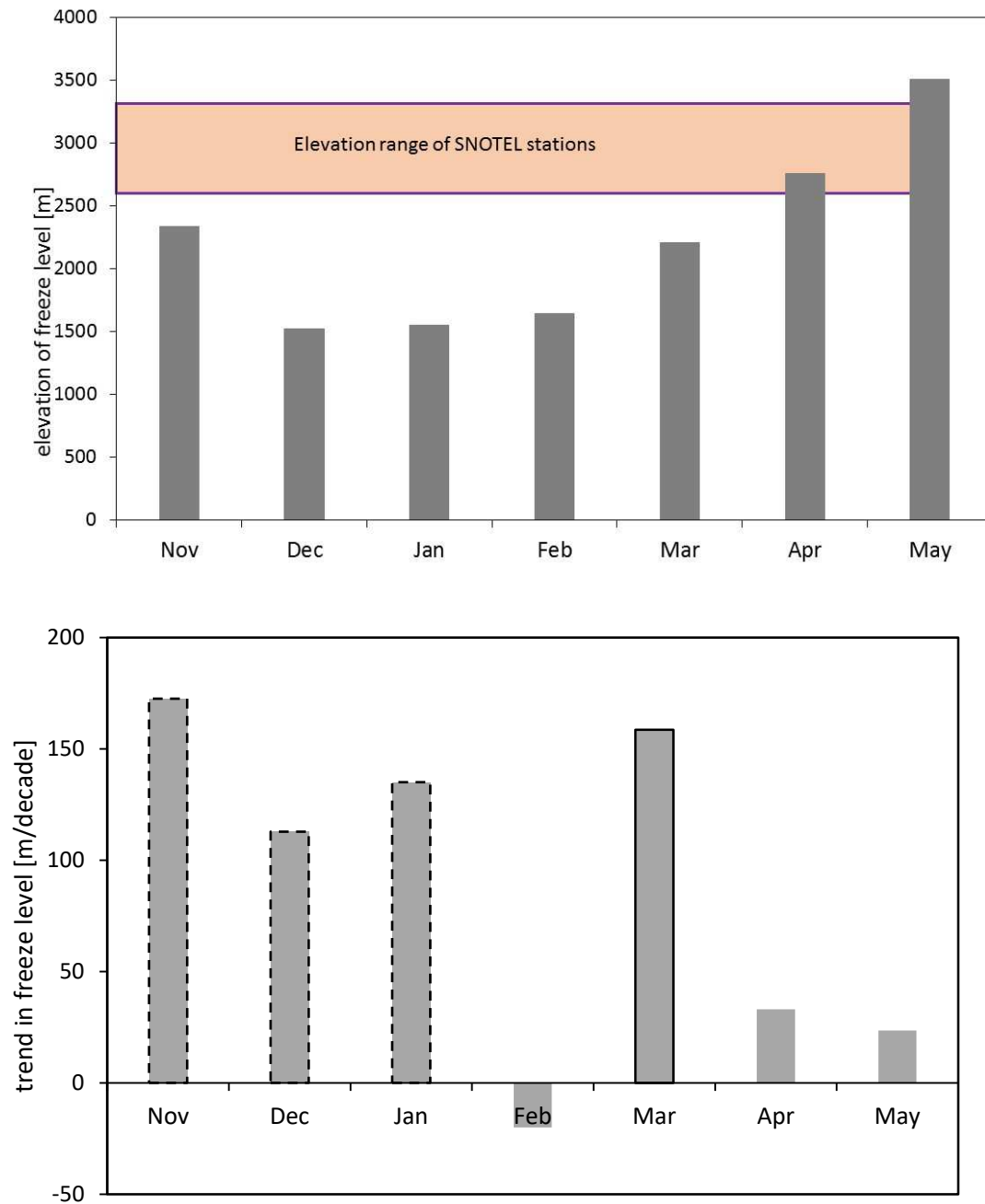


Figure 4.14. a) Average monthly elevation of freeze level (zero-degree isotherm), 1981-2015, and b) trends in elevation of freeze level.

Results of the analysis of warmer-then-freezing weather at Lake Irene and Copeland Lake showed consistent seasonal patterns for the two SNOTEL stations, with Copeland Lake having

about 100-200 more maximum-daily degrees each month than Lake Irene (Figure A.25a). At both stations, November and March had similar values for this measurement. Analysis of trends in these monthly maximum-daily degree totals over their respective periods of record (1986-2015 for Lake Irene, 1989-2015 for Copeland Lake), showed that November had the strongest increasing trend at both stations (Figure A.25b). January, March, and July also had increasing trends, while October, February, and May had decreasing trends.

4.6 Paleoclimate SWE Reconstructions

The three selected SWE reconstructions, with their equations, coefficients of determination, and Nash-Sutcliffe coefficients of efficiency, are listed in Table 4.3. The tree-ring chronologies used for the reconstructions are listed in Table A.1. An example of the fit of one of the equations, for April 1 SWE at the North Inlet Grand Lake snow course, is shown in Figure 4.15. The reconstructed and moving 35-year linear trends in SWE estimates for North Inlet based on these equations are shown in Figures 4.16 and 4.17. Similar SWE reconstructions and moving 35-year trends for Cameron Pass and Longs Peak are shown in Figures A.26 through A.29. While there is greater variability in the observed (historical) SWE compared to the reconstructed SWE, the same pattern exists. The recent observed decrease in SWE at a rate of almost 40 mm/decade at North Inlet of Grand Lake has occurred during the paleo-record, specifically around 1610 (Figure 4.17, Table 4.3), and an even larger increase (~75 mm/decade) may have occurred around 1580.

Table 4.3. Results of trend analysis of paleo-SWE reconstructions based on tree rings.

Location	Reconstruction date	Equation	Fit statistics		Comparable trend present?
			R ²	NSCE	
North Inlet Grand Lake	April 1	26.1PUM + 126HOT + 26.1BTU + 49.6	0.29	0.29	Decrease ~1610 Increase ~1580
Cameron Pass	May 1	162GMR + 202NPU + 355	0.42	0.4	No
Longs Peak	May 1	101GMR + 53.5ENC + 36.2HOT + 85.2BTU + 65.4STU + 0	0.53	0.52	Decrease ~1830

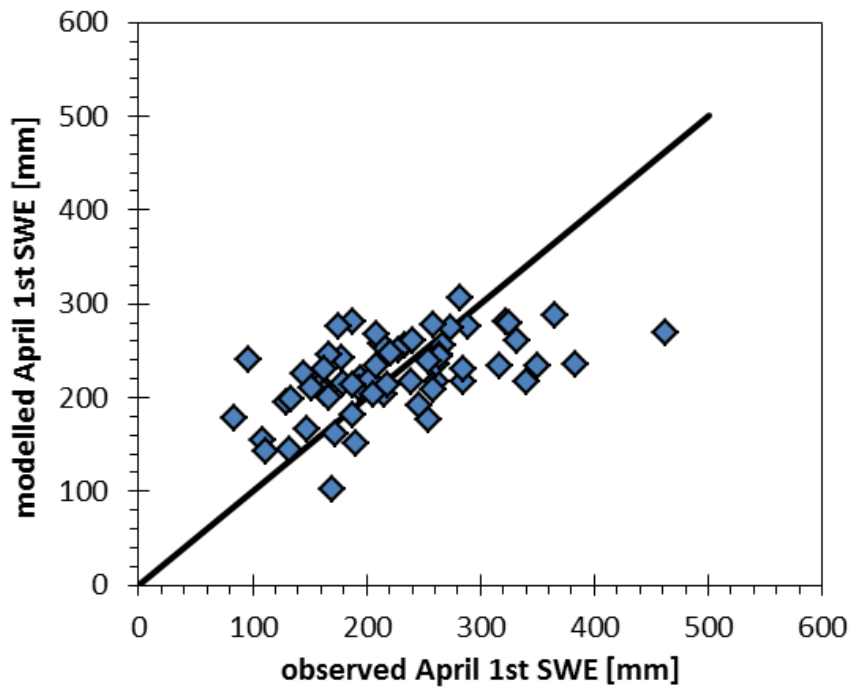


Figure 4.15. Correlation between the modeled (tree ring estimated) and observed April 1st SWE for the North Inlet of Grand Lake snow course. Data were for the period 1938 (start of snow course) to 1999 (end of tree ring chronology).

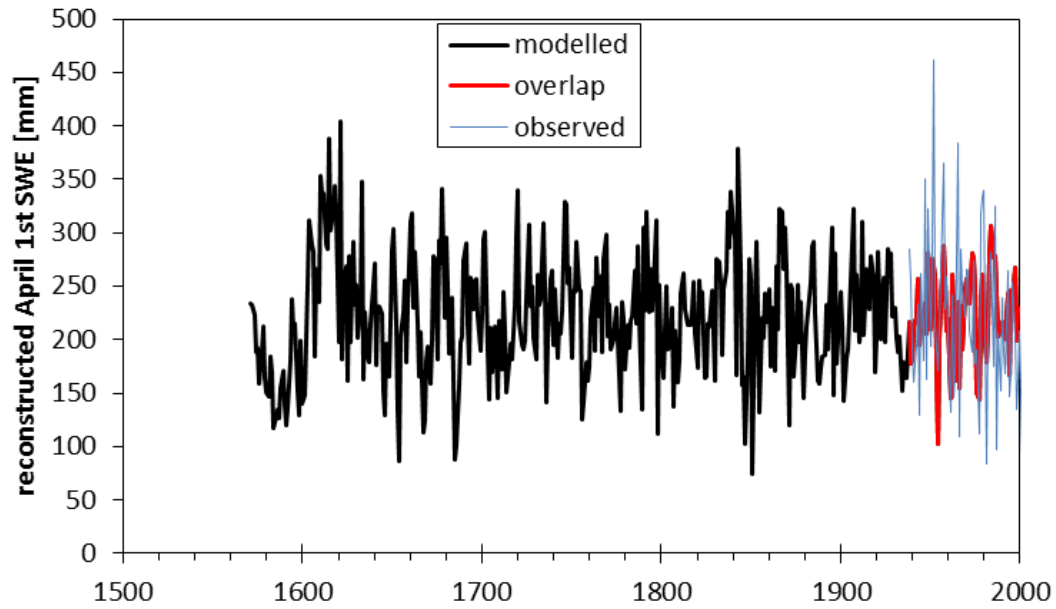


Figure 4.16. North Inlet of Grand Lake April 1st SWE reconstruction from 1571 to 1999.

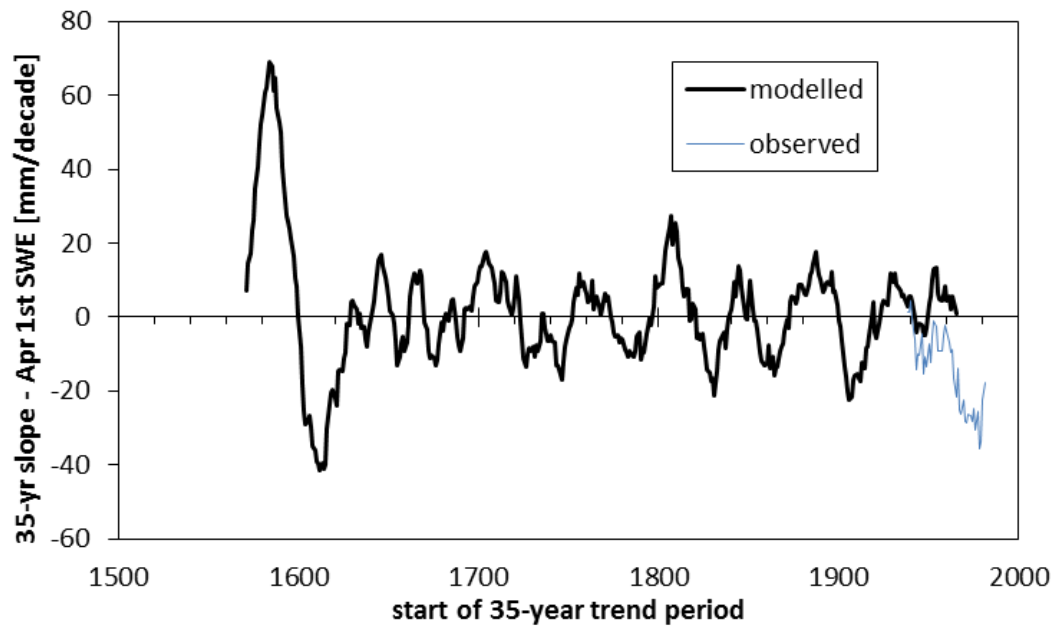


Figure 4.17. Slope over 35-year time period for the reconstructed and observed (historical) April 1st SWE at North Inlet of Grand Lake snow course.

The above method was applied to the May 1st SWE at Cameron Pass (Figure A.26) and Longs Peak (Figure A.28) to yield different results (Figures A.27 and A.29). Specifically, the Cameron Pass SWE trends in the recent 80 years are unprecedented compared to the paleo-record (Figure A.27), while more extreme 35-year trends may have occurred at Longs Peak around 1830 (Figure A.29).

4.7 Projections of Future Temperature, Precipitation, and SWE

The nine 1/8 by 1/8 degree pixels for which CMIP5 climate model projections were retrieved had median elevations ranging from 2639 to 3430 m (Figure A.30). The range of these median elevations closely matches the elevation range of the snow courses and SNOTEL stations. The distribution of elevations within the pixels is shown in Figure A.31.

Projections from the climate models were examined to determine how closely they match observed trends in temperature, precipitation, and SWE during the study period, and to provide estimates of future conditions. The temperature projection of the ensemble average of CMIP5 climate models was made using projected values for monthly minimum temperature, as average temperatures were not available. The projected warming during the period 1981-2015 was about 1.2°C, or 0.34°C/decade. This is a faster rate of warming than the rates seen for average annual temperature at the stations used in the study, which ranged from 0.004 to 0.35°C/decade (Figure A.23). The ensemble mean projection for future increase of the average of monthly minimum temperatures during 2015-2099 was about 2.0 degrees, or 0.24°C/decade. This projected warming rate is similar to observed rates at the lower elevation stations in the study area. In the model projections, all months had similar warming trends. In contrast, the observed temperature trends varied monthly (Figure 4.13b).

The projection for annual precipitation from the ensemble average of CMIP5 climate models for the period 1981-2015 was similar to the observed annual precipitation at the centrally located Willow Park SNOTEL station, but the models did not display the inter-annual variability observed at the station (Figure A.32). On a monthly basis, the patterns of simulated and observed average monthly precipitation values were similar (Figure A.33). Trends in monthly precipitation also agreed in terms of direction of change for most months, with the exceptions of November and March (Figure A.34). In these two months the modeled trends projected increasing precipitation while the trends at the station were toward decreasing precipitation.

Average annual precipitation trends projected into the future by the CMIP5 model ensemble for the period 2015-2099 showed slightly increasing trends, averaging about 6.0 mm/decade. On a monthly basis, the projected monthly trends showed a slightly different pattern from the simulated 1981-2015 trends (Figure A.35). These future trends emphasized increasing precipitation in the early part of the snow season through December, and much smaller increases, or decreases, in trend for the remainder of the snow season, through June.

Projections of SWE from the Variable Infiltration Capacity (VIC) hydrologic model linked to the ensemble CMIP5 climate models showed some notable differences compared with observed values. The models simulated slower accumulation and a later and lower peak SWE compared to observed SWE at Willow Park (Figure A.36). Simulated April 1 SWE was much less than observed, by about 200 mm, with much less inter-annual variability. On a monthly basis, there is little similarity between the simulated and observed trends in SWE, in both magnitude and direction. Average annual SWE trends projected into the future by the CMIP5 model ensemble showed a continued zero to slightly decreasing trend in April 1 SWE for the period 2015-2099, averaging only -2.0 mm/decade.

Examination of projections of individual CMIP5 models, rather than the ensemble mean of all of the models, showed that one model, IPSL model (see Chapter 2), computed April 1 SWE patterns that were similar to the declining trends noted at many of the snow courses and SNOTEL stations in this investigation, as illustrated over a 65 year period at the Longs Peak snow course (Figure 4.18). As the observed trend in April 1 SWE at Longs Peak during 1951-2015 of -9.6 mm/decade is very similar to the average April 1st trend at all of the snow courses of -10.2 mm/decade, it was used to compare with IPSL results. The observed April 1 SWE time series at Longs Peak was very similar to the IPSL model during the period from 1951 to 2015 (Figure 4.18). The trend simulated using the IPSL model through 2099 has a slope of -7.2 mm/decade, according to the linear best-fit trend line.

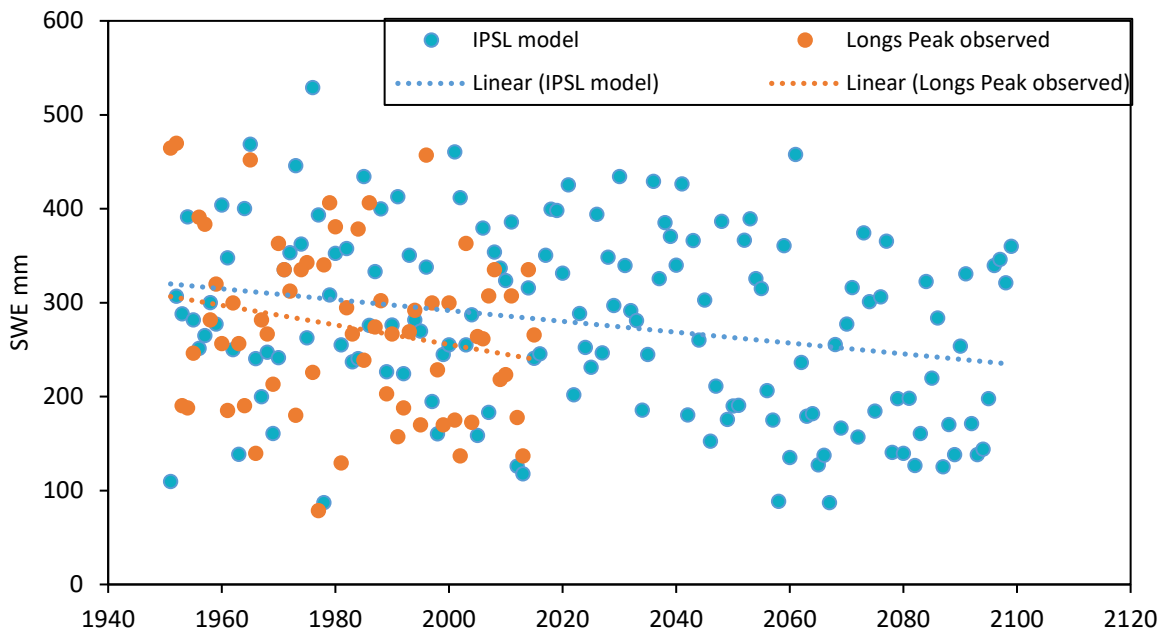


Figure 4.18. Comparison of trends in April 1 SWE between observed Longs Peak snow course data and IPSL model.

The monthly distribution of SWE trends for the period 1981-2015, simulated by the IPSL model, has a few important similarities with observed SWE trends from snow courses and SNOTEL stations (Figure 4.19). Both the simulated and observed monthly SWE trends show a general pattern of more SWE accumulation, or less SWE loss, during the early part of the snow season, and greater SWE loss during the latter part of the snow season, particularly March through May. IPSL model projections through 2099 suggest that trends toward SWE loss will intensify in all cold-season months and expand into the early part of the snow season (Figure 4.20).

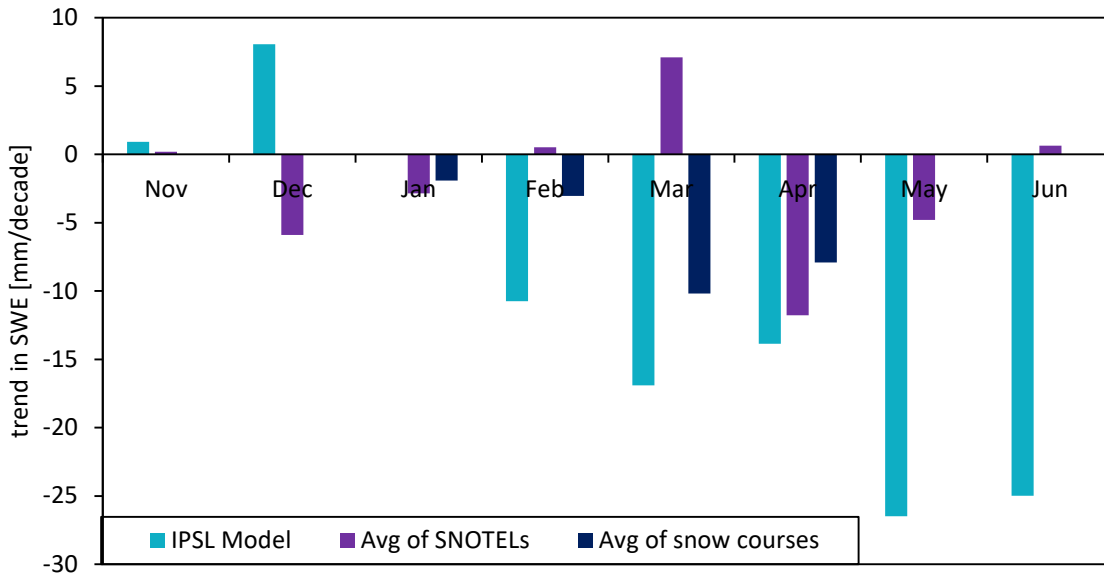


Figure 4.19. Trend in first-of-month SWE, 1981-2015, simulated by IPSL model and observed averages at SNOTELs and snow courses.

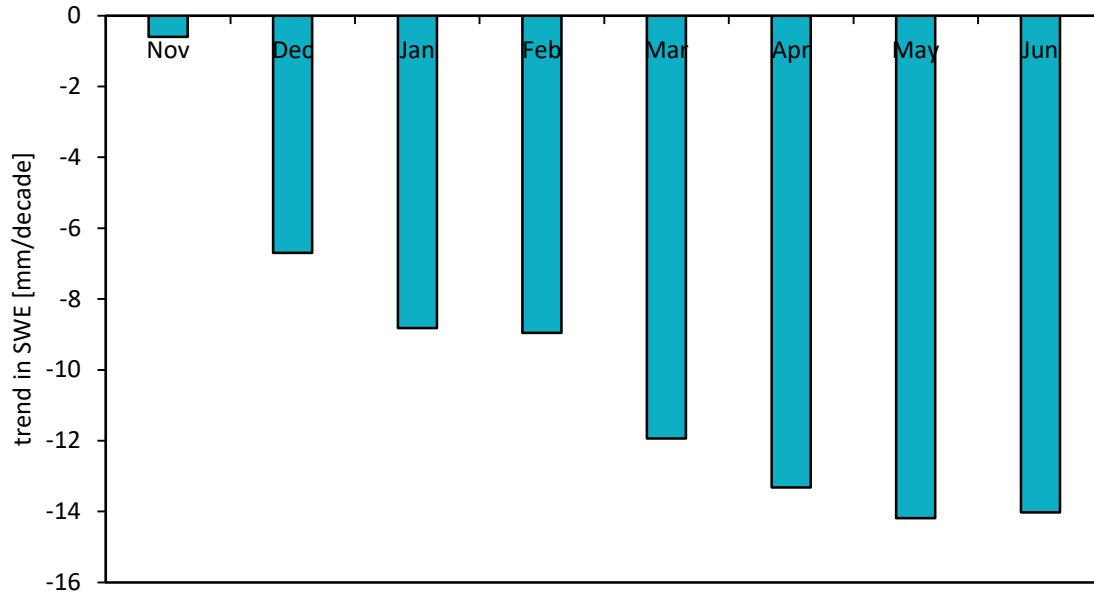


Figure 4.20. IPSL model projections for trends in first-of-month SWE, 2015-2099.

CHAPTER 5. DISCUSSION

5.1 Trends in Snow Water Equivalent

5.1.1 *Variability in Annual Measures of SWE*

Evaluating trends in an annual time series of data involves making a distinction between inter-annual variability and long-term trends (Bradley *et al.*, 2007; Venable *et al.*, 2012). In general, longer time series produce more accurate estimation of trends than shorter ones. Time series shorter than 15 years were found to produce inaccurate estimates of temperature trends (IPCC, 2013). Precipitation in the western United States is often said to vary according to the double sunspot cycle, which has a period of about 22 years (Vines, 1982; Fu *et al.*, 2012), suggesting that the period for trend analysis of precipitation should exceed 22 years. As temperature and precipitation are the primary factors that influence accumulation and ablation of the seasonal snowpack in the western United States (Hamlet *et al.*, 2005), trends in measures of snowpack accumulation and ablation should also be based on time series that exceed these minimum durations. The availability of SWE data dictates the maximum length of record that can be considered. For example, there are 80 years for the earliest snow courses, such as Wild Basin established in 1936, and 36 years for the first group of SNOTEL stations, such as Lake Irene established in 1980. Fortunately, the latter periods provide annual series of SWE values sufficiently long for meaningful analysis of long-term trends despite the strong inter-annual variability.

In this investigation, the short-term, inter-annual variability in April 1 SWE at a typical SNOTEL station, such as Willow Park, was more closely related to precipitation than to

temperature (Figure A.3). Regression analysis (Figure A.4) showed this greater correlation of April 1 SWE with precipitation than with temperature, indicating that short-term SWE variability, on the order of a few years, in the western United States, and particularly in the colder inland mountains, is primarily related to variability in precipitation. On the other hand, long-term SWE trends, on the order of several decades, are primarily related to trends in temperature (Hamlet *et al.*, 2005; Serreze *et al.*, 1999).

5.1.2 Monthly Trends in SWE

The generally declining trends in snow water equivalent at snow courses and SNOTEL sites in and near Rocky Mountain National Park are consistent with previous studies (see below) that have found trends toward rising temperatures and decreasing snowpack in the region. This study, however, goes further to more closely examine patterns of variability in SWE trends throughout the snow season. For example, this study examined SWE trends in relation to trends in near-freezing temperatures during the months of November and March, near the beginning and end of the core accumulation season, and explored SWE trends in the context of elevation-dependent warming.

Monthly trends in April 1 SWE at snow courses and SNOTEL sites in this investigation ranged from an increase of 20 mm/decade to a decrease of 50 mm/decade, but most trends were decreasing. This is consistent with trends for various recent periods found for the northern Front Range of Colorado (Hamlet *et al.*, 2005, about -2r mm/decade; Regonda *et al.*, 2005, -20 to -40 mm/decade; Clow, 2010, -12 to -27 mm/decade); the Upper Colorado River Basin (Harpold *et al.*, 2012, -10 to -50 mm/decade for annual peak SWE); and the Rocky Mountains from Colorado to British Columbia (Mote *et al.*, 2005, about -1 to -5 mm/decade).

While the average rate of decreasing SWE trend with elevation is similar for most months (slopes in Figure 4.7), the trend lines vary with respect to their location along the x-axis, and hence where they cross the zero line. The lowest y-intercept was approximately 2650m and was for January and April, indicating that in these months most SWE trends were increasing. Conversely, the y-intercept for March 1st is the highest (~3075m), indicating that in March most SWE trends were decreasing. The change in SWE from March 1st to April 1st is evident as March is the month with the most negative trends in change in SWE (Figure 4.6b). The change in SWE over the month of November also decreases at most stations (Figure 4.6b). Thus the months near the beginning (November) and end (March) of the core snow accumulation season are times that have seen the greatest shift toward less accumulation (November) and/or more ablation (March) (Figure 4.8b).

The decreasing trends in March change in SWE are observed over both long-term and short-term time scales, as illustrated in the lower left quadrant of Figure A.5b. All but five of the trends for March change in SWE occur to the left of the 1:1 line in Figure A.5b. This indicates that the pattern of negative trends in March change in SWE was stronger during the period 1981-2015 than during the longer period. Finally, the stronger clustering of trends for March change in SWE in the lower left quadrant in Figure A.5b, compared with the more scattered pattern of April 1 SWE in Figure A.5a, indicates that the negative shift in March change in SWE (less accumulation or more ablation or both) is more pronounced than the trend in April 1 SWE. Since more SWE accumulates during February (Figure 4.6b) and less is still present on April 1, the change in SWE between March 1 and April 1 is accentuated.

Although the negative trend in March change in SWE was stronger during the period 1981-2015 than during the longer period of snow course records, the general pattern of declining

trends in April 1 SWE was slightly stronger over the longer period (Figure A.5a). This suggests that the trend toward increased SWE accumulation during February (Figure 4.6b) may have occurred mostly during the recent 35 years. It also indicates that the general trend toward declining April 1 SWE is consistent over at least 8 decades. This is consistent with an earlier conclusion that the cause of declining trends in April 1 SWE in the western United States is widespread long-term warming, and not decadal climate variability such as would be caused by the cyclical patterns of the Pacific Decadal Oscillation (Hamlet *et al.*, 2005).

At some of the northerly stations, for the longer period of record, there were increasing trends in SWE from the beginning (~1936) to the mid-1970s, followed by a decreasing trend afterwards (Fassnacht and Hultstrand, 2015). This is similar to what Chen and Grasby (2009) hypothesized with synthetic data, but contrary to what Venable *et al.* (2012) found with temperature data.

5.1.3 Other Measures of SWE Derived from Daily Data

The daily time step of SNOTEL stations provides opportunities for examining a variety of measures defining snowpack accumulation and ablation (e.g., Fassnacht *et al.*, 2014), in addition to the traditional measure of SWE on the first of the month. The most obvious measure is annual peak SWE (Figure 3.1). As in an earlier study (Clow, 2010), this investigation did not find a clear pattern of trends in annual peak SWE in this part of Colorado. However, Clow (2010) did find clear declining trends in annual peak SWE in southern and western Colorado. Derry and Fassnacht (2015) found declines in SWE south of 38.75 degrees North latitude, suggesting that weather patterns influencing snowpack development in the north-central mountains of Colorado are probably different from those affecting other parts of the state. Also,

Clow (2010) used a shorter time period (~1987 to 2007) and used bulk trends from the Regional Kendall Test, that Fassnacht *et al.* (2016) illustrated masked local climate trends. One pattern that did emerge in the trends in annual peak SWE is a tendency for high-elevation sites to have declining trends, while low-elevation sites had increasing trends (Figure A.6a). This is consistent with studies that have found a tendency for more rapid warming at higher elevation (Diaz and Eischeid, 2007; McGuire *et al.*, 2012). It is also consistent with trends toward greater April and May precipitation at SNOTEL sites in the study area (Figure A.19).

The combination of increasing and decreasing trends for date of annual peak SWE (Figure A.6b) found in this investigation are consistent with the finding of little change in date of peak SWE (Harpold *et al.*, 2012). They are also mostly consistent with the finding of limited trends toward earlier peak SWE on the western side of the Front Range and later peak SWE on the eastern side, as well as towards an earlier peak SWE at warmer (lower) sites (Hamlet *et al.*, 2005).

Comparison of annual peak SWE with April 1 SWE (Figure A.7) confirms the earlier finding that April 1 SWE can significantly underestimate annual peak SWE (Bohr and Aguado, 2001). In this investigation the difference averaged 22 percent, a much larger difference than the 12 percent reported in the earlier study. This reflects the fact that SNOTEL stations in the study area include many of the higher, colder, and snowier stations in the state, but the result is also affected by the outlier of Copeland Lake, a low-elevation SNOTEL station where the median date for annual peak SWE is as early as March 6. Using May 1 SWE to estimate annual peak SWE would a better approximation for most of the sites in this study area, but would still average 7 percent less than actual peak SWE.

5.1.4 Patterns in SWE Trends

The day-by-day analysis of SWE trends shows both similarities and differences among SNOTEL stations (Figures 4.9 - 4.11). At most stations, the trend on most days is toward less SWE, but at some stations, such as Bear Lake and Copeland Lake, most or all days have positive trends in SWE. The climatic influences on these daily SWE trends involve monthly patterns of trends in temperature and precipitation (Figure 5.1). This pattern of different climatic forcing mechanisms controlling snowpack accumulation and ablation at different times of the snow season has been noted in previous studies (Knowles *et al.*, 2006). In some months such as November and March, decreasing precipitation and increasing temperatures combine to reduce SWE accumulation. In others, such as December, February, April, and May, the reverse is true, resulting in positive trends in SWE change. During January, precipitation and temperature trends are both increasing, and apparently the increasing precipitation trend outweighs the temperature trend. The apparent discrepancies between SWE and change in SWE in December and April are explained by the strong negative trends in SWE during the preceding months, November and March, respectively. These strong negative antecedent trends mean that the SWE trend in the following month can still be negative, even while the trend in change in SWE can be positive, since the SWE change is measured from an increasingly lower base.

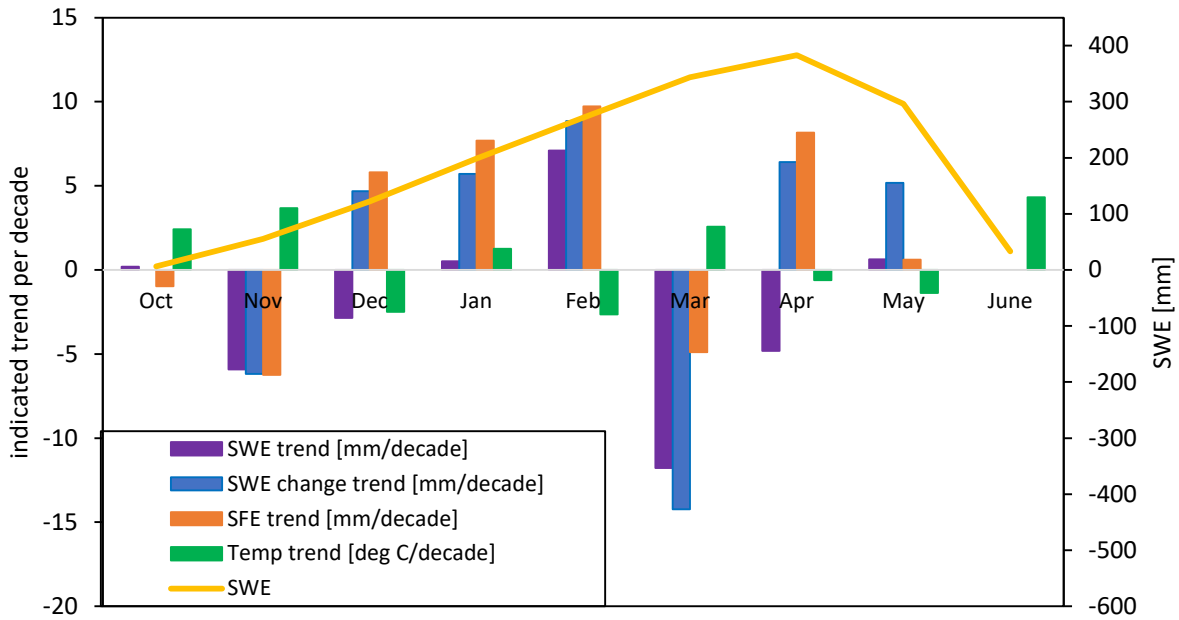


Figure 5.1. Average trends in SWE, monthly change in SWE, SFE, and temperature, by month.

The fluctuating pattern of greater decrease or less increase in SWE during November; less decrease or greater increase during December to early March; greater decrease or less increase during mid-March to early April; less decrease or greater increase during mid-April to early May; and finally greater decrease or less increase during mid-May to June, is consistent at the six SNOTEL stations analyzed in detail (Figures 4.8 and A.9 – A.11). This suggests that the pattern of climatic forcing mechanisms described above is consistent across the study area.

5.1.5 Trends in Number of Days per Year with Threshold Accumulation and Ablation Values

Five of the SNOTEL stations have trends toward slightly fewer days per year with SWE accumulation exceeding 10 mm (Figure A.15). The two that had positive trends, which were the only statistically significant trends, were Deadman Hill and Copeland Lake, both of which had positive trends. These stations are both on the eastern side of the Front Range (in Clow's purple grouping), and frequently receive snow from upslope storms that bring moisture from the east up into the Front Range. This further explains the positive SWE trends at Copeland Lake.

Trends in days with accumulation exceeding 5 mm were mostly positive, but none were statistically significant. Trends in days with accumulation exceeding 0 mm were all positive, and almost all statistically significant. The daily SWE increases during those times are mostly less than 5 mm, as seen by the difference in significant trends for the 0 and 5 mm threshold. This consistent pattern of increasing trends in number of days with small increases in accumulation is likely a reflection of the trends toward increased snowfall equivalent and increased SWE accumulation during December, January, February, and April (Figure 5.1). An alternate explanation, however, could be increased variability, or noise, in sensor readings (Avanzi *et al.*, 2014.) Trends toward ablation also increased. Nearly all of the trends in days with ablation exceeding these three thresholds are positive (meaning more loss of SWE). The lowest threshold, 0 mm, has the most significant trends, while the highest threshold, -10 mm, has the least significant trends. This may indicate that more ablation is occurring in small daily amounts, but can also include increased sensor noise.

5.2 Niveograph Interpolation from Snow Course Data

The technique of model adjustment using time pro-rated multipliers provides a simple method that allows the model niveographs to be bent and shaped to closely match the observed monthly data. As there is also significant interannual variability in the specific shape of the niveograph, this flexibility to bend the model to fit each year's data helps to improve overall accuracy. The close fit between adjusted niveograph models based on daily niveographs at four index SNOTEL stations and observed daily niveographs at Willow Park and Lake Irene suggest that SNOTEL records can be used to estimate daily niveographs at nearby snow courses. The estimation technique is improved if the peak phase is extended and the melt phase delayed for years when SWE is still increasing on 1 May. The validity of the estimation technique is expected to diminish with increasing distance between the SNOTEL stations and the snow course site. The interpolated niveographs were found to produce improved accuracy in estimates of annual peak SWE compared with the assumption that the peak occurred on April 1 (Patterson and Fassnacht, 2014).

5.3 Trends in Precipitation

While the pattern of monthly trends in precipitation helps to explain the observed trends in SWE, the magnitudes of the precipitation trends observed in this study, on the order of 10 mm/decade, are small compared with trends observed in other parts of the western United States, which exceed 30 mm/decade (Mote, 2003; Regonda *et al.*, 2005). This is consistent with other studies that have found little change in precipitation in this part of Colorado (Hamlet *et al.*, 2005; Ray *et al.*, 2008; Lukas *et al.*, 2014). The time series of total cold-season (October to June) precipitation for the Willow Park SNOTEL station during 1981-2015, when smoothed

with a 4-year moving average, appears to follow a cyclical pattern that might indicate a correlation with the 11-year solar magnetic activity cyclical (Figure 5.2) (NASA, 2016). This would indicate a different source of influence on local precipitation, compared to the influence of sea-surface temperature cycles that was noted for locations closer to the ocean in the western United States (Hamlet, 2005). For example, the Willow Park precipitation record does not synchronize with the Pacific decadal oscillation, which exhibits a positive phase during the 1985 positive precipitation phase, but also a negative phase during the 2005 positive precipitation phase NOAA, 2016b).

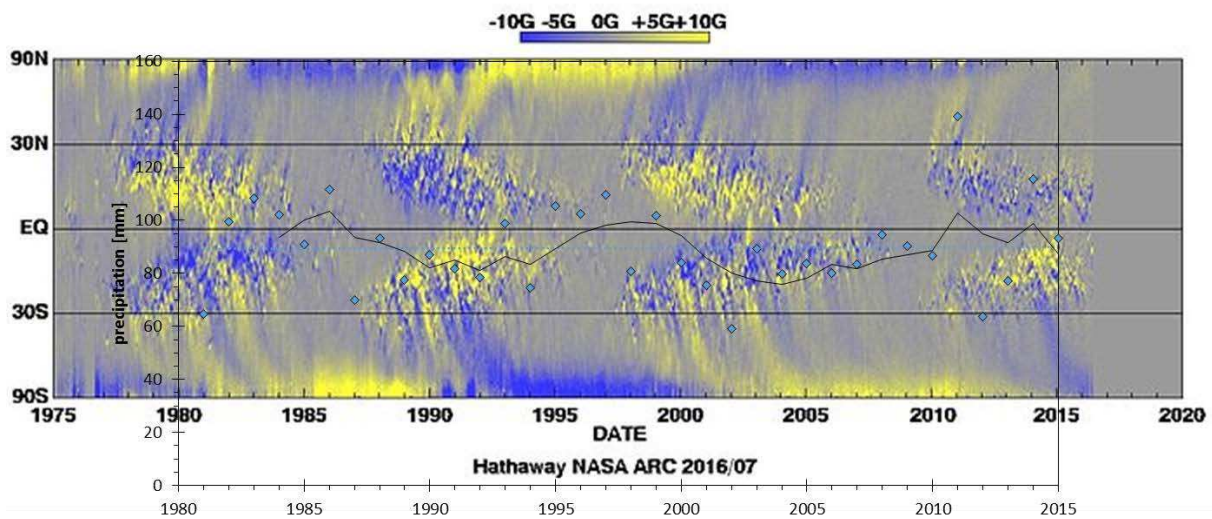


Figure 5.2 Four-year moving average of Oct-June precipitation at Willow Park SNOTEL, 1981-2015, superimposed over time vs. solar latitude diagram of the radial component of the solar magnetic field based on the 11-year sunspot cycle (from the solar group at NASA Marshall Space Flight Center, <<http://solarscience.msfc.nasa.gov/SunspotCycle.shtml>>, accessed 10-26-2016).

In the Sierra and Cascade mountain ranges, the fraction of winter precipitation falling as snow has been decreasing by as much as 60 percent in 54 years, or about 40 mm/decade

(Knowles *et al.*, 2006), but in this study area, the ratio of SFE to cold-season precipitation has been more consistent (Figure 4.12). The average trend in the ratio of total annual SFE/total Oct-June precipitation varied from zero to about +20 percent over 35 years, or about 0 to +10 mm/decade. The largest single-month decreasing trend was October at Joe Wright, which had a rate of about -20 percent over 35 years (1981-2015), or about -10 mm/decade. This is consistent with findings that the Colorado Rockies are sufficiently cold that the fraction is minimally affected by recent warming trends (Knowles *et al.*, 2006).

Many studies of precipitation trends depend on data from weather stations that do not measure snow, or do not use snow data. Also, most of these weather stations are at elevations below the zone of persistent seasonal snow accumulation (Richer *et al.*, 2013). Accordingly, it can be difficult to determine the phase of precipitation, i.e., rain or snow, on a particular day in the snow zone (Fassnacht and Soulis, 2002). Temperature records are used to make this determination, but the temperature threshold below which precipitation falls in frozen form is not always constant (Fassnacht *et al.*, 2013; Harder and Pomeroy, 2014). This underscores an advantage of calculating precipitation trends using records from SNOTEL stations, as the SWE data are available to help determine precipitation phase.

5.4 Trends in Temperature

The general trends during 1981-2015 toward warmer temperatures in the study area are similar to observations found in other recent reports (Hamlet *et al.*, 2005; Knowles *et al.*, 2006; Diaz and Eischeid, 2007). The Loch Vale temperature trend in this investigation represents an update to the trend reported for 1983-2007 in Clow (2010), including new and revised data (Colorado State University, 2016). Strongest warming trends were in November, March, June,

and July, when trends exceeded $0.4^{\circ}\text{C}/\text{decade}$ (Figure 4.13b). By comparison, average annual statewide temperatures in Colorado during 1980-2010 have been increasing at about $0.37^{\circ}\text{C}/\text{decade}$ (Lukas *et al.*, 2014). The northern Colorado Rockies appear to be warming more quickly than other parts of the state (Ray *et al.*, 2008; Lukas *et al.*, 2014). A comparison of seasonal temperature trends from 1957 to 2006 in four mountainous areas of the globe found that the Colorado Rocky Mountains and the Swiss Alps had the strongest overall warming trends, and that the warming trend in the Colorado Rockies (about $0.5^{\circ}\text{C}/\text{decade}$) was particularly strong in the spring (Rangwala and Miller, 2012). Wet-day (days with precipitation) daily minimum temperatures, too, showed strong warming trends, especially during March, in the Colorado Rockies and elsewhere, with increasing trends of $0.25^{\circ}\text{C}/\text{decade}$ during 1949-2004 (Knowles *et al.*, 2006). Based on temperature records recorded at SNOTEL stations from 1991 to 2012, homogenized to adjust for effects of sensor upgrades, Oyler *et al.* (2015) found that warming trends in maximum temperatures in the mountains of Colorado, like those of other interior mountain ranges in the western U.S., averaged in the range of 0.25 to $0.75^{\circ}\text{C}/\text{decade}$.

Temperature records from SNOTEL stations have been shown to contain a positive bias related to changes in sensors, sensor locations, and operational protocols (Oyler *et al.*, 2015). Nevertheless, temperature records from SNOTEL stations can be useful in making relative comparisons among stations. Using the temperature records from the SNOTEL stations preserves the association with the other data collected at the same stations, notably SWE and precipitation. These were used to analyze trends in April 1 SWE in relation to trends in temperature and precipitation.

The results of the analysis of trends in April 1 SWE in relation to trends in October-June precipitation and temperature for the study area (Figure A.22) are similar to those in the Pacific

Northwest (Mote, 2003), in that most of the April 1 SWE trends were decreasing, most were associated with slightly decreasing October-June precipitation at SNOTEL stations, and all were associated with increasing October-June temperatures. However, these temperature trends (Figure A.22) were artificially amplified (Oyler *et al.* 2015). If the data were properly homogenized, the temperature trends could be in the range of zero to 3 degrees C/decade, similar to those found at Allenspark, Grand Lake, and Loch Vale. One station (Lake Eldora) had increasing temperature, increasing precipitation, and significantly increasing SWE, suggesting that the greater precipitation was sufficient to counteract the effects of warming and resulted in increased SWE. Another station (Deadman Hill) had increasing temperature and precipitation, but decreasing SWE, suggesting that at this station the greater precipitation was not sufficient to counteract the effects of warming. A further station (Willow Creek Pass) had increasing temperature, decreasing precipitation, and increasing SWE, suggesting that other factors may also be involved. The overall range of the three variables in this study area was less than the variability reported for the same variables in the Pacific Northwest (Mote, 2003). This is consistent with Losleben and Pepin (2003) who showed the northern Colorado Rockies are less susceptible to temperature-induced negative SWE trends and variability is less than other mountainous areas in the western U.S.

The warming trends observed in this investigation do not appear to follow a cyclical pattern, but instead are relatively consistent in their rate of warming (Figure A.23). The longer period of record (1949-2015) at the Grand Lake cooperative weather station provides an indication of when this recent warming trend may have begun (Figure 4.24). The time series of average annual temperature at Grand Lake shows a cooling trend from 1949 to 1973, followed by the warming trend that continues to the present. This is consistent with other studies that have

identified the early to mid-1970s as the beginning of the current warming trend (Tebaldi *et al.*, 2012), and the 1990s to the present as the period with the strongest warming signal (Ray *et al.*, 2008; Santer *et al.*, 2011).

5.5 Trends in Freezing Level and Maximum Daily Temperatures above Zero

Results of the analysis of simulated free-atmosphere freezing level showed that only during November and March, the average level of the zero-degree Celsius isotherm was about 400 m below the elevation of the lowest SNOTEL stations (Figure 4.14a). In addition, trends in average freezing level were rising more rapidly in November and March than in other cold-season months in between. The trend in freezing level for February was slightly negative. This suggests that during November and March the daily temperature cycle brings warmer-than-freezing temperatures to the elevation zone of the SNOTEL stations for some portion of each of those months. It would then follow that warming trends during these two months are likely to increase the portion of the month with warmer-than-freezing weather, resulting in increased snowmelt. The monthly patterns and trends in daily maximum temperatures warmer than zero at the highest (Lake Irene) and lowest (Copeland Lake) SNOTEL stations provided a test of this hypothesis. Results show that November and March had similar values (Figure A.25a). During these two months the summation of daily maximum temperatures warmer than zero at these two stations ranged from 75 to 250 total degrees, implying a monthly average maximum temperature of about 2.5 to 8.3 degrees. Therefore, both November and March have temperature ranges based on this measure such that a relatively small increase in temperature would cause a relatively large proportional increase in the amount of warmer-than-freezing weather available to help melt snow.

5.6 Climatic Influence on SWE Trends

Trends in both precipitation and temperature influence trends in SWE in and near Rocky Mountain National Park. While year-to-year variability in SWE is influenced primarily by variability in precipitation, the primary reason for the long-term SWE declines in and near Rocky Mountain National Park appears to be increased ablation during periods of the snow season formerly characterized by little ablation. This increased ablation is associated with long-term trends toward warming temperatures, especially during November and March. In their assessment of the Rocky Mountains from Colorado to British Columbia, Mote *et al.* (2005) concluded that warming produces lower spring SWE largely by increasing the frequency of melt events. Hamlet *et al.* (2005) concluded that decreased April 1 SWE in the Rockies from 1947-2003 is due primarily to widespread warming. In this study, we looked at total cold-season precipitation and snowfall at SNOTEL sites, and found no trend toward decreased precipitation or snowfall. Also, snowfall as a proportion of total cold-season precipitation showed no trend, except at the lowest SNOTEL station (Copeland Lake), where there was a trend of increasing snowfall. This agrees with Clow (2010), Mote *et al.* (2005), and Harpold *et al.* (2012), indicating that the SWE declines are not related to an overall decrease in winter precipitation, or a change from snow to rain. While there was a shift from snow to rain widespread over much of western North America and even for parts of Colorado, no such shift was observed for the northern Colorado Front Range (Knowles *et al.*, 2006).

As shown in Figure 4.13b, March and November are also the two months during the snow accumulation season with the strongest warming trends. This finding reinforces an earlier finding (Mote *et al.*, 2005) that warming produces lower spring SWE largely by increasing the frequency of melt events, not by simply enhancing the likelihood of rain instead of snow.

Indeed, Mote *et al.* (2005) found significant correlation between April 1 SWE and total daily melt events. In this study there was no significant correlation between April 1 SWE and number of ablation events, but trends in number of days with ablation (>5 mm loss in SWE) were significantly increasing at five SNOTEL stations and not significantly increasing at six other, closely matching the downward trends in April 1st SWE.

5.7 Trends in Magnitude and Timing of Peak SWE versus SWE Change

Annual peak SWE has decreased at 7 stations (increased at 5) and timing of the annual peak has shifted earlier at four and later at eight SNOTEL stations. The timing of peak SWE, in part, explains why some stations have had a shift in date of peak SWE while others have not. The period during mid-March to early April is characterized by warming and drying trends, when SWE trends become less positive or more negative (Figures 4.8a, 4.9 – 4.11, 5.1). For simplicity, this period will be called the “March thaw”. At the higher and colder sites such as Joe Wright and Willow Park (Figure 5.3), the March thaw occurs prior to the peak, during a period of net SWE accumulation. The March thaw inhibits SWE accumulation, but as of 2015 has not caused the SWE trends to shift from net accumulation to net loss. At the lower and warmer sites, such as Copeland Lake (Figure 5.4), the March thaw occurs after the peak, during a period of net SWE loss, when further acceleration of the SWE loss trend has no impact on the earlier annual peak. At both of these types of sites, peak SWE therefore occurs during a period with a trend toward cooler and wetter conditions. Therefore, the warming trends during the March thaw do not affect the timing or magnitude of the annual peak, which is actually likely to have a trend toward increasing magnitude and later timing, in response to the trends toward cooler and wetter conditions.

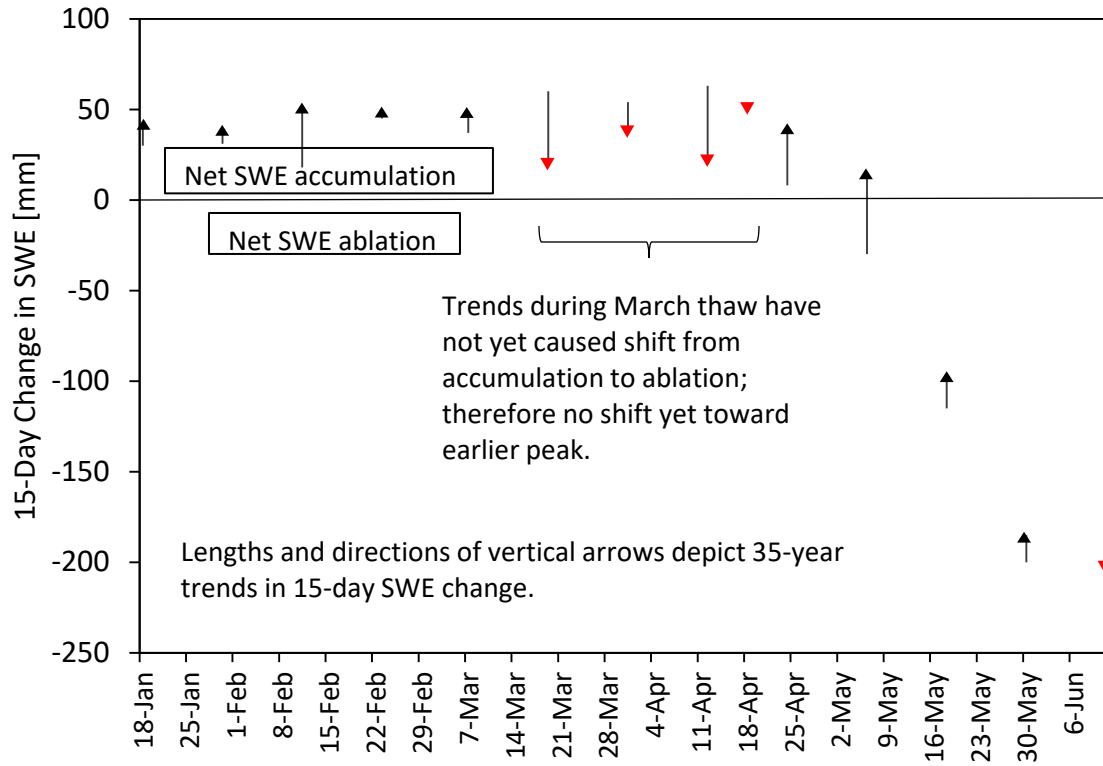


Figure 5.3. Magnitudes and trends in 15-day change in SWE at Willow Park SNOTEL, 1981-2015, for selected days.

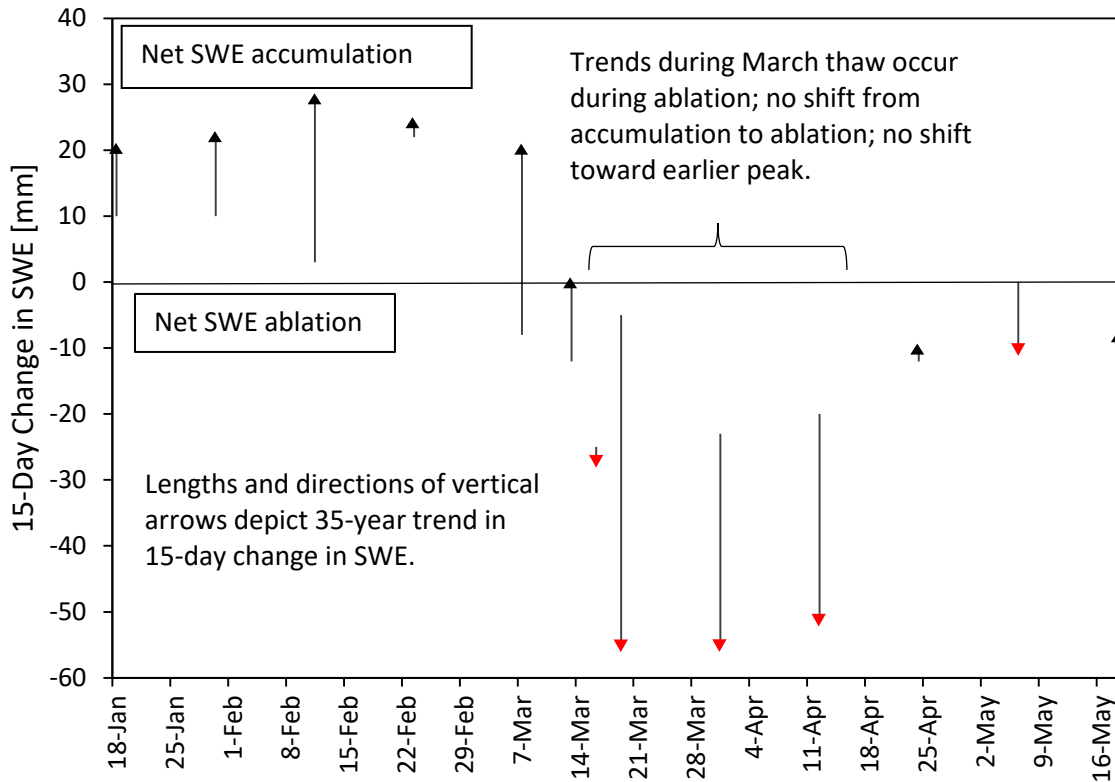


Figure 5.4. Magnitudes and trends in 15-day change in SWE at Copeland Lake SNOTEL, 1981-2015, for selected days.

However, at some sites, such as Phantom Valley (Figure 5.5), which is intermediate in elevation, annual peak SWE occurs during the March thaw. Moreover, at this site, the temperatures during the March thaw are such that the trend in 15-day SWE change has shifted from net accumulation to net loss of SWE (Figure A.12b). This is the requisite for a shift toward an earlier peak SWE, and as a result, the timing of peak SWE has shifted 10 days earlier over 35 years. The relation between trend in date of peak SWE and peak SWE, therefore, is a curvilinear pattern, in which early and late dates of peak SWE show trends toward later peak SWE, while dates of peak SWE during the March thaw show trends toward earlier peak SWE (Figure 5.6). The basic point of Figure 5.6 is that if peak SWE occurs during the March thaw, the trend is toward an earlier peak, while if peak SWE occurs prior to or after the March thaw, the trend is

toward a later peak. In the future, if the March thaw trend continues, SNOTEL stations such as Willow Park are likely to see SWE trends during the March thaw shift from net accumulation to net loss, and at that time the magnitude and timing of annual peak SWE are likely to shift toward smaller and earlier values.

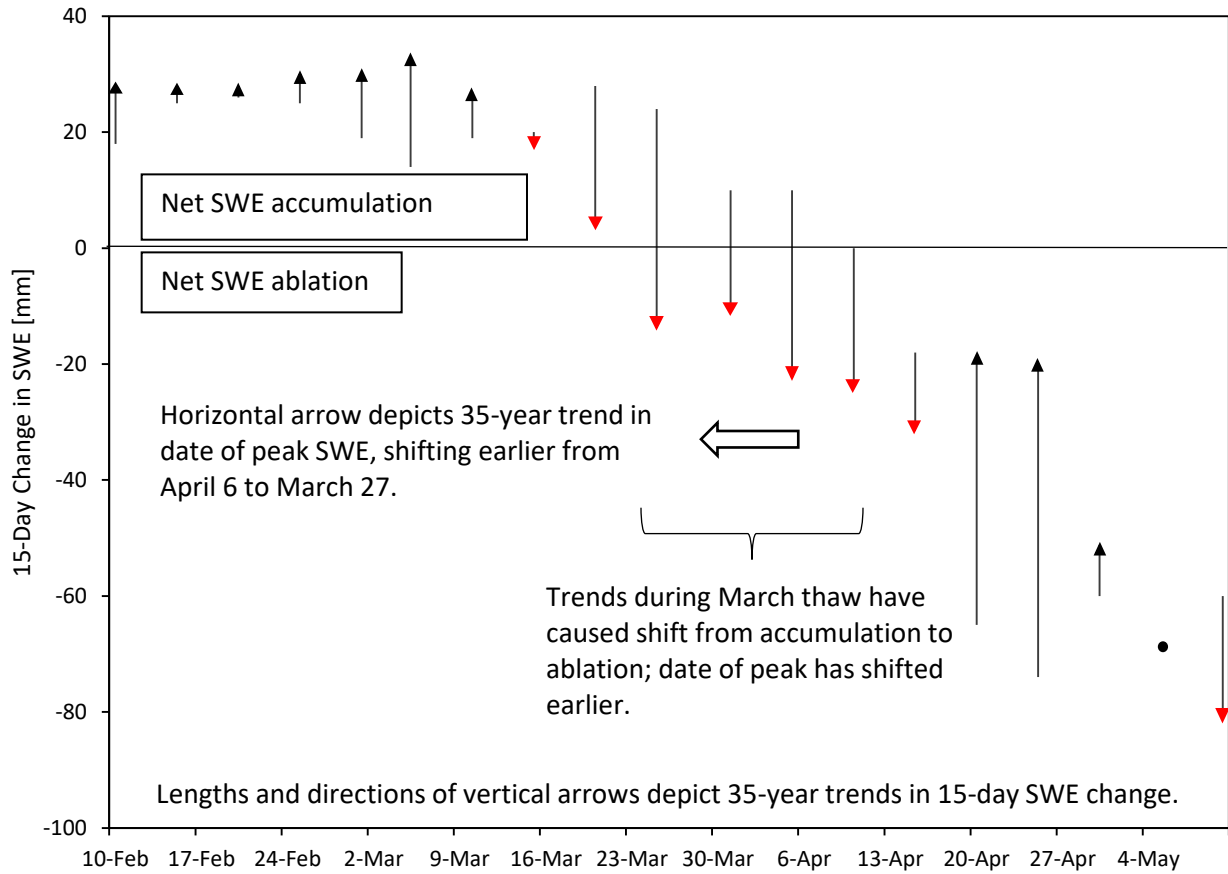


Figure 5.5. Magnitudes and trends in 15-day change in SWE at Phantom Valley SNOTEL, 1981-2015, for selected days.

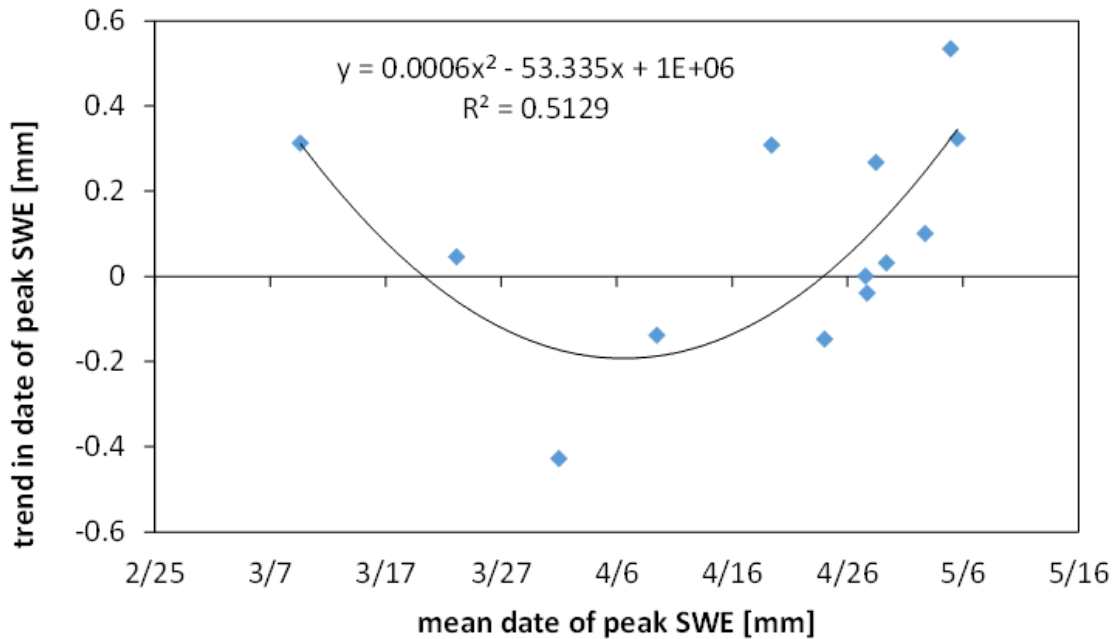


Figure 5.6. Relation between trend in date of peak SWE and date of peak SWE at SNOTEL stations. The fitted function is a second-order polynomial.

5.8 Elevation Dependent SWE Loss

Negative trends in several measures of SWE in this investigation are more prevalent at higher elevations in the zone that includes the SNOTEL stations, than at lower ones. All of the monthly SWE trends from snow courses and SNOTEL stations have a negative correlation with elevation (Figure 4.6). Similarly, the trends in annual peak SWE (Figure A.6a), and in days per year with SWE over 100 mm (Figure A.14) show more negative trends at higher elevations than lower ones.

Trends in some other measures, however, suggest an opposite pattern. Trends in date of annual peak SWE show more shifts to later dates at higher-elevation sites, and more shifts to earlier dates at lower-elevation sites (Figure A.6b). Warming of annual average temperature is

limited at the higher-elevation site (Loch Vale), and greater at the lower-elevation sites (Allenspark and Grand Lake) (Figure 4.13b). Similarly, trends in average cold-season temperature as measured at the SNOTEL stations show no correlation with elevation (not shown). A factor other than temperature is likely influencing the elevation dependence of negative SWE trends. Trends in October-June snowfall equivalent also show a negative correlation with elevation (Figure A.21). This suggests that the predominance of negative trends in SWE at higher elevation sites may be related to less accumulation, rather than more temperature-induced melt. The elevation dependence of negative SWE trends in the study area contrasts with results of a study in the Pacific Northwest, which found a positive correlation between elevation and April 1 SWE (Mote, 2003). The negative correlation between SWE trends and elevation found in this investigation contrasts with the earlier conclusion that higher-elevation, colder sites in the Colorado Rockies tend to be more immune to effects of climate change than lower sites (Mote *et al.*, 2005).

Some researchers have found evidence for elevation-dependent warming in and near the study area. Along an elevation transect in the Front Range of the Colorado Rockies just south of Rocky Mountain National Park, the strongest warming trend (0.42-0.44°C/decade) during 1953-2008 was in maximum temperatures at the sites with elevations similar to the SNOTEL stations (2591–3048 m) (McGuire *et al.*, 2012). The strongest warming trends in that study during 1989-2008 were in maximum temperatures at 2591m (0.85°C/decade), and in minimum temperatures at 3048 m (0.5°C/decade). Using data for 1979-2006 from the PRISM (Parameter-elevation Regressions on Independent Slopes Model), Diaz and Eischeid (2007) found mean annual warming of 0.3°C/decade at 1500 m, compared to 0.7 °C/decade at 3500 m, and 0.96 °C/decade at 4000 m. Models of atmospheric processes over mountains, as well as numerous other

observational studies, support the conclusion that several atmospheric warming mechanisms are stronger at higher elevations, or at least in the subalpine zone, than at lower elevations (Rangwala and Miller, 2012; Pepin *et al.*, 2015). Apparently the complex interaction of temperature, precipitation, snowfall, topography, and weather patterns in these mountainous areas creates some opportunities for additional research into elevation dependence of trends.

5.9 Albedo-Feedback and Humidity Effects

One of the more likely mechanisms that would account for the warming and SWE loss during March and November is albedo-feedback warming (Pepin *et al.*, 2015; Rangwala and Miller, 2012). This process tends to occur near the zero isotherm, which is in the vicinity of the SNOTEL sites during November and March. Loss of snow cover reduces the albedo, which enhances absorption of solar radiation, leading to more warming, and hence delayed SWE accumulation and earlier melt. The effect is to shorten the snow accumulation season at both ends. Thus, while the high, cold mountains of the northern Front Range are still cold enough to support a strong snow accumulation season during December-February, they are showing the typical signs of warming and SWE loss during November and March. Another elevation-dependent warming mechanisms is positive feedback related to increased humidity that yields more downward longwave radiation; this has been found to be significant in Colorado (Naud *et al.*, 2013).

The occurrence of dust on snow has been mentioned as a possible factor enhancing melt through albedo feedback at higher elevations (Lukas *et al.*, 2014; Rangwala and Miller, 2012; Painter *et al.*, 2010). However, the influence of dust on elevation dependent warming in the study area is likely to be limited as the Front Range is distant from the Four Corners area, the

source of most dust affecting snow in Colorado, and there appears to be little or no relation between dust deposition and elevation (Painter, T.H., personal communication, 2015). Another possible factor could be additional albedo feedback caused by deposition of black carbon and other organic-matter particles on snow (Flanner *et al.*, 2009).

5.10 Paleoclimate SWE Reconstructions

Tree-ring reconstructions have been found to be useful proxies for long-term climate records in comparing recent and paleo trends in temperature (Esper *et al.*, 2012), precipitation (Yang *et al.*, 2014), streamflow (Chen *et al.*, 2016), and SWE (Wood and Smith, 2013). The paleo SWE reconstructions examined in this study show that at least some of the recent 35-year trends in observed SWE have comparable precedents during the preceding five centuries (Table 4.3). This finding is consistent with paleo trends that appear in a tree-ring SWE reconstruction for the Gunnison region of Colorado, about 200 km SW of the study area (Woodhouse, 2003). The SWE reconstruction in the Gunnison region showed at least one period in the paleo record, around 1613-25, with a declining trend in SWE similar to those found in this investigation (Figure A.37). The duration of the Gunnison paleo trend, about 13 years, was shorter than the 35 years used in this study, however. If the current declining trends continue into the future, then it becomes likely that the current trends may extend over a longer period than seen in records from the past five centuries.

5.11 Future Projections of SWE Trends

The climate and hydrologic model projections discussed in the results section consider the atmospheric greenhouse gas loading that distinguishes the current period of warming trends from past warming trends (Maurer *et al.*, 2007). Therefore, the projections for continued warming throughout the 21st century, common to all the models discussed, suggest that climatic conditions driving snowpack accumulation and ablation for the remainder of this century will be different from the cyclical patterns of the past. The IPSL model, one of the CMIP5 models that best matches the observed SWE record for 1981-2015, projects a pattern of declining monthly SWE trends, with greater declining trends, up to 14 mm/decade, toward the later part of the snow year. At this rate, annual peak SWE, which now averages about 400 mm in the study area, would be reduced by about 14 percent by 2055, and about 30% by 2099.

The regionally downscaled CMIP5 climate models have a spatial resolution of 1/8 of latitude by 1/8 degree of longitude, or about 11 x 14 km (U.S. Bureau of Reclamation, 2014). Finer-resolution models have been shown to provide more accurate representation of complex topography in mountain areas, and hence of the complex weather patterns that influence the snowpack in these areas (Rasmussen *et al.*, 2011, Rasmussen *et al.*, 2014). The Weather Research and Forecasting-Hydrology (WRF-Hydro) model, which has a resolution of 4 x 4 km, was found to have close agreement with observed snowfall and SWE data observed at SNOTEL stations in the Colorado mountains (Rasmussen *et al.*, 2014). Monthly trends in precipitation and SWE for the next 3.5 decades for the Colorado mountains, simulated using the WRF-Hydro model, were quite similar to trends observed at snow courses and SNOTEL stations in this investigation. Specifically, the simulated trends for precipitation showed increasing precipitation early in the snow season, especially December through April, and decreasing precipitation later

in the spring. The simulated trends for SWE showed little or no loss in SWE during October through February, but greater SWE loss during March through June.

The general agreement between the high-resolution WRF-Hydro model and observed monthly trends in SWE lend some additional credence to this model (Rasmussen *et al.*, 2014). The primary discrepancies are for the months of November and March, during which the modeled trends projected more precipitation while the trends at Willow Park were toward less precipitation. The general pattern of future precipitation and SWE, however, appears to reflect current trends. Monthly trends in precipitation and SWE for the next 3.5 decades for the Colorado mountains, simulated using the WRF-Hydro model, were quite similar to trends observed at snow courses and SNOTEL stations in this investigation. Specifically, the simulated trends for precipitation showed increasing precipitation early in the snow season, especially December through April, and decreasing precipitation later in the spring. The simulated trends for SWE showed little or no loss in SWE during October through February, but greater SWE loss during March through June. Therefore, enhanced precipitation during the early part of the snow season (October to February), especially higher than 3000 m, is likely to preserve and, in some places, even raise the average SWE during those months. This enhancement of precipitation and SWE is likely to maintain or raise current SWE conditions as late as April 1 in parts of the study area. As spring progresses, enhanced warming and decreased precipitation are likely to accelerate rates of SWE loss, leading to earlier and lower peak SWE, more rapid melt, and earlier runoff. By 2055 April 1 SWE in much of Colorado is projected to decrease by 25% compared with 2014 (Rasmussen *et al.*, 2014), with probably lesser declines in this study area due to the high elevation.

5.12. Ramifications for Natural Resource Management

The findings of this investigation suggest some points that are likely to be of interest to natural resource managers with interests in the study area. These points pertain to water supply, wildfire, ecological resources, and winter recreation.

Like other areas of the western United States that depend on the seasonal snowpack for water supply and other natural resources benefits, Rocky Mountain National Park and vicinity are undergoing climatic changes that are altering patterns of accumulation and ablation of the snowpack. In comparison to areas such as the Sierra and Cascade mountain ranges in California and the Pacific Northwest, as well as mountains farther south and west in Colorado, the north-central Colorado mountains in the study area are experiencing less variability in temperature, precipitation, and snow water equivalent (SWE), and weaker long-term trends. However, the observed and projected trends are still noteworthy. December, January, and February are still dependable months for snow accumulation, and are likely to continue as such for much of the rest of this century. In November and March, however, warming and drying trends are reducing SWE accumulation at the beginning and end of the winter. March is shifting from a month of dependable SWE accumulation to a month with less accumulation and, in some years and some places, net loss in SWE. Spring storms often bring additional SWE accumulation, but rising temperatures create variable conditions and lead to rapid melt.

In terms of water supply, overall precipitation is not decreasing in the study area. In December, January, and February, April, and May, precipitation trends are positive. However, trends toward less accumulation or greater loss of SWE during March result in less SWE in the snowpack on April 1, and variable warming trends later in the spring are likely to enhance snowmelt and create greater uncertainty regarding water supplies during the crucial spring runoff

period. Water managers will have to rely less on the snowpack for water storage, and more on artificial storage projects, whether above or underground. Warming trends during the growing season are projected to enhance evapotranspiration. This will reduce soil moisture and streamflow, stress vegetation, and will probably result in increased demand for water for irrigation. Enhanced SWE accumulation during the core winter months of December, January, and February will concentrate the snowpack during these months, with the potential for earlier and more rapid snowmelt runoff during the spring. One mitigating factor for water managers will be the trend toward cooler and wetter conditions during mid-April to early May, especially at lower elevation parts of the snow zone, at least for the next few decades. This trend is likely to help mitigate the SWE losses during November and March.

The results also have ramifications for ecological resources and wildfire. Reduced soil moisture and streamflow, and increased stress on vegetation, are likely to lead to increased risk of wildfires during longer, drier summers in the study area (Westerling *et al.*, 2006). This will impact risk to structures and people, put more aerosols into the atmosphere, and, together with the reduced streamflow, alter aquatic and riparian ecosystems. Terrestrial ecosystems that rely on snow for habitat or protection will also be altered as spring SWE is reduced, and will have drier soil and vegetation in the summer.

Snow-based recreation is likely to become more concentrated during the months with more dependable SWE accumulation, January and February. It is also likely to become more concentrated in higher-elevation parts of the park and vicinity, where snow will be more dependable. Variable conditions during the spring may result in increased danger of avalanches. As warming continues there will be fewer days with snow suitable for skiing or snowshoeing.

CHAPTER 6. CONCLUSIONS

The seasonal snowpack in and near Rocky Mountain National Park is undergoing changes that will pose challenges for water providers, natural resource managers, and winter recreation enthusiasts. Assessing long-term trends in measures of the seasonal snowpack, and in the climatic factors that influence its accumulation and ablation, helps to characterize those challenges. In particular, evaluating the patterns of variation in those trends during the snow season provides new understanding as to the causes, specific ramifications, and likely future course of the trends. In addition, placing the current 35-year trends in the longer context of longer-term observational records, and paleoclimate tree-ring reconstructions provides useful comparisons of current and past trends. Finally, projections of future trends provided by linked climate and hydrologic models offer a sense of how these trends are likely to affect the snowpack of the future.

Several factors are working to limit snowpack changes in the study area, in comparison to snowpack changes elsewhere in the western United States, at least for the next few decades. One mitigating factor is the relatively limited variability in temperature and precipitation, and hence snow water equivalent (SWE), in the study area, compared with other areas such as the Cascades, Sierras, and mountains of western and southern Colorado. The relatively limited variability applies mostly to time scales of one to a few years; over longer time scales, the study areas appears to have warming trends as rapid or more rapid than those found in other parts of the western U.S. Short-term variability in precipitation is correlated with short-term variability in SWE, while long-term trends in both precipitation and temperature appear to influence long-term trends in SWE. A second mitigating factor is the inland location and continental climate of the study area. This tends to isolate the study area from influences of the ocean, including

moderate temperatures, and the cyclical oscillations that bring stronger variability to mountains closer to the coast. The continental climate also helps to keep winter temperatures sufficiently cool to support snowpack development and retention. A third mitigating factor is the relatively high elevation of the snow zone in the study area, which reinforces the cool winter temperatures. A fourth mitigating factor is an observed trend toward greater precipitation in the core winter months of December, January, and February. This trend is crucial to maintaining and, in some cases, enhancing the snowpack during these months. All four of these mitigating factors are likely to continue influencing the snowpack in the study area throughout the present century. A fifth mitigating factor is an observed trend toward enhanced precipitation and cooler temperatures during mid-April to early May, a crucial period for retaining SWE into the beginning of the drier summer months. This trend may be related to the occurrence of spring upslope conditions that bring moisture to the Front Range of the Rockies from the east. This factor is not as wide-spread geographically as the other factors mentioned. In addition, linked climate and hydrologic models that are capable of simulating the effects of the first four factors do not project this fifth factor as a significant influence on snowpack accumulation and ablation in the future. Therefore, there is some uncertainty about the future persistence of this trend in the study area. Model projections suggest that spring warming will reduce SWE accumulation and enhance melt during April and May. These mitigating factors help to explain why, at most of the 13 SNOTEL stations in the study, the timing of annual peak SWE has not shifted to an earlier date, and monthly SWE trends during February are positive.

In spite of these mitigating factors, declining trends in several measures of SWE in the study area are apparent. In every month, some of the trends in monthly SWE at the 23 snow courses and 13 SNOTELs included in the study are decreasing. During November, December,

March, and April most of the trends in monthly SWE are decreasing. Annual peak SWE is decreasing at most of the 13 SNOTEL stations, number of days per year with measurable SWE loss is increasing at all of the SNOTELs, and number of days per year with over 100 mm of SWE is decreasing at most of the SNOTELs.

The strongest negative trends in SWE occur during November and March. These trends are associated with both increasing temperatures and decreasing precipitation in those months. The increasing temperatures bring more above-freezing weather, and hence more snowmelt, to SNOTEL stations in the study area. At SNOTEL stations such as Phantom Valley, where the “March thaw” coincides with the timing of annual peak SWE, annual peak SWE is reduced and the timing of the peak is shifted earlier. At other stations, where annual peak SWE occurs prior to or after the March thaw, trends toward cooler and wetter conditions tend to preserve or enhance the magnitude and timing of annual peak SWE.

While most of the trends discussed in this investigation pertain to the 35-year period 1981-2015, evaluation of SWE data from snow courses starting in the 1930s shows that declining SWE trends have been consistent for the full 80-year record of these snow courses. In contrast, evaluation of temperature data starting in 1949 at Grand Lake shows that, consistent with trends in many other areas, the current warming trend in the study area began about 1973, following a period of cooling.

As found by Clow (2010), there are some differences in SWE trends at SNOTEL stations on the western (orange cluster) and eastern (purple cluster) sides of the Front Range. The sites on the western side have more negative monthly trends in SWE, while the sites on the eastern side have fewer such trends. This difference is especially noteworthy during February, April, and May.

Trends in October-June precipitation are relatively small in comparison with trends seen in other parts of the western United States, and there is as yet no trend toward decreased fraction of October-June precipitation falling as snow. The precipitation trends that do exist, along with the temperature trends, help to explain the pattern of SWE trends that tend to decrease in November and March and increase in other months.

In contrast to results from the Pacific Northwest, which found stronger decreasing trends in SWE at lower elevations in the mountains, in this investigation several of the measures of SWE had trends indicating greater SWE loss at higher elevations. This pattern was not consistent with all measures of SWE, however, and the temperature trends examined in this investigation did not show a consistent pattern of more rapid warming at higher elevation.

The paleo SWE reconstructions based on tree-ring chronologies show that at least some of the recent 35-year trends in observed SWE described in this study have comparable precedents during the preceding five centuries. If the 80-year period of declining trends at snow courses is considered, and especially if the current declining trends continue into the future, then it becomes likely that the current trends are unprecedented over the past five centuries.

Linked climate and hydrologic models, especially the high-resolution WRF-Hydro model designed for accurate simulation of atmospheric processes over the complex topography of the study area, project that the current warming trends will continue, and will overcome the effects of increased precipitation to enhance spring snowmelt in most of the study area. At some of the highest elevation sites the models project that, even with warming, the temperatures will remain below freezing, and continued enhanced precipitation may preserve the snowpack.

These findings suggest that, in Rocky Mountain National Park and vicinity, the core winter months of December, January, and February are likely to continue with current or perhaps even enhanced trends in snow water equivalent. However, the snow season is likely to begin later, due to continued warming and drying trends in November. March is likely to shift from being a key month for snow accumulation, to being a period with less accumulation and some loss of SWE. Conditions during April and May are likely to be variable, with strong SWE accumulation from upslope storms in some years, but increased warming causing more rapid melt. Spring runoff is likely to begin earlier. During the longer, warmer, summers, soil moisture is likely to decline, contributing to decreased streamflow, stress for vegetation, and increased fire danger. Winter recreation will become more concentrated during January and February. The variable conditions during the spring will create increased risk for avalanches. Downstream water users will need to rely less on snowmelt runoff and more on stored water.

REFERENCES

- Avanzi, F., C.D. Michele, A. Ghezzi, C. Jommi, and M. Pepe, 2014. A processing-modeling routine to use SNOTEL hourly data in snowpack dynamic models. *Advances in Water Resources*, 73, 16-29.
- Bales, R.C., N.P. Molotch, T.H. Painter, M.D. Dettinger, R. Rice, and J. Dozier, 2006. Mountain hydrology of the western United States. *Water Resources Research*, 42, W08432, 13 pp.
- Barnett, T.P., D.W. Pierce, H.G. Hidalgo, C. Bonfils, B.D. Santer, T. Das, G. Bala, A.W. Wood, T. Nozawa, A.A. Mirin, D.R. Cayan, and M.D. Dettinger, 2008. Human-induced changes in the hydrology of the western United States. *Science*, 319, 5866, 1080-1083.
- Berkelhammer, M.B., 2010, *Perspectives on drought and temperature variability for the southwestern United States from a new hydro-isotopic network*. Ph.D. Dissertation, Geological Sciences, University of Southern California, December 2010. UMI Number: 3434545. <http://digitallibrary.usc.edu/cdm/ref/collection/p15799coll127/id/681462>, accessed 7-10-16.
- Bohr, G.S., and E. Aguado, 2001. Use of April 1 SWE measurements as estimates of peak seasonal snowpack and total cold-season precipitation. *Water Resources Research*, 37(1), 51-60.
- Bradley, B.A., R.W. Jacob, J.F. Hermance, and J.F. Mustard, 2007, A curve fitting procedure to derive inter-annual phenologies from time series of noisy satellite NDVI data. *Remote Sensing of the Environment*, 106(2):137-145.
- Brekke, L, A Wood, and T Pruitt, 2014, *Downscaled CMIP3 and CMIP5 Hydrology Projections: Release of Hydrology Projections, Comparison with Preceding Information, and Summary of User Needs*. 111 p. http://gdo-dcp.ucllnl.org/downscaled_cmip_projections/techmemo/BCSD5HydrologyMemo.pdf, accessed 7-23-16.
- Burakowski, E., and M. Magnusson, 2012. *Climate impacts on the winter tourism economy in the United States*. Report by Protect Our Winters and the Natural Resources Defense Council, 36 p. <https://www.nrdc.org/sites/default/files/climate-impacts-winter-tourism-report.pdf>, accessed 7-8-2016.
- Chen, Z., and S. Grasby, 2009. Impact of Decadal and Century-Scale Oscillations on Hydroclimate Trend Analyses. *Journal of Hydrology*, 365(1-2), 122-133.
- Chen, Feng, Qing He, Bakytbek, E., Shulong Yu & Ruibo Zhang, 2016, Reconstruction of a long streamflow record using tree rings in the upper Kurshab River (Pamir-Alai Mountains) and its application to water resources management. *International Journal of Water Resources Development*, 0(0.0):1-11, October 14, 2016. [DOI: 10.1080/07900627.2016.1238347].
- Clarke, L., J. Edmonds, H. Jacoby, H. Pitcher, J. Reilly, R. Richels, 2007. *Scenarios of Greenhouse Gas Emissions and Atmospheric Concentrations*. Sub-report 2.1A of Synthesis and

Assessment Product 2.1 by the U.S. Climate Change Science Program and the Subcommittee on Global Change Research. Department of Energy, Office of Biological & Environmental Research, Washington, 7 DC, USA, 154 pp.

Clow, D.W., 2010, Changes in the timing of snowmelt and streamflow in Colorado: a response to recent warming. *Journal of Climate*, 23, 2293-2306.

Colorado Climate Center, 2016, *Drought Resources*, <http://climate.colostate.edu/droughtqanda.php>, accessed 7-8-16.

Colorado State University, 2016, *Loch Vale Watershed data*. https://www.nrel.colostate.edu/projects/lvws/data.html#Meteorological_data, accessed 7-10-16.

Denver Botanical Gardens, 2016, *Krummholz*. 23p. <http://www.botanicgardens.org/system/files/resources/docent/krummholz.pdf>, accessed 7-18-16.

Denver Post, 2015, *Skiers' economic impact in Colorado adds up to \$4.8 billion*. <http://www.denverpost.com/2015/12/09/skiers-economic-impact-in-colorado-adds-up-to-4-8-billion/>, accessed 7-8-16.

Derry, J.E., and S.R. Fassnacht, 2015. *Snowpack Variability and Trends across the San Juan Mountains of Southwestern Colorado from Snow Telemetry and Snowcourse Stations*. Poster presentation at the American Geophysical Union Fall Meeting, San Francisco CA, December 14-18, 2015 (C33C-0836).

Diaz, H.F., and J.K. Eischeid, 2007. Disappearing "alpine tundra" Köppen climatic type in the western United States. *Geophysical Research Letters*, 34, L18707 [DOI:10.1029/2007GL031253].

Dressler, K.A., S.R. Fassnacht, and R.C. Bales, 2006. A comparison of snow telemetry and snow course measurements in the Colorado River Basin. *Journal of Hydrometeorology*, 7, 705-712.

Dufresne, J.-L., et al., 2013, Climate change projections using the IPSL-CM5 Earth System Model: from CMIP3 to CMIP5. *Climate Dynamics*, 40(9-10), 2123-2165, 2013, [DOI:10.1007/s00382-012-1636-1].

Esper, J., and co-authors, 2012, Orbital forcing of tree-ring data. *Nature Climate Change*, 2:862-866. [DOI:10.1038/nclimate1589].

Fassnacht, S.R., K.A. Dressler, and R.C. Bales, 2003. Snow water equivalent interpolation for the Colorado River Basin from snow telemetry (SNOTEL) data. *Water Resources Research*, 39(8), 1208 [DOI:10.1029/2002WR001512].

Fassnacht, S.R., and J.E. Derry, 2010. Defining similar regions of snow in the Colorado River Basin using self-organizing maps. *Water Resources Research*, 46, W04507 [DOI:10.1029/2009WR007835].

- Fassnacht, S.R., and E.D. Soulis, 2002. Implications during transitional periods of improvements to the snow processes in the Land Surface Scheme - Hydrological Model WATCLASS. *Atmosphere-Ocean*, 40(4), 389-403.
- Fassnacht, S.R., and G.G. Patterson, 2013. Niveograph Interpolation to Estimate Peak Accumulation at Two Mountain Sites. *Cold and Mountain Region Hydrological Systems Under Climate Change: Towards Improved Projections* (Proceedings of symposium H02, IAHS-IAPSO-IASPEI Assembly, Gothenburg, Sweden, July 2013) IAHS, 360, 59-64.
- Fassnacht, S.R., N.B.H. Venable, J. Khishigbayar, and M.L. Cherry, 2013. The Probability of Precipitation as Snow Derived from Daily Air Temperature for High Elevation Areas of Colorado, United States. *Cold and Mountain Region Hydrological Systems Under Climate Change: Towards Improved Projections* (Proceedings of symposium H02, IAHS-IAPSO-IASPEI Assembly, Gothenburg, Sweden, July 2013) IAHS, 360, 65-70.
- Fassnacht, S.R., D.C. Deitemeyer, and N.B.H. Venable, 2014. Capitalizing on the Daily Time Step of Snow Telemetry Data to Model the Snowmelt Components of the Hydrograph for Small Watersheds. *Hydrological Processes*, 28(16), 4654-4668 [DOI: 10.1002/hyp.10260].
- Fassnacht, S.R., and M. Hultstrand, 2015. Snowpack Variability and Trends at Long-term Stations in Northern Colorado, USA. *Proceedings of the International Association of Hydrological Sciences* (Hydrologic Non-Stationarity and Extrapolating Models to Predict the Future), [DOI:10.5194/piahs-92-1-2015].
- Fassnacht, S.R., and R.M. Records, 2015. Large Snowmelt versus Rainfall Events in the Mountains. *Journal of Geophysical Research*, 120, 2375-2381 [DOI:10.1002/2014JD022753]
- Fassnacht, S.R., M.L. Cherry, N.B.H. Venable, and F. Saavedra, 2016. Snow and Albedo Climate Change Impacts across the United States Northern Great Plains. *The Cryosphere*, 10, 329-339, [DOI:10.5194/tc-10-329-2016].
- Flanner, M. G., Zender, C. S., Hess, P. G., Mahowald, N. M., Painter, T. H., Ramanathan, V., and Rasch, P. J., 2009, Springtime warming and reduced snow cover from carbonaceous particles, *Atmos. Chem. Phys.*, 9, 2481-2497, DOI:10.5194/acp-9-2481-2009, 2009.
- Flanner, M.G., K.M. Shell, M. Barlage, D.K. Perovich, and M.A. Tschudi, 2011. Radiative forcing and albedo feedback from the northern hemisphere cryosphere between 1979 and 2008. *Nature Geoscience*, 4, 151-155 [DOI:10.1038/ngeo1062].
- Fritze, H., I.T. Stewart, and E. Pebesma, 2011. Shifts in western North American snowmelt runoff regimes for the recent warm decades. *Journal of Hydrometeorology*, 12, 989-1006.
- Fu C., A.L. James, and M. Wachowiak, 2012. Analyzing the combined influence of solar activity and El Nino on streamflow across southern Canada. *Water Resources Research*, 48(5), [DOI:10.1029/2011WR011507].

- Gilaberte-Burdalo, M., F. Lopez-Martin, M.R. Pino-Otin, and J.I. Lopez-Moreno, 2014. Impacts of climate change on ski industry. *Environmental Science and Technology*, 44, 51-61 [DOI: 10.1016/j.envsci.2014.07.003].
- Gilbert, R.O. 1987. *Statistical Methods for Environmental Pollution Monitoring*, Wiley, NY.
- Hamlet, A.F., P.W. Mote, M.P. Clark, and D.P. Lettenmaier, 2005, Effects of temperature and precipitation variability on snowpack trends in the western United States. *Climate*, 18, 4545-4561.
- Harder, P, and Pomeroy, J.W., 2014, Hydrological model uncertainty due to precipitation-phase partitioning methods. *Hydrological Processes*, 28(14), 4311–4327. [DOI: 10.1002/hyp.10214].
- Harding, B.L., and E.A. Payton, 1990. Marginal economic value of streamflow. *Water Resources Research*, 26(12), 2845-2859.
- Harpold, A., P. Brooks, S. Rajagopal, I. Heidbuchel, A. Jardine, and C. Stielstra, 2012. Changes in snowpack accumulation and ablation in the intermountain west. *Water Resources Research*, 48, W11501-W11511.
- Helsel, D.R. and R.M. Hirsch. 1995. *Statistical Methods in Water Resources*, Elsevier, New York.
- Intergovernmental Panel on Climate Change, 2013, *Climate change 2013--the physical science basis: Working Group I Contribution to the Fifth Assessment Report of the Intergovernmental Panel on Climate Change*. Cambridge University Press, p. 194 of 1535.
- Jones, H.G., J.W. Pomeroy, D.A. Walker, and R.W. Hoham, (eds), 2001. *Snow Ecology*, chapters 5 and 6. Cambridge University Press, Cambridge, U.K., 378 p.
- Kendall, M.G. 1975. *Rank Correlation Methods*, 4th edition, Charles Griffin, London.
- Knowles, N, M.D Dettinger, and D.R. Cayan, 2006, Trends in snowfall versus rainfall in the western United States. *Climate* 19: 4545-4559.
- Knowles, N., M.D. Dettinger, and D.R. Cayan. 2007. *Trends in snowfall versus rainfall for the western United States, 1949–2001*. California Energy Commission, PIER Energy-Related Environmental Research Program. CEC-500-2007-032.
- LaMarche, V.C., and Stockton, C.W., 1974, *Chronologies from temperature-sensitive bristlecone pines at upper treeline in western United States*. University of Arizona Laboratory of Tree Ring Research Tree Ring Bulletin, 34:21-45. <http://arizona.openrepository.com/arizona/handle/10150/260057>, accessed 7-10-16.
- Lazar, B., and M. Williams, 2008. Climate change in western ski areas: Potential changes in the timing of wet avalanches and snow quality for the Aspen ski area in the years 2030 and 2100. *Cold Regions Science and Technology*, 51, 219-228.

- Losleben, M, and N. Pepin, 2003, Spatial and Temporal Variability in Snowpack Controls: Two Decades of SnoTel Data from the Western U.S. 2003 PACLIM Conference Proceedings, pp. 23-32. http://tenaya.ucsd.edu/~dettinge/PACLIM/05_Losleben_03.pdf, accessed 7-23-16.
- Lukas, J., J. Barsugli, N. Doesken, I. Rangwala, and K. Wolter, 2014, *Climate change in Colorado: A synthesis to support water resources management and adaptation* (2nd ed.). Report to the Colorado Water Conservation Board. Western Water Assessment, Cooperative Institute for Research in Environmental Sciences, University of Colorado, Boulder, 114 p.
- Mann, H.B. 1945. Non-parametric tests against trend. *Econometrica* 13:163-171.
- Maurer, E. P., L. Brekke, T. Pruitt, and P. B. Duffy (2007), Fine-resolution climate projections enhance regional climate change impact studies, *Eos Trans. AGU*, 88(47), 504. Note: The regionally downscaled projections were retrieved from http://gdo-dcp.ucllnl.org/downscaled_cmip_projections/dcpInterface.html, accessed 7-10-16.
- McGuire, C.R., C.R. Nufio, M.D. Bowers, and R.P. Guralnick, 2012, Elevation-dependent temperature trends in the Rocky Mountain Front Range: Changes over a 56- and 20-year record. *PLoS ONE* 7(9): e44370. [DOI:10.1371/journal.pone.0044370].
- Milly, P.C.D., K.A. Dunne, and A.V. Vecchia, 2005, Global pattern of trends in streamflow and water availability in a changing climate. *Nature* 438:347-350. [DOI:10.1038/nature04312].
- Mote, P.W., 2003, Trends in snow water equivalent in the Pacific Northwest and their climatic causes. *Geophysical Research Letters* 30(12):1601-1604. [DOI:10.1029/2003GL017258]. <http://onlinelibrary.wiley.com/doi/10.1029/2003GL017258/epdf>, accessed 7-23-16.
- Mote, P.W., A.F. Hamlet, M.P. Clark, and D.P. Lettenmaier, 2005, Declining mountain snowpack in western North America. *Bulletin of the American Meteorological Society*, 86(1), 39-49.
- National Aeronautics and Space Administration, 2016. *The sunspot cycle*. <http://solarscience.msfc.nasa.gov/SunspotCycle.shtml>, accessed 11-26-16.
- National Oceanic and Atmospheric Administration, National Centers for Environmental Information, 2016a. Climate data online. <http://www.ncdc.noaa.gov/cdo-web/search>, accessed 7-10-16.
- National Oceanic and Atmospheric Administration, National Centers for Environmental Information, 2016b. *Pacific decadal oscillation*. <https://www.ncdc.noaa.gov/teleconnections/pdo/>, accessed 10-26-16.
- National Park Service, 2016a. *National Park Service Visitor Use Statistics*. <https://irma.nps.gov/Stats/Reports/Park>, accessed 2-24-16.
- National Park Service, 2016b, *Alpine tundra ecosystem*. https://www.nps.gov/romo/learn/nature/alpine_tundra_ecosystem.htm, accessed 7-9-16.

- National Park Service, 2016c, *Park statistics*. <https://www.nps.gov/romo/learn/management/statistics.htm>, accessed 7-9-16.
- National Park Service, 2016d, *Weather—Rocky Mountain National Park*. <https://www.nps.gov/romo/planyourvisit/weather.htm>, accessed 7-20-16.
- Natural Resources Conservation Service, 2016a, *Snow survey sampling guide*. <http://www.wcc.nrcs.usda.gov/factpub/ah169/ah169.htm>, accessed 7-9-16.
- Natural Resources Conservation Service, 2016b, *SNOTEL and snow survey and water supply forecasting*. National Water and Climate Center brochure, rev. 01-2014. http://www.wcc.nrcs.usda.gov/snotel/SNOTEL_brochure.pdf, accessed 7-9-16.
- Natural Resources Conservation Service, 2016c, *Snow telemetry (SNOTEL) and snow course data and products*. <http://www.wcc.nrcs.usda.gov/snow/>, accessed 7-9-16.
- Naud, C.M., Y. Chen, I. Rangwala, and J.R. Miller, 2013, Sensitivity of downward longwave surface radiation to moisture and cloud changes in a high-elevation region. *Journal of Geophysical Research: Atmospheres*, 118:10,172-81, DOI:10.1002/jgrd.50644.2013.
- Oyler, J.W., S.Z. Dobrowski, A.P. Ballantyne, A.E. Klene, and S.W. Running, 2015, Artificial amplification of warming trends across the mountains of the western United States. *Geophysical Research Letters*, 42(1), [DOI:10.1002/2014GL062803].
- Painter, T.H., J.S. Deems, J. Belnap, A.F. Hamlet, C.C. Landry, and B. Udall, 2010, Response of Colorado River runoff to dust radiative forcing in snow. *Proceedings of the National Academy of Sciences*, 107(40):17125–17130, [DOI: 10.1073/pnas.0913139107].
- Pagano, T.C., 2012, Quantification of the influence of snow course measurement date on climatic trends. *Climatic Change*, 114: 549. [DOI:10.1007/s10584-012-0446-0].
- Papadogiannaki, E., Y. Le, and S.J. Hollenhorst, 2011. *Rocky Mountain National Park Visitor Study, Winter 2011*. Visitor Services Project, Park Studies Unit, University of Idaho, Moscow, ID, NPS 121/111373, 115 p. http://psu.sesrc.wsu.edu/vsp/reports/235.2_ROMO_rept.pdf, accessed 2-24-16.
- Patterson, G.G., and S.R. Fassnacht, 2014, Niveograph interpolation to estimate peak accumulation of snow water equivalent in Rocky Mountain National Park. *Proceedings of the 82nd Annual Western Snow Conference*, (Durango CO), 109-116.
- Pepin, N., R.S. Bradley, H.F. Diaz, M. Baraer, E.B. Caceres, N. Forsythe, H. Fowler, G. Greenwood, M.Z. Hashmi, X.D. Liu, J.R. Miller, L. Ning, A. Ohmura, E. Palazzi, I. Rangwala, W. Schöner, I. Severskiy, M. Shahgedanova, M.B. Wang, S.N. Williamson, and D.Q. Yang, 2015, Elevation-dependent warming in mountain regions of the world. *Nature Climate Change* 5: 424-430. Published online: 23 APRIL 2015 | [DOI: 10.1038/NCLIMATE2563].
- Pfohl, A.K.D., 2016. *Trends in snowmelt contribution to streamflow in the southern Rocky Mountains of Colorado*. Unpublished Master's Thesis, Watershed Science, Colorado State University.

- Rangwala, I., and J.R. Miller, 2012, Climate change in mountains: a review of elevation-dependent warming and its possible causes. *Climatic Change* (2012) 114: 527–547, [DOI 10.1007/s10584-012-0419-3].
- Rasmussen, R. M., and coauthors, 2011: High resolution coupled climate-runoff simulations of seasonal snowfall over Colorado: A process study of current and warmer climate. *Journal of Climate*, 24, 3015-3048, [DOI:10.1175/2010JCLI3985.1].
- Rasmussen, R., and co-authors, 2014. Climate Change Impacts on the Water Balance of the Colorado Headwaters: High-Resolution Regional Climate Model Simulations. *Journal of Hydrometeorology*, 15, 1091-1116 [DOI:<http://dx.doi.org/10.1175/JHM-D-13-0118.1>].
- Ray, A.J., J.J. Barsugli, and K.B. Averyt, 2008. *Climate change in Colorado: A synthesis to support water resources management and adaptation*. Report for the Colorado Water Conservation Board. Western Water Assessment, Cooperative Institute for Research in Environmental Sciences, University of Colorado, Boulder, 58 p.
- Regonda, S.K., B. Rajagopalan, M. Clark, and J. Pitlick, 2005, Seasonal cycle shifts in hydroclimatology over the western United States. *Climate* 18:372-384.
- Rense, W.P., Rocky Mountain Hydrologic Research Center, Allenspark, Colo., 2016, personal communication.
- Richer, E.E., S.K. Kampf, S.R. Fassnacht, and C.C. Moore, 2013, Spatiotemporal index for analyzing controls on snow climatology: application in the Colorado Front Range. *Physical Geography* 34(2):85-107.
- Salmi, T, A Määttä, P Anttila, T Ruoho-Airola, and T Amnell, 2002, *Detecting trends of annual values of atmospheric pollutants by the Mann-Kendall test and Sen's slope estimates—the Excel template application MAKESENS*. Finnish Meteorological Institute, Helsinki, 2002, 35 p. http://www.ilmanlaatu.fi/ilmansaasteet/julkaisu/pdf/MAKESENS-Manual_2002.pdf, accessed 7-22-16.
- Santer, B.D., and co-authors, 2011. Separating signal and noise in atmospheric temperature changes: The importance of timescale. *Journal of Geophysical Research*, 116(D22105), 19p, [DOI:10.1029/2011JD016263].
- Sen, P.K. 1968. Estimates of the regression coefficient based on Kendall's tau. *Journal of the American Statistical Association* 63:1379-1389.
- Serreze, M.C., M.P. Clark, R.L. Armstrong, D.A. McGinnis, and R.S. Pulwarty, 1999. Characteristics of the Western United States snowpack from snowpack telemetry (SNOTEL) data. *Water Resources Research*, 35(7), 2145-2160.
- Skamarock, W. C., J. B. Klemp, J. Dudhia, D. O. Gill, D. M. Barker, W. Wang, and J. G. Powers, 2005: *A description of the Advanced Research WRF version 2*. NCAR Tech. Note NCAR/TN-4681STR, 88 pp. [Available online at www.mmm.ucar.edu/wrf/users/docs/arw_v2.pdf.]

Stahl, K., R. D. Moore, J. M. Shea, D. Hutchinson, and A. J. Cannon (2008), Coupled modelling of glacier and streamflow response to future climate scenarios. *Water Resources Research*, 44, W02422, [DOI:10.1029/2007WR005956].

Stewart, I.T., D.R. Cayan, and M.D. Dettinger, 2005. Changes toward earlier streamflow timing across western North America. *Journal of Climate*, 18, 1136-1155.

Stewart, I.T., D.R. Cayan, and M.D. Dettinger, 2004. Changes in snowmelt runoff timing in western North America under a “business as usual” climate change scenario. *Climatic Change*, 62, 217-232.

Tebaldi, C., Adams-Smith, D., and Heller, N., 2012, *The heat is on: U.S. Temperature Trends*. Climate Central, 22p. <http://www.climatecentral.org/wgts/heat-is-on/HeatIsOnReport.pdf>, accessed 7-26-16.

Theil, H. 1950. A rank-invariant method of linear and polynomial regression analysis, 1, 2, and 3: *Ned. Akad. Wentsch Proc.*, 53:386-392, 521-525, and 1397-1412.

U.S. Bureau of Reclamation, 2014, *Downscaled CMIP3 and CMIP5 Climate and Hydrology Projections: Release of Hydrology Projections, Comparison with preceding Information, and Summary of User Needs*, prepared by the U.S. Department of the Interior, Bureau of Reclamation, Technical Services Center, Denver, Colorado. 110 pp. Note: The hydrology projections were retrieved from http://gdo-dcp.ucllnl.org/downscaled_cmip_projections/dcpInterface.html, accessed 7-10-16.

U.S. Forest Service, 2016, *National visitor use monitoring results*. http://www.fs.fed.us/recreation/programs/nvum/reports/year1/R2_Arapaho_final.htm#Toc524932933, accessed 7-9-16.

Venable, N.B.H., S.R. Fassnacht, G. Adyabadam, Tumenjargal S., M. Fernández-Giménez, and B. Batbuyan, 2012. Does the Length of Station Record Influence the Warming Trend That is Perceived by Mongolian Herders near the Khangai Mountains? *Pirineos*, 167, 71-88 [doi: 10.3989/Pirineos.2012.167004].

Vines, R.G., 1982. Rainfall patterns in the western United States. *Journal of Geophysical Research*, 87(C9), 7303-7311, [DOI: 10.1029/JC087iC09p07303].

Viviroli, D., H.H. Dürr, B. Messerli, M. Meybeck, and R. Weingartner, 2007. Mountains of the world, water towers for humanity: Typology, mapping, and global significance. *Water Resources Research*, 43(7), W07447, [DOI: 10.1029/2006WR005653].

Westerling, A.L., H.G. Hidalgo, D.R. Cayan, and T.W. Swetnam, 2006. Warming and earlier spring increase western U.S. forest wildfire activity. *Science*, 313, 5789, 940-943.

Western Regional Climate Center, 2016, *North American freezing level tracker*. <http://www.wrcc.dri.edu/cwd/products/>, accessed 7-10-16.

Wood, L.J., and D.J. Smith, 2013, Climate and glacier mass balance trends from AD 1780 to present in the Columbia Mountains, British Columbia, Canada. *Holocene*, 23(5):739-748.

Woodhouse, C.A., 2003, A 431-year reconstruction of western Colorado snowpack from tree rings. *Journal of Climate* 16:1551-1561.

Woodhouse, C.A., and Lukas, J.J., 2006, Multi-century tree-ring reconstructions of Colorado streamflow for water-resource planning. *Climatic Change*, 23p. [DOI: 10.1007/s10584-006-9055-0]. <http://www.u.arizona.edu/~conniew1/papers/WoodhouseLukasClCh.pdf>, accessed 7-10-16.

Woodhouse, CA, 2016, *Streamflow reconstructions from tree rings: an example from Middle Boulder Creek*. NOAA Paleoclimatology Program.

<http://bcn.boulder.co.us/basin/forum/basindendro.html>, accessed 7-23-16.

Yang, B., Chun Qin, Jianglin Wang, Minhui He, Melvin, T.M., Osborn, T.J., and Briffa, K.R., 2014, A 3,500-year tree-ring record of annual precipitation on the northeastern Tibetan Plateau. *Proc. Natural Academy of Sciences USA*, 111(8): 2903–2908. [DOI:10.1073/pnas.1319238111].

APPENDIX

Table A.1. Tree-ring reconstructions used in this investigation (from Woodhouse, 2003).

Code	Name	Species	Begin [year]	End [year]	Length [yrs]	Basin	Latitude [N]	Longitude [W]	Elev [m]
BTU	Big Thompson	Douglas-fir	1520	2000	481	South Platte	40° 25'	105° 17'	2012
ENC	Encampment	Douglas-fir	1380	2001	622	North Platte	41° 09'	106° 47'	2500
GM R	Green Mtn. Res.	Douglas-fir	1378	2000	623	Colorado	39° 51'	106° 14'	2514
HOT	Hot Sulphur Springs	Douglas-fir	1571	1999	429	Colorado	40° 04'	106° 08'	2499
NPU	North Park update	Douglas-fir	1486	2001	516	North Platte	40° 57'	106° 20'	2450
PUM	Pump House	pinyon	1320	2002	683	Colorado	39° 58'	106° 31'	2194
STU	Stultz Trail	Douglas-fir	1480	1997	518	Arkansas	38° 20'	105° 16'	2465

Table A.2. Half matrix of April 1st SWE correlations for the study period 1981-2015 with three levels of correlation ($R^2 > 0.5, 0.7, 0.9$) highlighted.

	Roach	Joe Wright	Lake Irene	Phantom Valley	Willow Creek Pass	Stillwater Creek	Deadman Hill	Willow Park	Bear Lake	Copeland Lake	University Camp	Niwot	Lake Eldora	Copeland Lake	Deer Ridge	Hidden Valley	Lake Irene	Long Draw Reservoir	Longs Peak	Milner Pass	North Inlet Grand Lake	Wild Basin	Bennett Creek	Big South	Boulder Falls	Cameron Pass	Chambers Lake	Deadman Hill	Granby	Hourglass Lake	McIntyre	Park View	Red Feather	University Camp	Ward	Willow Creek Pass
Roach	0.6	0.7	0.5	0.5	0.5	0.7	0.7	0.6	0.2	0.6	0.5	0.3	0.2	0.1	0.3	0.4	0.7	0.7	0.7	0.7	0.7	0.6	0.4	0.4	0.7	0.5	0.7	0.5	0.5	0.7	0.6	0.5	0.5	0.3	0.7	
Joe Wright	0.6	0.5	0.5	0.5	0.5	0.4	0.6	0.3	0.1	0.2	0.3	0.2	0.1	0.3	0.4	0.6	0.6	0.5	0.3	0.6	0.6	0.3	0.3	0.4	0.2	0.6	0.5	0.5	0.3	0.3	0.5	0.6	0.4	0.5	0.2	0.5
Lake Irene	0.7	0.5	0.7	0.5	0.6	0.7	0.8	0.6	0.2	0.7	0.6	0.5	0.3	0.3	0.4	0.9	0.9	0.6	0.9	0.8	0.7	0.4	0.3	0.5	0.9	0.7	0.6	0.4	0.5	0.6	0.7	0.5	0.5	0.3	0.7	
Phantom Valley	0.5	0.5	0.7	0.5	0.8	0.4	0.7	0.4	0.3	0.5	0.5	0.6	0.4	0.4	0.3	0.7	0.7	0.4	0.8	0.6	0.5	0.4	0.6	0.5	0.7	0.8	0.4	0.4	0.4	0.5	0.7	0.5	0.5	0.3	0.6	
Willow Creek Pass	0.5	0.5	0.5	0.5	0.6	0.3	0.5	0.5	0.1	0.3	0.2	0.2	0.1	0.1	0.2	0.5	0.5	0.3	0.6	0.5	0.3	0.1	0.2	0.3	0.5	0.4	0.3	0.3	0.2	0.4	0.5	0.2	0.4	0.0	0.6	
Stillwater Creek	0.5	0.5	0.6	0.8	0.6	0.3	0.6	0.5	0.4	0.4	0.5	0.6	0.4	0.3	0.6	0.6	0.5	0.4	0.7	0.6	0.4	0.4	0.6	0.5	0.6	0.6	0.3	0.4	0.3	0.5	0.7	0.4	0.5	0.3	0.7	
Deadman Hill	0.7	0.4	0.7	0.4	0.3	0.3	0.6	0.5	0.2	0.6	0.5	0.3	0.3	0.3	0.3	0.7	0.7	0.5	0.6	0.6	0.3	0.3	0.4	0.7	0.5	0.8	0.6	0.6	0.5	0.7	0.5	0.5	0.3	0.5		
Willow Park	0.7	0.6	0.8	0.7	0.5	0.6	0.6	0.5	0.2	0.6	0.5	0.5	0.3	0.4	0.4	0.8	0.8	0.6	0.9	0.7	0.6	0.4	0.5	0.5	0.8	0.7	0.6	0.4	0.5	0.7	0.8	0.5	0.4	0.4	0.7	
Bear Lake	0.6	0.3	0.6	0.4	0.5	0.5	0.5	0.5	0.2	0.6	0.5	0.4	0.3	0.3	0.3	0.5	0.7	0.6	0.5	0.6	0.7	0.2	0.2	0.6	0.5	0.4	0.5	0.4	0.5	0.5	0.4	0.4	0.5	0.3	0.5	
Copeland Lake	0.2	0.1	0.2	0.3	0.1	0.4	0.2	0.2	0.2	0.3	0.4	0.5	0.6	0.5	0.3	0.3	0.3	0.4	0.3	0.2	0.3	0.5	0.6	0.3	0.3	0.4	0.1	0.3	0.4	0.4	0.4	0.3	0.4	0.3	0.4	0.3
University Camp	0.6	0.2	0.7	0.5	0.3	0.4	0.6	0.6	0.6	0.3	0.8	0.8	0.6	0.5	0.5	0.6	0.7	0.7	0.6	0.6	0.8	0.4	0.4	0.9	0.6	0.6	0.4	0.4	0.7	0.7	0.5	0.4	0.9	0.5	0.5	
Niwot	0.5	0.3	0.6	0.5	0.2	0.5	0.5	0.5	0.5	0.4	0.8	0.8	0.7	0.6	0.6	0.5	0.6	0.6	0.8	0.5	0.5	0.7	0.6	0.5	0.8	0.5	0.6	0.4	0.4	0.8	0.7	0.5	0.6	0.7	0.7	0.4
Lake Eldora	0.3	0.2	0.5	0.6	0.2	0.6	0.3	0.5	0.4	0.5	0.8	0.8	0.6	0.6	0.5	0.4	0.7	0.6	0.5	0.4	0.6	0.5	0.4	0.6	0.5	0.5	0.8	0.5	0.6	0.2	0.4	0.6	0.5	0.4	0.5	0.3
Copeland Lake	0.2	0.1	0.3	0.4	0.1	0.4	0.3	0.3	0.3	0.6	0.6	0.7	0.6	0.5	0.4	0.3	0.4	0.5	0.3	0.2	0.5	0.5	0.5	0.6	0.3	0.5	0.2	0.2	0.5	0.5	0.3	0.6	0.6	0.5	0.3	0.6
Deer Ridge	0.3	0.3	0.3	0.4	0.1	0.3	0.3	0.4	0.3	0.5	0.5	0.6	0.6	0.5	0.7	0.4	0.5	0.5	0.4	0.4	0.5	0.4	0.5	0.4	0.5	0.4	0.5	0.4	0.5	0.3	0.2	0.4	0.4	0.6	0.5	0.6
Hidden Valley	0.4	0.4	0.4	0.3	0.2	0.3	0.3	0.4	0.3	0.3	0.5	0.6	0.5	0.4	0.7	0.4	0.4	0.5	0.4	0.4	0.5	0.4	0.4	0.5	0.4	0.5	0.4	0.4	0.5	0.4	0.4	0.4	0.7	0.4	0.5	0.3
Lake Irene	0.7	0.6	0.9	0.7	0.5	0.6	0.7	0.8	0.5	0.3	0.6	0.5	0.4	0.3	0.4	0.4	0.8	0.6	0.9	0.9	0.7	0.5	0.5	0.8	0.7	0.6	0.4	0.5	0.6	0.8	0.6	0.5	0.4	0.7	0.8	
Long Draw Reservoir	0.7	0.5	0.9	0.7	0.5	0.7	0.8	0.7	0.3	0.7	0.6	0.7	0.4	0.5	0.4	0.8	0.6	0.6	0.6	0.8	0.7	0.8	0.3	0.5	0.6	0.9	0.7	0.7	0.7	0.6	0.8	0.6	0.5	0.7	0.3	0.6
Longs Peak	0.7	0.3	0.6	0.4	0.3	0.4	0.5	0.6	0.6	0.4	0.7	0.8	0.6	0.5	0.5	0.5	0.6	0.6	0.6	0.6	0.5	0.7	0.5	0.3	0.6	0.6	0.5	0.5	0.4	0.7	0.6	0.6	0.5	0.6	0.6	0.6
Milner Pass	0.7	0.6	0.9	0.8	0.6	0.7	0.6	0.9	0.5	0.3	0.6	0.5	0.5	0.3	0.4	0.4	0.9	0.8	0.6	0.8	0.7	0.4	0.5	0.5	0.8	0.7	0.6	0.5	0.5	0.7	0.8	0.5	0.6	0.4	0.8	
North Inlet Grand Lake	0.7	0.6	0.8	0.6	0.5	0.6	0.7	0.6	0.2	0.6	0.5	0.4	0.2	0.4	0.5	0.9	0.7	0.5	0.8	0.6	0.4	0.5	0.4	0.8	0.7	0.6	0.4	0.5	0.6	0.7	0.5	0.6	0.3	0.7		
Wild Basin	0.6	0.3	0.7	0.5	0.3	0.4	0.6	0.6	0.7	0.3	0.8	0.7	0.6	0.5	0.5	0.7	0.8	0.7	0.7	0.6	0.6	0.4	0.4	0.4	0.7	0.6	0.6	0.6	0.6	0.6	0.7	0.5	0.6	0.5	0.5	
Bennett Creek	0.4	0.3	0.4	0.4	0.1	0.4	0.3	0.4	0.2	0.5	0.4	0.6	0.5	0.5	0.4	0.4	0.5	0.3	0.5	0.4	0.4	0.4	0.4	0.6	0.4	0.4	0.5	0.3	0.2	0.7	0.4	0.4	0.7	0.2	0.8	
Big South	0.4	0.4	0.3	0.6	0.2	0.6	0.3	0.5	0.2	0.6	0.4	0.5	0.5	0.5	0.4	0.5	0.5	0.3	0.5	0.5	0.4	0.6	0.4	0.5	0.8	0.3	0.3	0.5	0.5	0.4	0.6	0.4	0.3	0.3		
Boulder Falls	0.4	0.2	0.5	0.5	0.3	0.5	0.4	0.5	0.6	0.3	0.9	0.8	0.8	0.6	0.5	0.5	0.8	0.6	0.6	0.8	0.8	0.6	0.4	0.4	0.4	0.5	0.5	0.3	0.4	0.6	0.5	0.4	0.4	0.9	0.5	0.3
Cameron Pass	0.7	0.6	0.9	0.7	0.5	0.6	0.7	0.8	0.5	0.3	0.6	0.5	0.5	0.3	0.4	0.4	0.8	0.9	0.6	0.8	0.8	0.6	0.4	0.5	0.5	0.8	0.6	0.4	0.5	0.7	0.7	0.5	0.5	0.3	0.7	
Chambers Lake	0.5	0.5	0.7	0.8	0.4	0.6	0.5	0.7	0.4	0.4	0.6	0.6	0.6	0.5	0.5	0.7	0.7	0.5	0.7	0.7	0.6	0.5	0.8	0.5	0.8	0.4	0.4	0.6	0.7	0.6	0.6	0.6	0.4	0.6		
Deadman Hill	0.7	0.5	0.6	0.4	0.3	0.3	0.8	0.6	0.5	0.1	0.4	0.4	0.2	0.2	0.3	0.3	0.6	0.7	0.5	0.6	0.6	0.3	0.3	0.3	0.6	0.4	0.5	0.7	0.5	0.7	0.4	0.3	0.5			
Granby	0.5	0.3	0.4	0.4	0.3	0.4	0.6	0.4	0.4	0.3	0.4	0.4	0.2	0.5	0.2	0.4	0.7	0.4	0.5	0.4	0.6	0.2	0.3	0.4	0.4	0.4	0.4	0.4	0.6	0.3	0.4	0.5	0.2	0.3		
Hourglass Lake	0.5	0.3	0.5	0.4	0.2	0.3	0.5	0.5	0.5	0.4	0.7	0.8	0.6	0.5	0.4	0.5	0.6	0.7	0.5	0.5	0.6	0.7	0.5	0.6	0.7	0.5	0.6	0.5	0.4	0.6	0.4	0.7	0.5	0.7	0.3	
McIntyre	0.7	0.5	0.6	0.5	0.4	0.5	0.7	0.7	0.5	0.4	0.7	0.7	0.5	0.5	0.5	0.4	0.6	0.8	0.6	0.7	0.6	0.7	0.4	0.5	0.7	0.7	0.7	0.6	0.6	0.6	0.6	0.5	0.7	0.4	0.5	
Park View	0.6	0.6	0.7	0.7	0.5	0.7	0.5	0.8	0.4	0.3	0.5	0.5	0.4	0.3	0.4	0.4	0.8	0.6	0.6	0.8	0.7	0.5	0.4	0.4	0.7	0.6	0.5	0.3	0.4	0.4	0.6	0.4	0.4	0.9		
Red Feather	0.5	0.4	0.5	0.5	0.2	0.4	0.5	0.5	0.4	0.4	0.4	0.6	0.5	0.6	0.6	0.7	0.5	0.5	0.5	0.5	0.5	0.7	0.6	0.4	0.5	0.6	0.7	0.4	0.7	0.5	0.4	0.5	0.6	0.3		
University Camp	0.5	0.5	0.5	0.5	0.4	0.5	0.5	0.4	0.5	0.3	0.9	0.7	0.7	0.6	0.5	0.4	0.5	0.7	0.6	0.6	0.6	0.6	0.2	0.4	0.9	0.5	0.6	0.4	0.5	0.5	0.7	0.4	0.5	0.3	0.4	
Ward	0.3	0.2	0.3	0.3	0.0	0.3	0.3	0.4	0.3	0.4	0.5	0.7	0.5	0.5	0.6	0.5	0.4	0.3	0.6	0.4	0.3	0.5	0.8	0.3	0.5	0.3	0.4	0.3	0.2	0.7	0.4	0.4	0.6	0.3	0.3	
Willow Creek Pass	0.7	0.5	0.7	0.6	0.6	0.7	0.5	0.7	0.5	0.3	0.5	0.4	0.3	0.3	0.3	0.3	0.7	0.6	0.6	0.8	0.7	0.5	0.3	0.3	0.3	0.7	0.6	0.5	0.3	0.3	0.5	0.9	0.3	0.4	0.3	

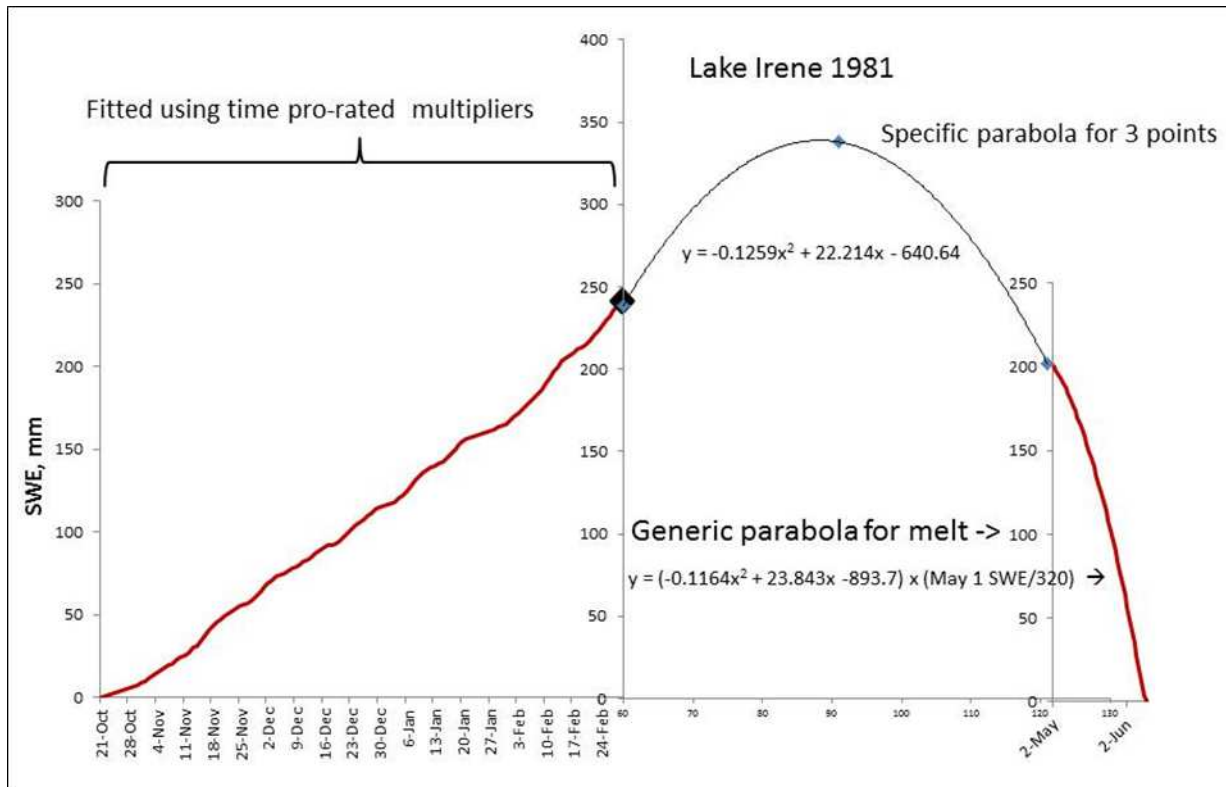


Figure A.1. Fitting the median niveograph to observed data for a given year using different techniques for accumulation, peak, and melt phases.

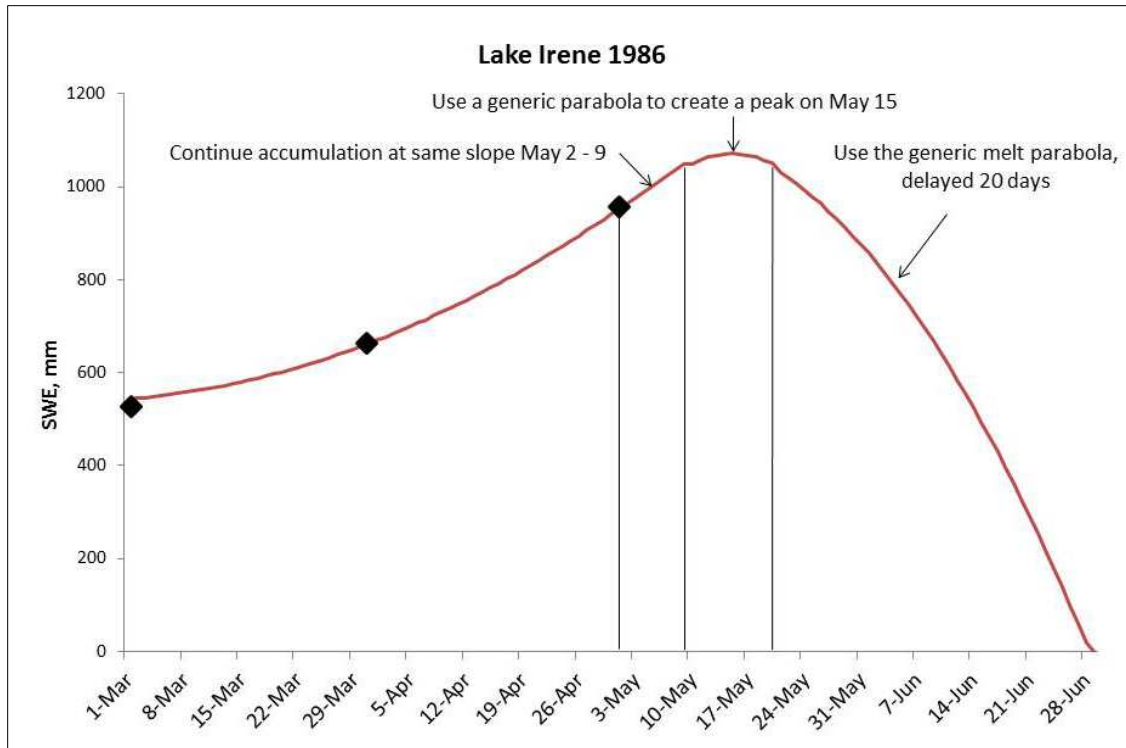


Figure A.2. Niveograph estimation procedure showing extension of the peak phase and delaying the melt phase when SWE is still increasing on May 1.

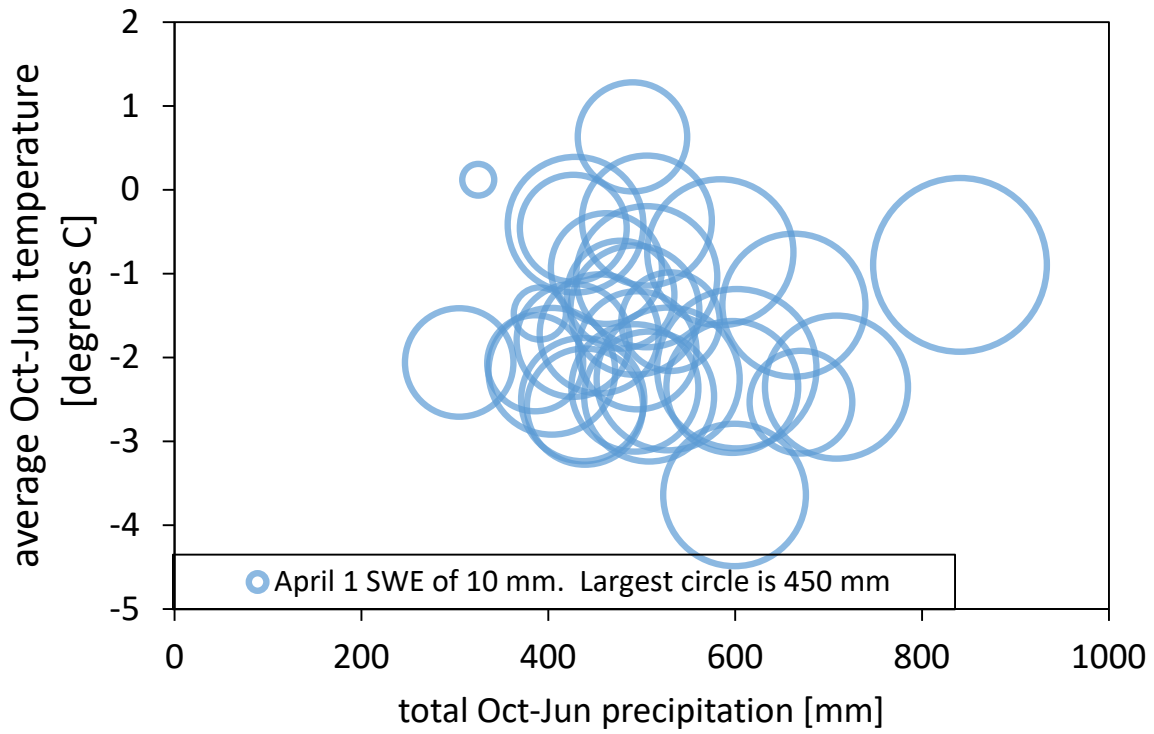


Figure A.3. April 1 SWE for each snow year, 1986-2015, at Phantom Valley SNOTEL, in relation to annual variations in total October-June precipitation and average October-June temperature as recorded at the SNOTEL station. Width of circle denotes magnitude of April 1 SWE.

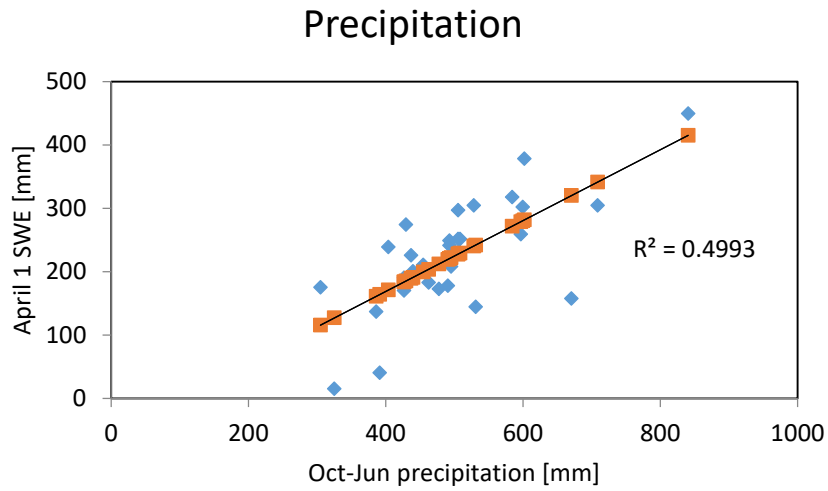
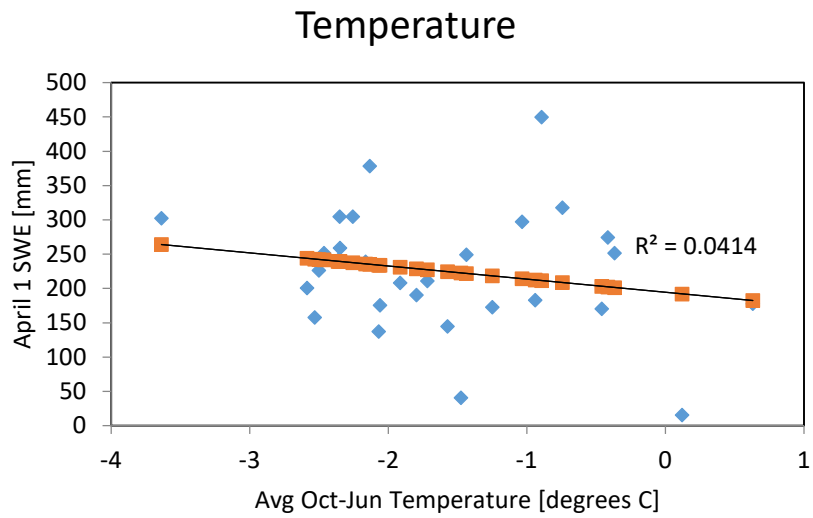


Figure A.4. Regression analyses of median April 1 SWE, 1981-2015, on October-June a) temperature and b) precipitation at Phantom Valley SNOTEL.

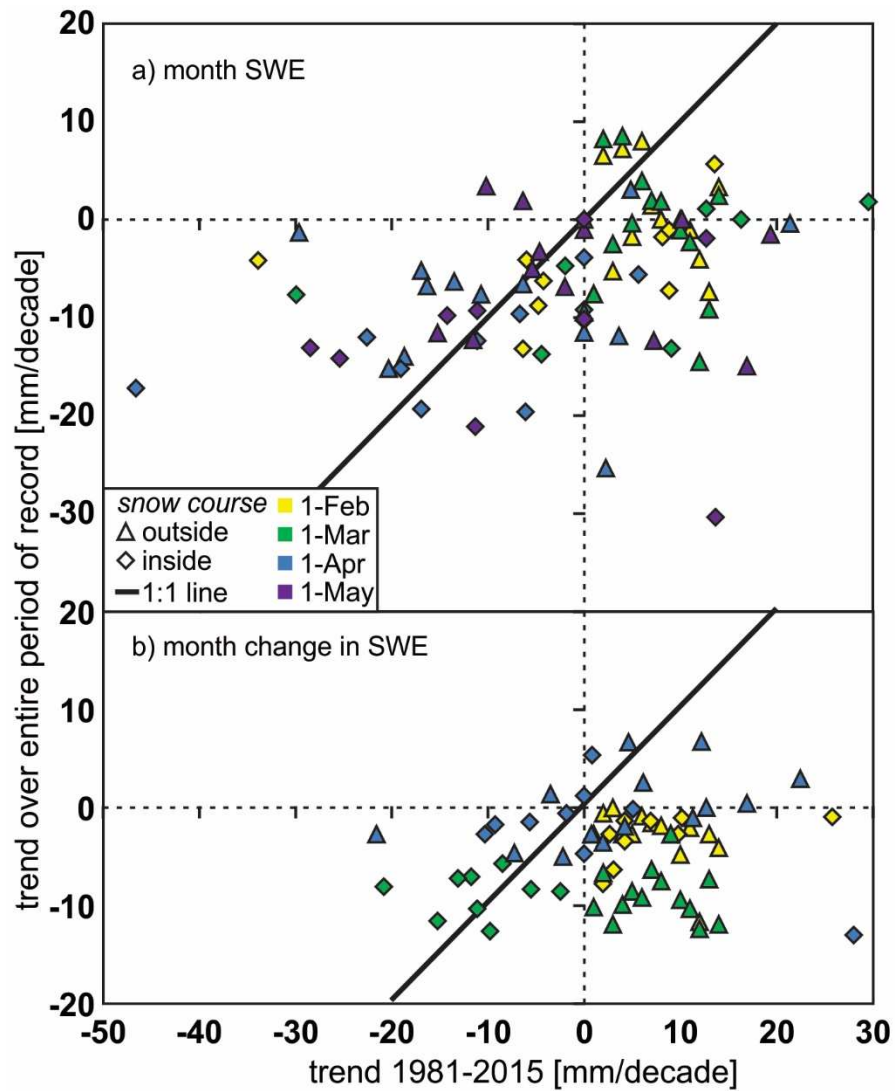


Figure A.5. a) Comparison of trends in SWE on first of month at snow courses inside and outside Rocky Mountain National Park for two different periods: 1981-2015, and entire period of record. b) Same comparison for trends in monthly change in SWE.

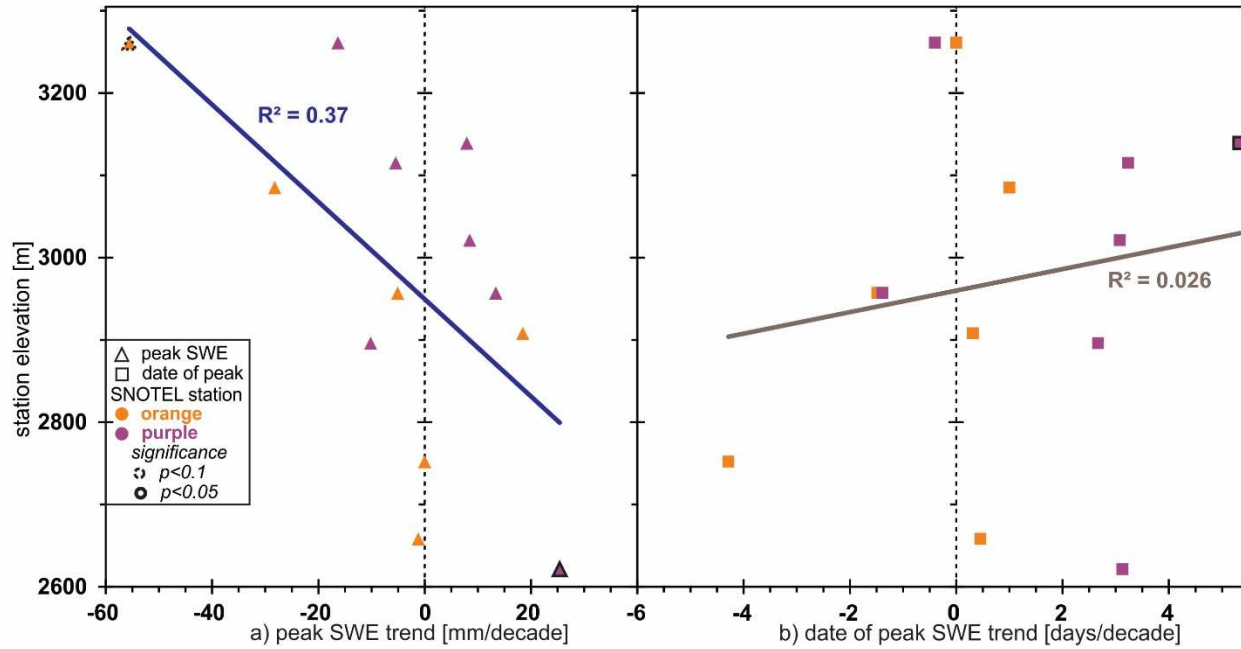


Figure A.6. a) Trends in annual peak SWE at SNOTEL stations in relation to elevation. b) Trends in date of peak SWE at SNOTEL stations in relation to elevation.

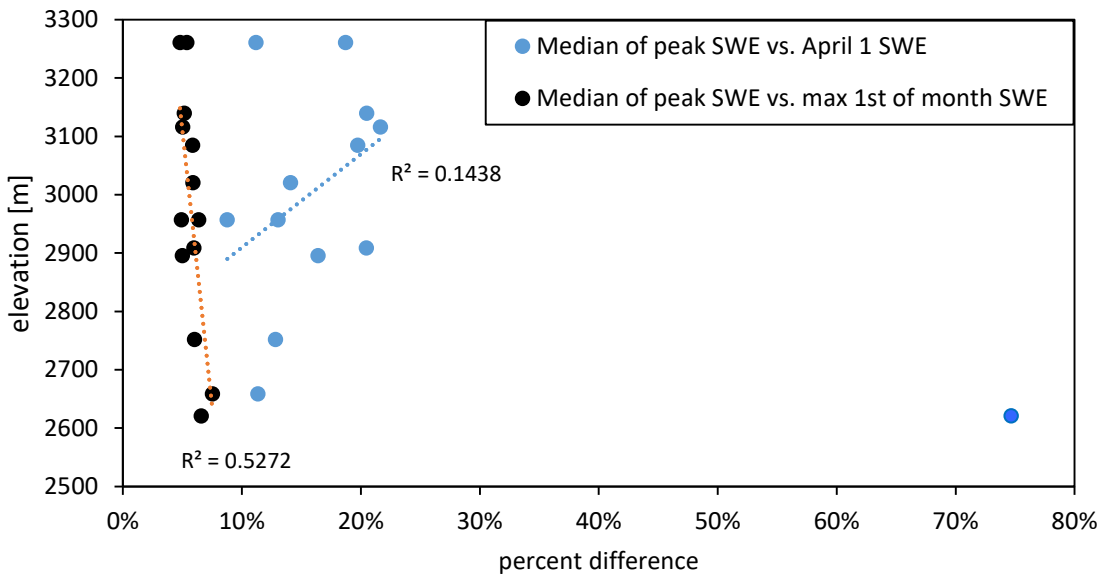


Figure A.7. Results of comparison of observed annual peak SWE with April 1 SWE, and with the maximum of first-of-month SWE values, in relation to elevation. Circles represent median differences over the period 1981-2015. Outlier is Copeland Lake. Data are listed in Table A.3.

Table A.3. Percent difference between observed peak SWE and indicated statistic, as percent of peak SWE.

station	peak SWE vs. April 1st SWE					peak SWE vs. max 1st of the month SWE (Feb-May)					peak SWE vs. max 1st of the month SWE (Feb-June)					Elevation [m]
	max	mean	median	std dev	min	max	mean	median	std dev	min	max	mean	median	std dev	min	
Joe Wright	56%	22%	20%	12%	1%	29%	7.6%	6.3%	6.2%	0%	12%	5.6%	5.9%	3.1%	0%	3085
Lake Irene	37%	13%	11%	9%	1%	15%	5.7%	5.9%	3.9%	0%	11%	5.2%	4.8%	3.6%	0%	3261
Willow Park	59%	21%	19%	13%	1%	28%	7.6%	5.8%	6.0%	0%	19%	6.6%	5.4%	4.8%	0%	3261
Bear Lake	41%	18%	16%	11%	1%	15%	6.0%	5.0%	4.6%	0%	15%	6.0%	5.0%	4.6%	0%	2896
Phantom Valley	92%	17%	13%	20%	0%	21%	7.4%	6.0%	5.9%	0%	21%	7.4%	6.0%	5.9%	0%	2752
Stillwater Creek	85%	20%	11%	23%	0%	23%	7.7%	7.5%	5.7%	0%	23%	7.7%	7.5%	5.7%	0%	2659
Roach	44%	15%	13%	11%	1%	28%	6.9%	5.5%	5.5%	1%	14%	6.1%	4.9%	3.9%	1%	2957
Willow Creek Pass	53%	21%	20%	11%	2%	18%	6.1%	6.0%	4.3%	0%	15%	5.7%	6.0%	3.8%	0%	2909
Deadman Hill	60%	23%	22%	11%	5%	38%	6.9%	5.2%	6.6%	0%	12%	5.6%	5.0%	3.4%	0%	3116
University Camp	49%	22%	20%	12%	1%	18%	6.5%	5.3%	5.1%	0%	18%	6.0%	5.2%	4.9%	0%	3140
Niwot	51%	17%	14%	15%	0%	23%	7.1%	6.2%	5.6%	0%	23%	6.7%	5.9%	5.5%	0%	3021
Lake Eldora	60%	15%	9%	15%	1%	31%	8.3%	6.4%	8.0%	1%	31%	8.3%	6.4%	8.0%	1%	2957
Copeland Lake	100%	64%	75%	34%	0%	36%	9.2%	6.6%	9.5%	0%	36%	9.2%	6.6%	9.5%	0%	2621
average	60%	22%	20%	15%	1%	25%	7%	6%	6%	0%	19%	7%	6%	5%	0%	

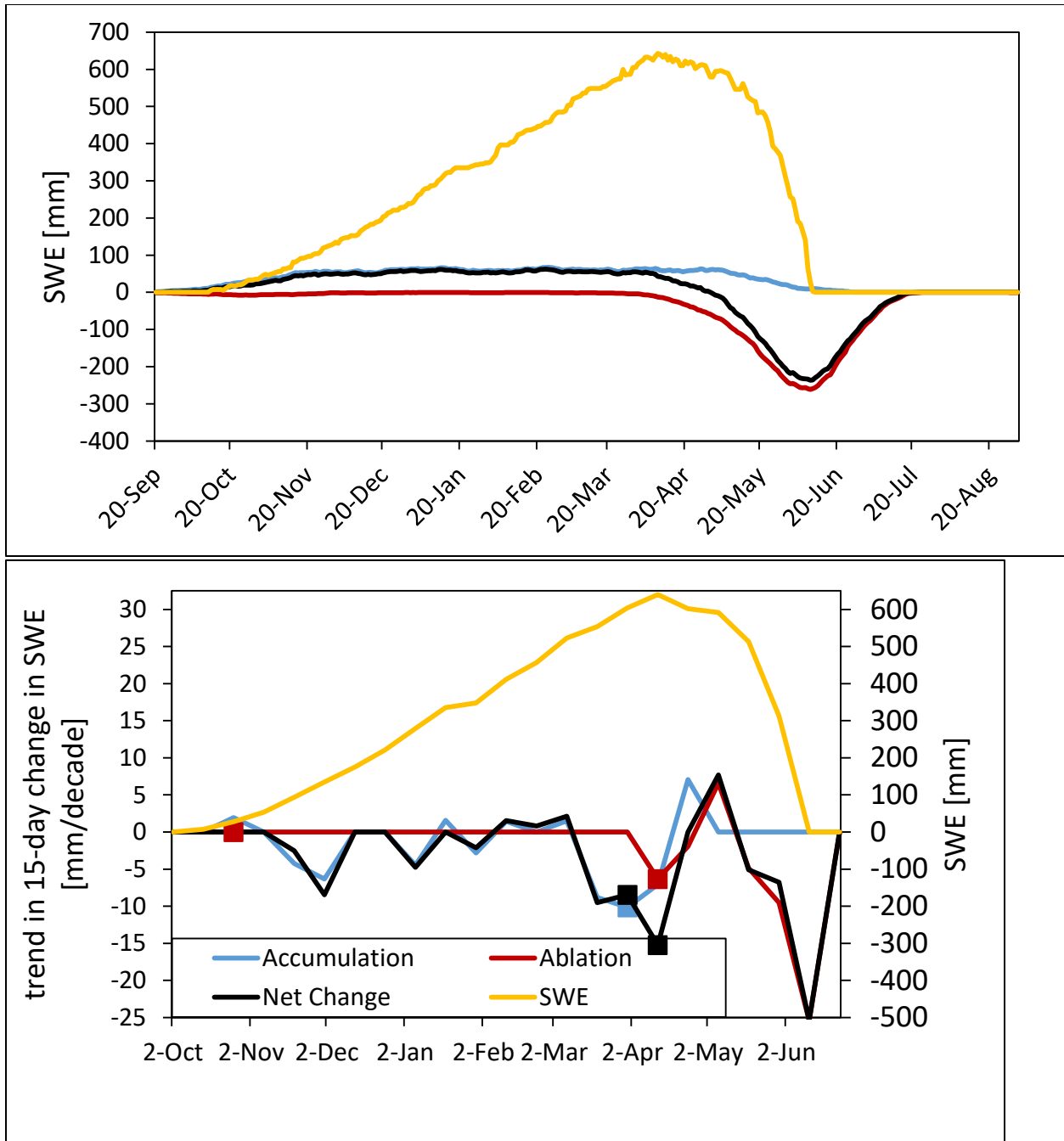


Figure A.8. a) Median SWE, 1981-2015, and average values for 15-day changes in SWE at Lake Irene SNOTEL. b) Trends in 15-day change in SWE. Square denotes statistically significant trend.

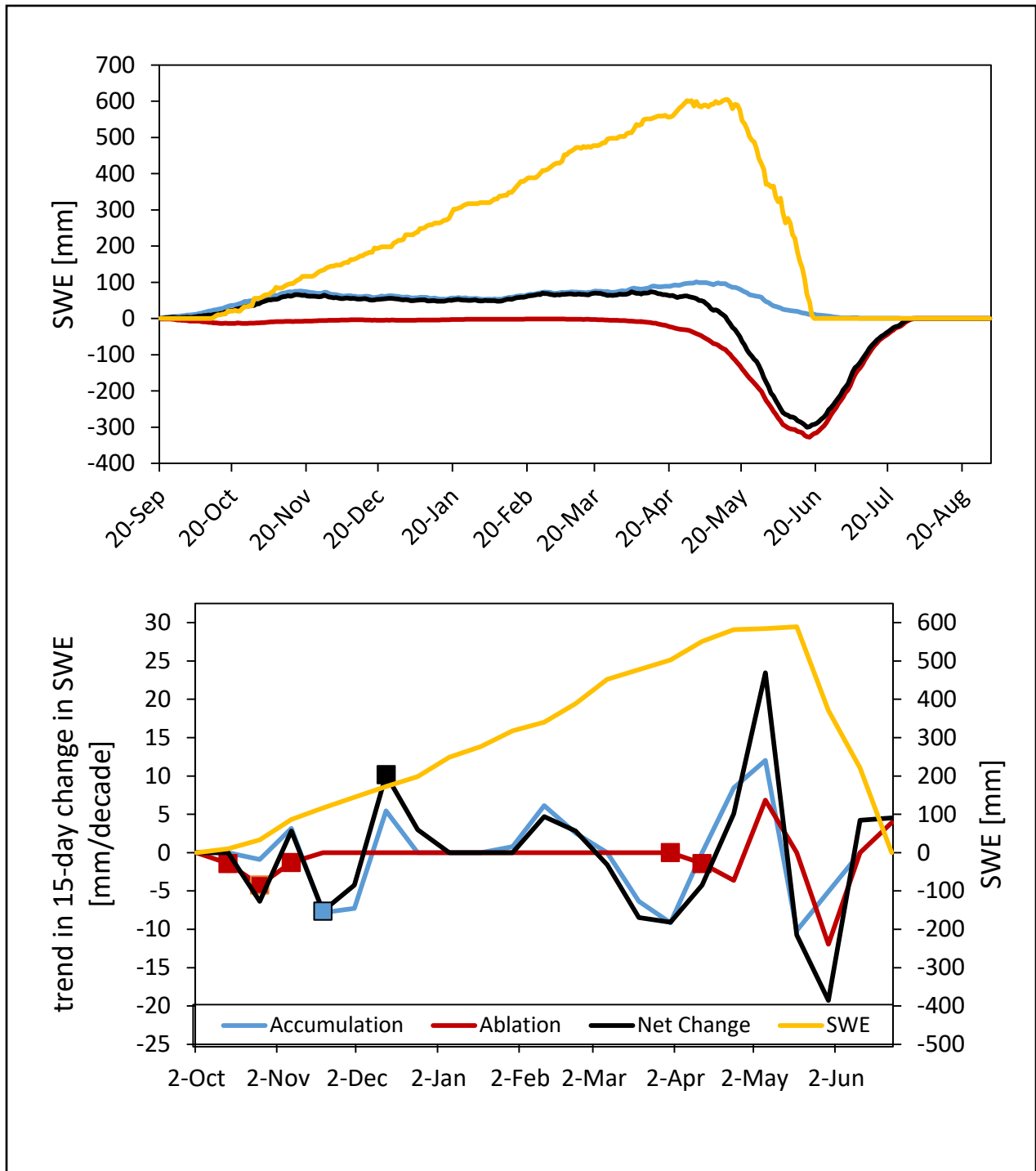


Figure A.9. a) Median SWE, 1981-2015, and average values for 15-day changes in SWE at Joe Wright SNOTEL. b) Trends in 15-day change in SWE. Square denotes statistically significant trend.

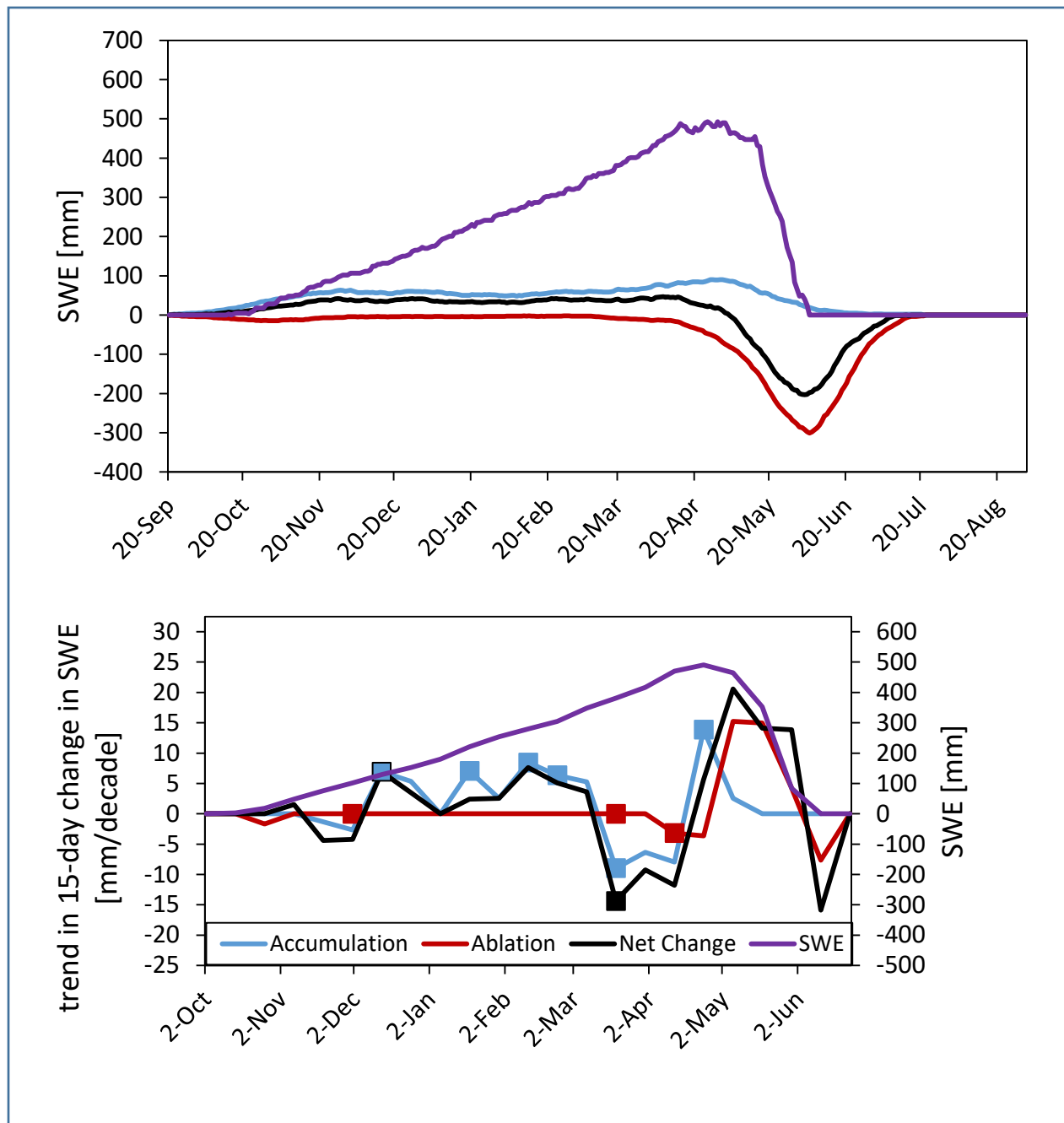


Figure A.10. a) Median SWE, 1981-2015, and average values for 15-day changes in SWE at Willow Park SNOTEL. b) Trends in 15-day change in SWE. Square denotes statistically significant trend.

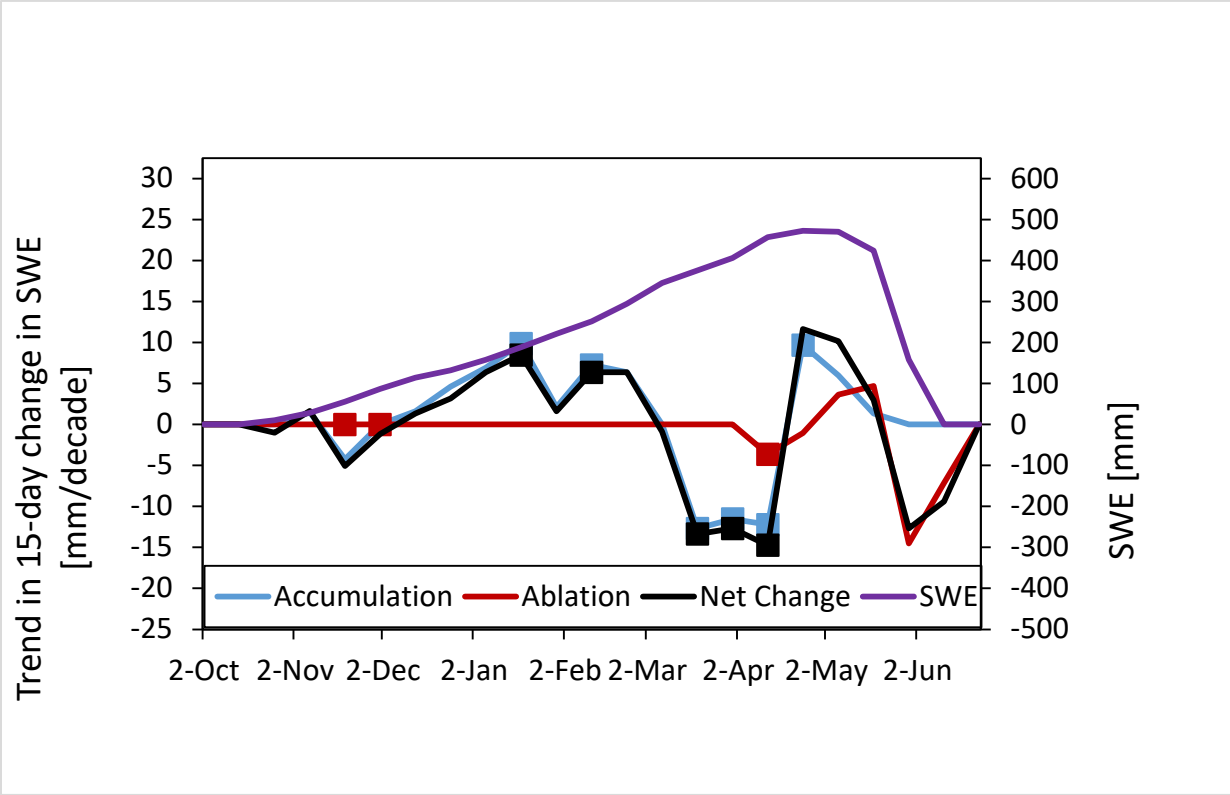
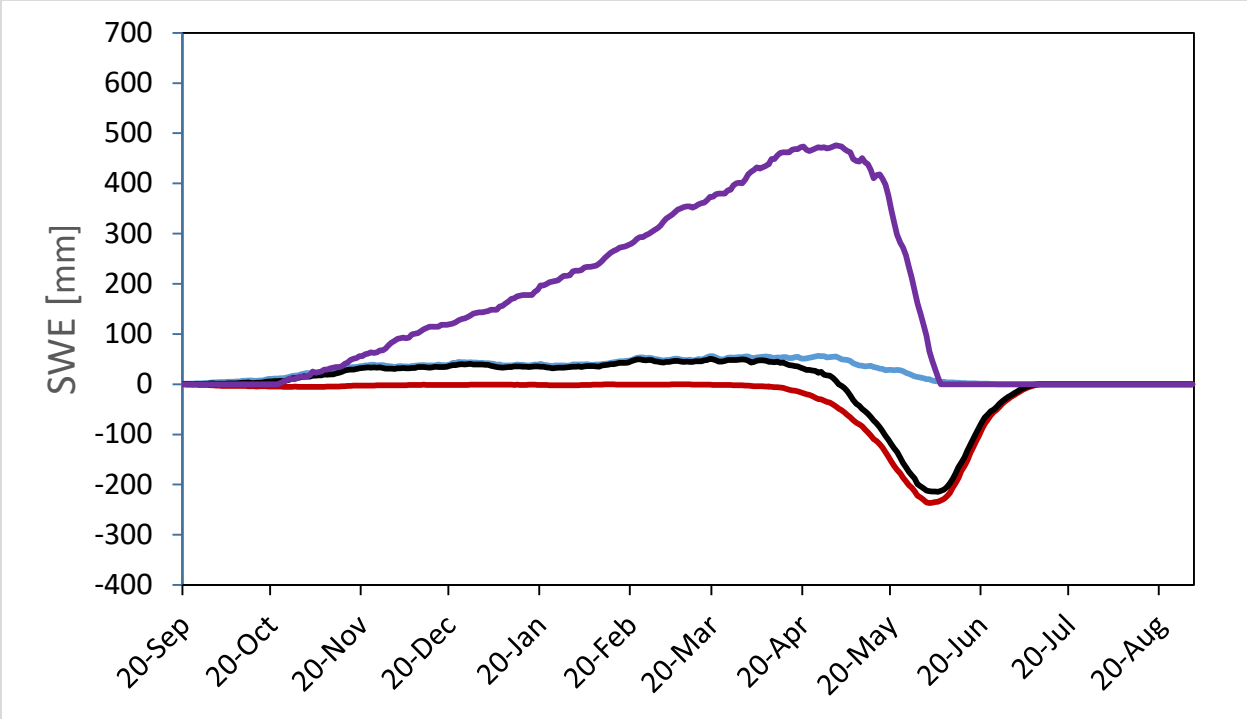


Figure A.11. a) Median SWE, 1981-2015, and average values for 15-day changes in SWE at Bear Lake SNOTEL. b) Trends in 15-day change in SWE. Square denotes statistically significant trend.

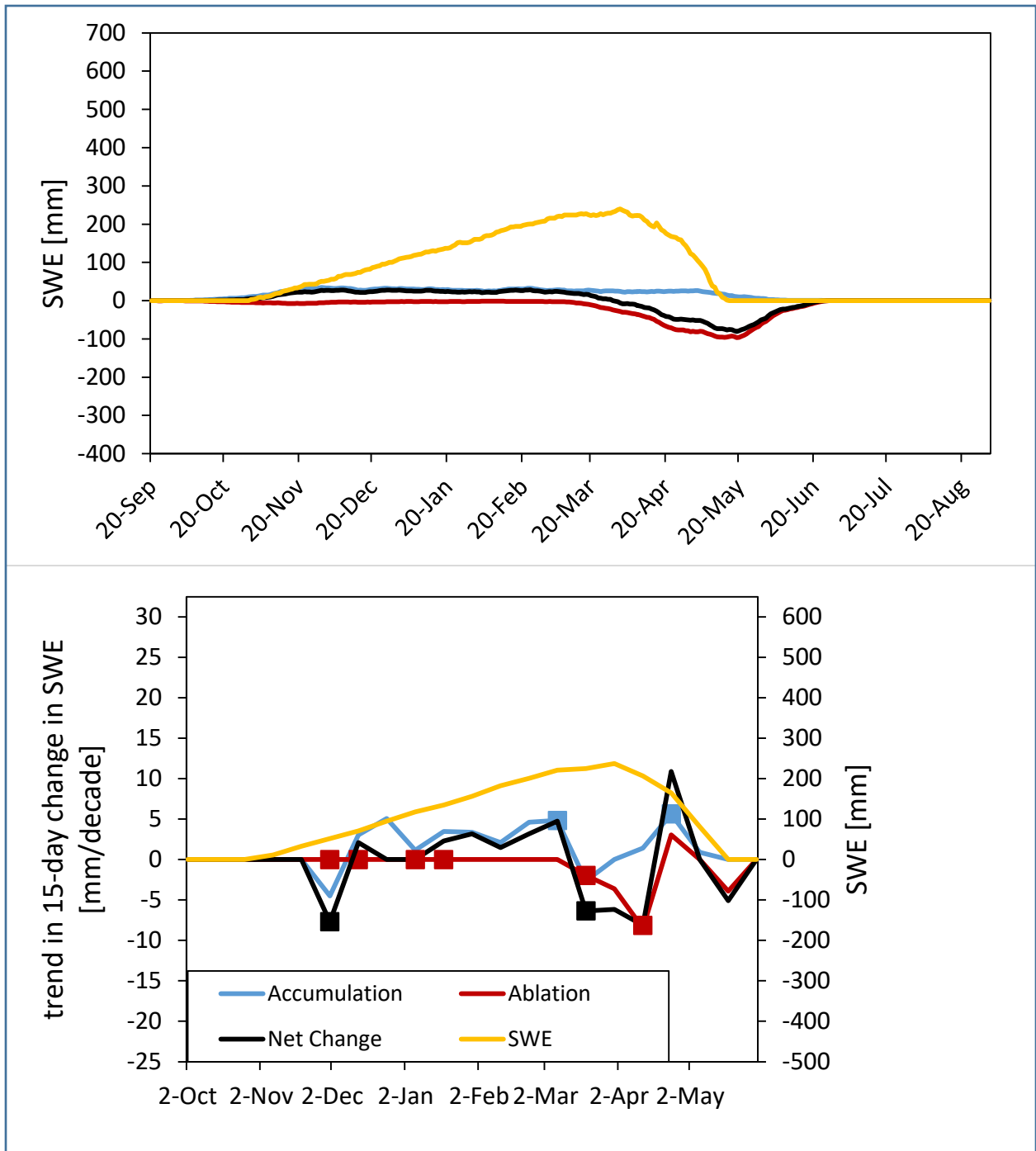


Figure A.12. a) Median SWE, 1981-2015, and average values for 15-day changes in SWE at Phantom Valley SNOTEL. b) Trends in 15-day change in SWE. Square denotes statistically significant trend.

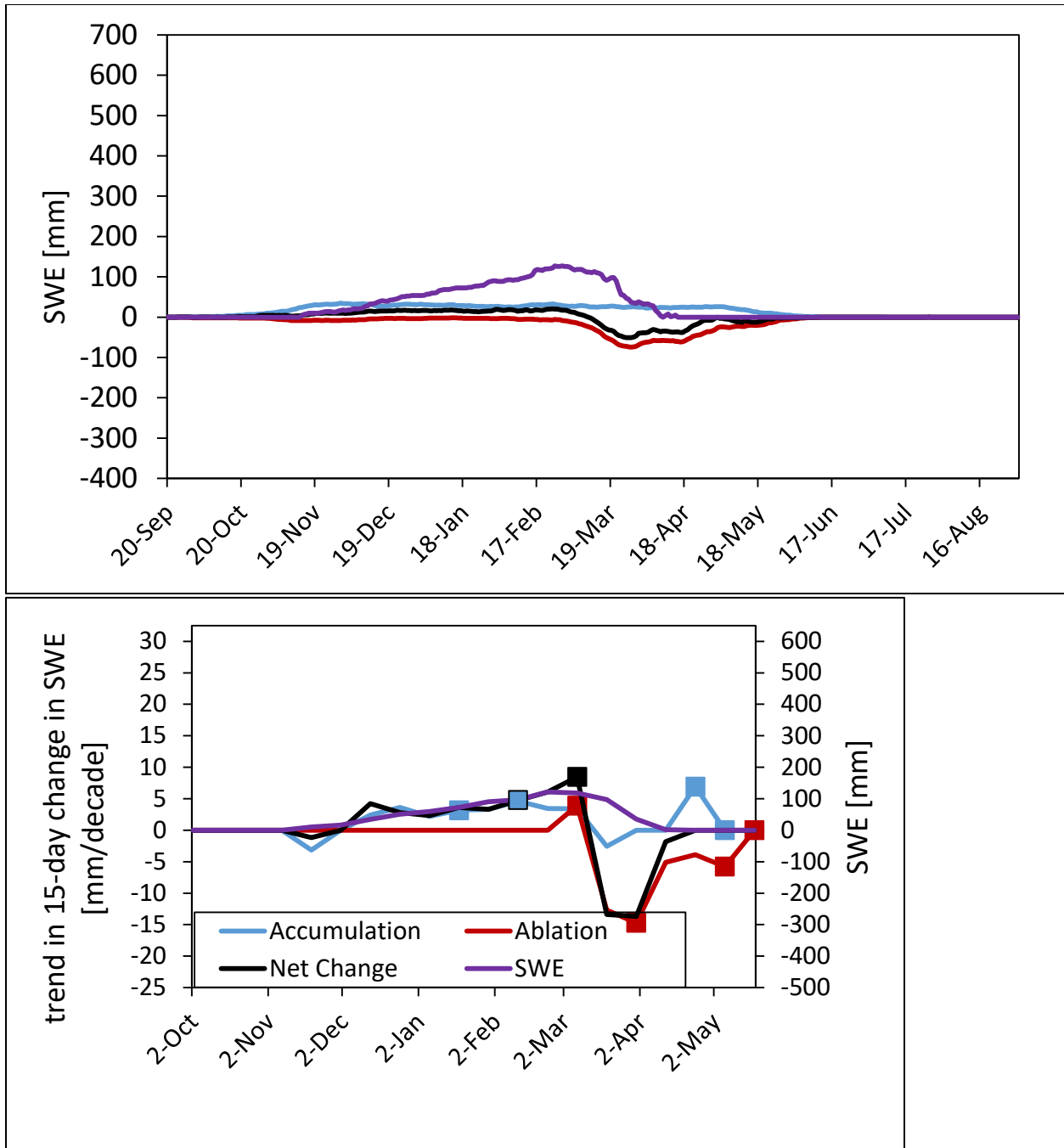


Figure A.13. a) Median SWE, 1981-2015, and average values for 15-day changes in SWE at Copeland Lake SNOTEL. b) Trends in 15-day change in SWE. Square denotes statistically significant trend.

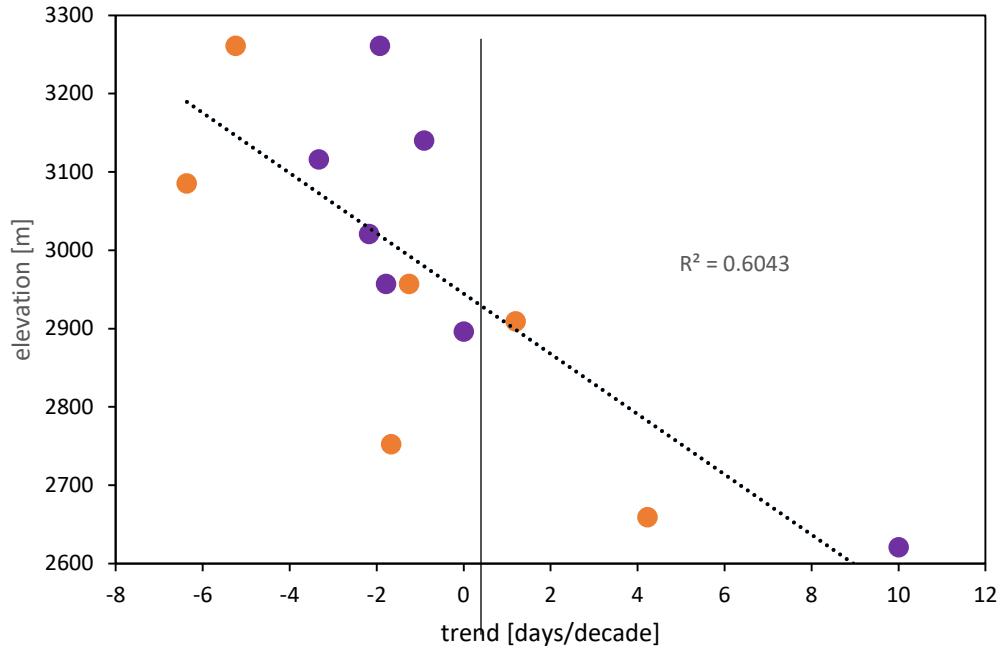


Figure A.14. Trends in number of days per year with SWE >100 mm at SNOTEL stations, 1981-2015, in relation to elevation.

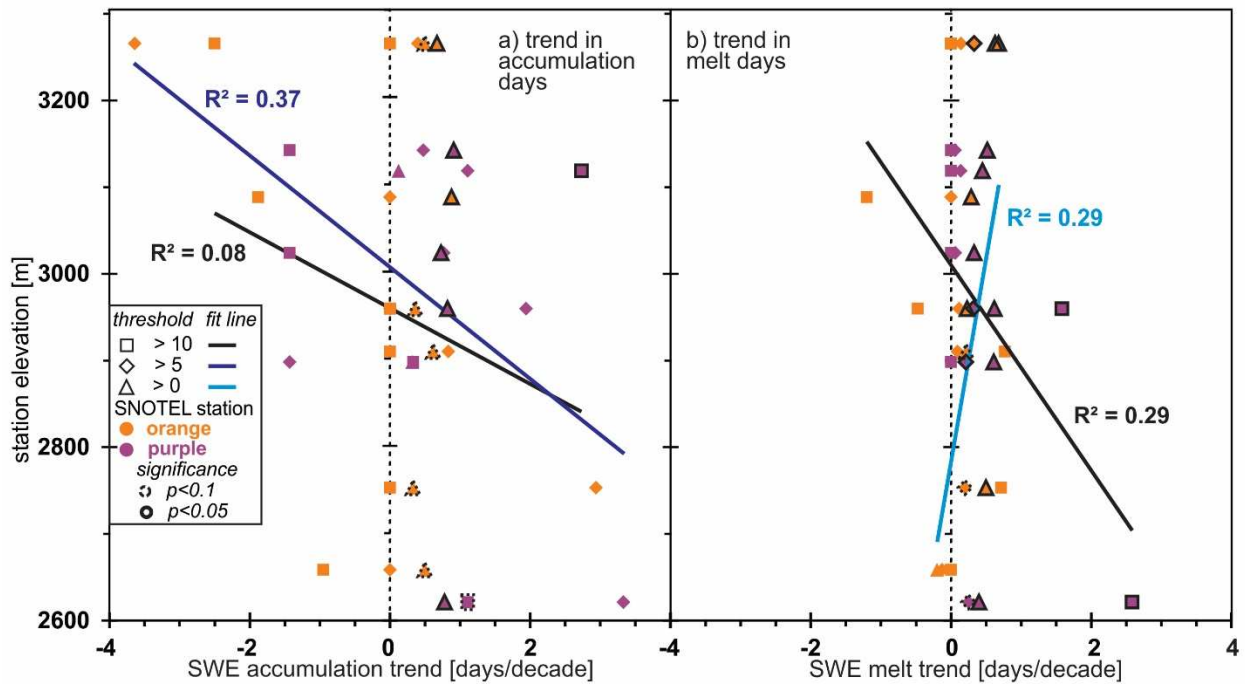


Figure A.15. Trends in number of days with a) SWE accumulation and b) SWE ablation greater than 0, 5 and 10 mm, 1981-2015, in relation to elevation.

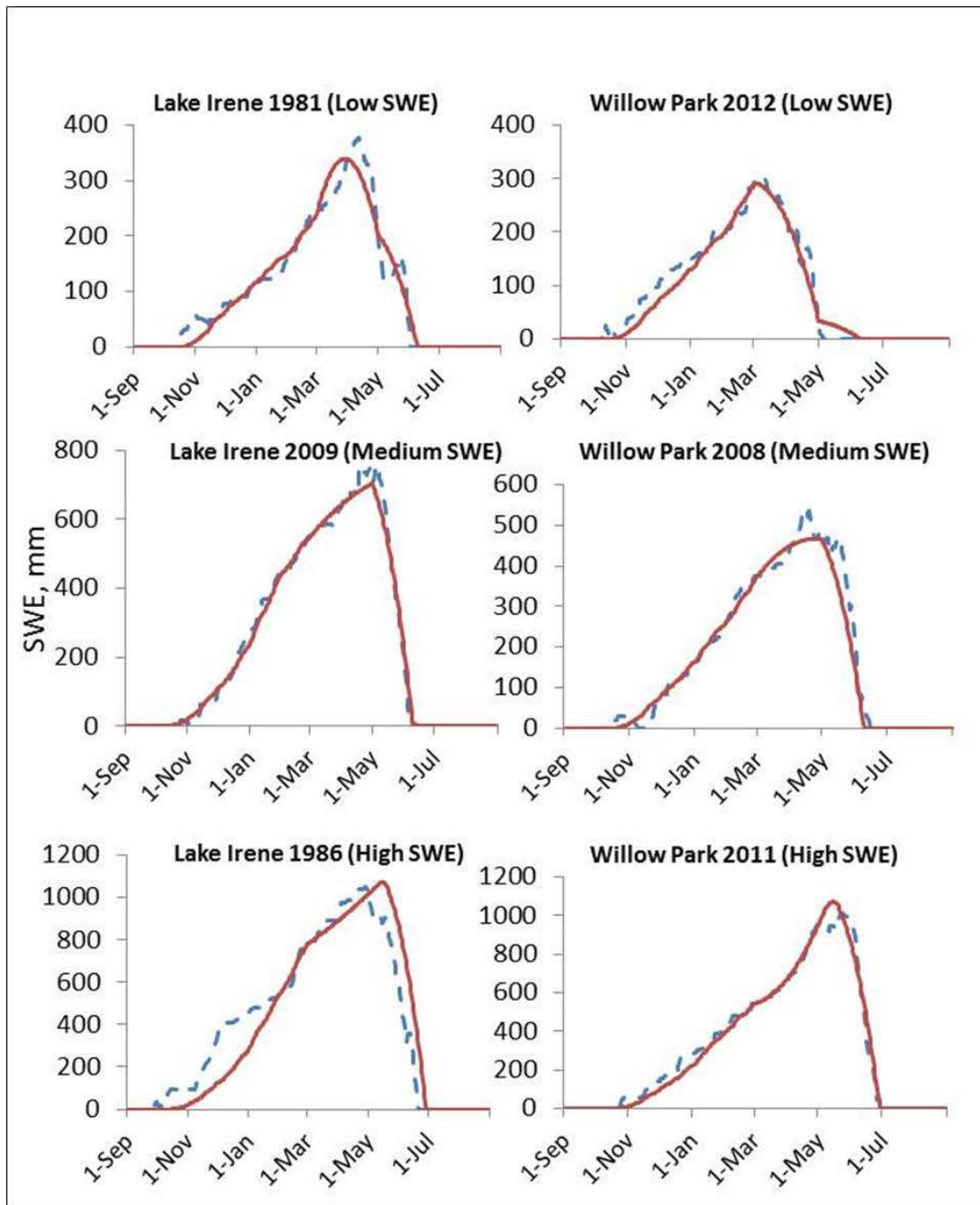


Figure A.16. Estimated (solid) and observed (dashed) niveographs for two SNOTEL stations for low, medium, and high SWE years.

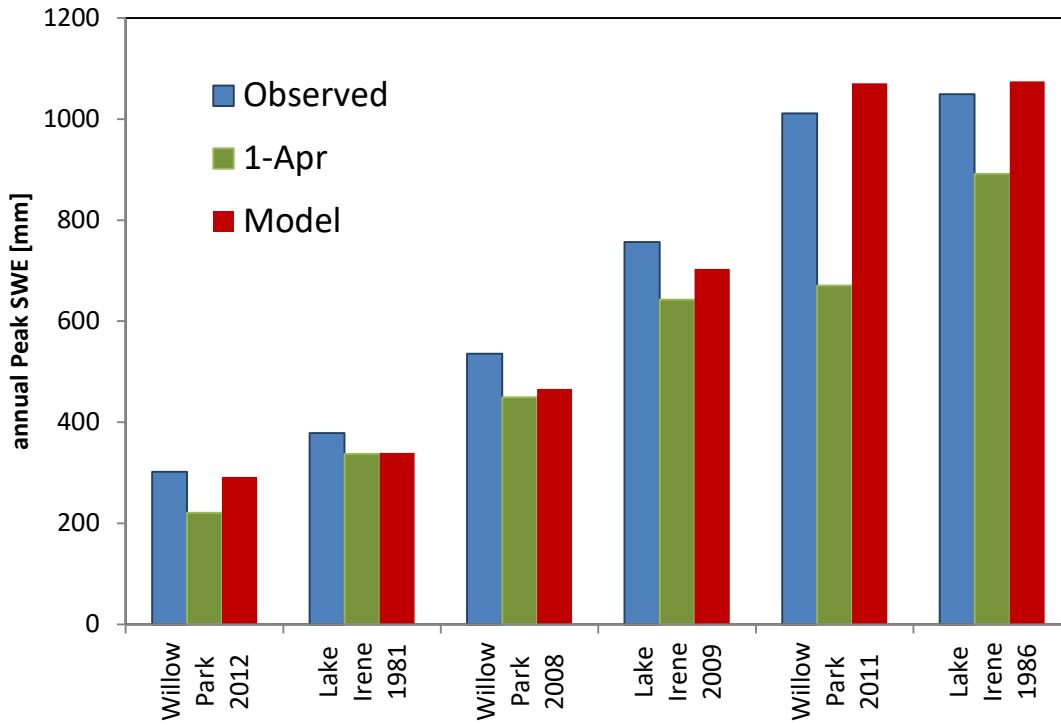


Figure A.17. Annual peak SWE from observed data, from the assumption of April 1 peak SWE, and from the estimated niveographs.

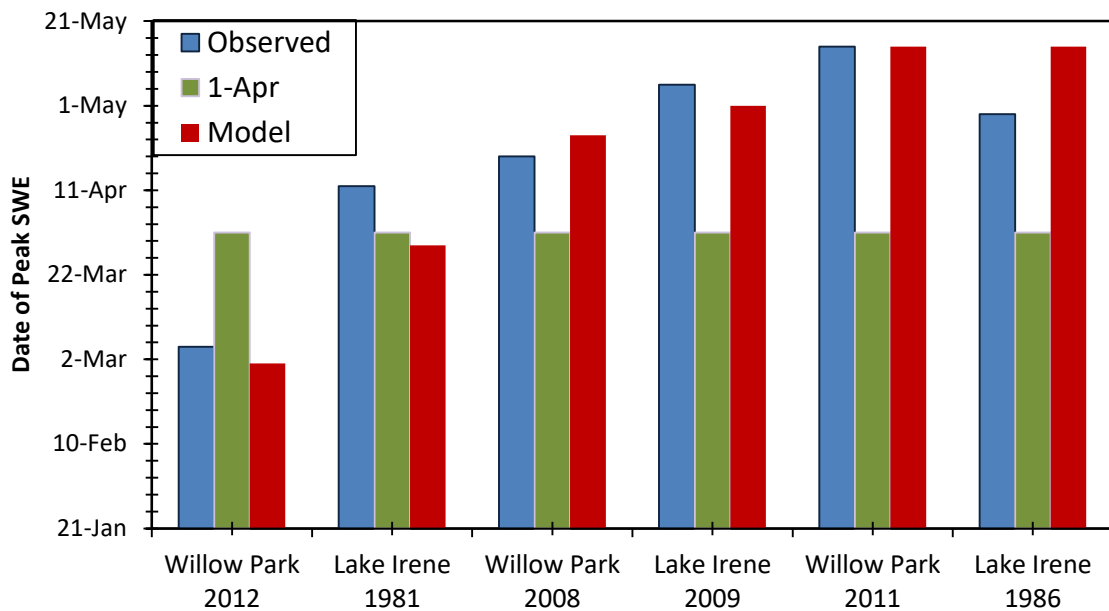


Figure A.18. Dates of peak SWE from observed data, from the assumption of April 1 peak SWE, and from the estimated niveographs.

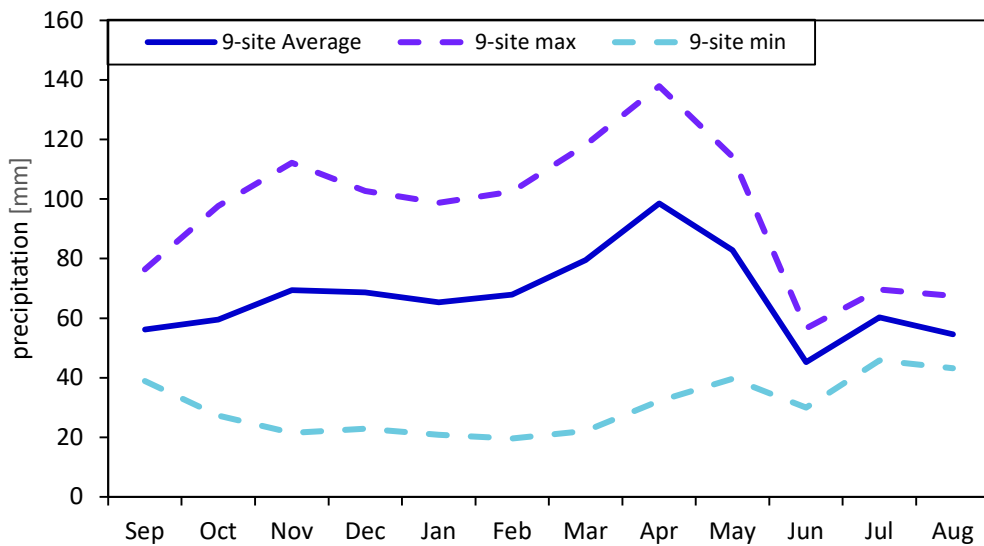


Figure A.19. Average, maximum, and minimum monthly precipitation, 1981-2015, at 6 SNOTEL stations and 3 weather stations.

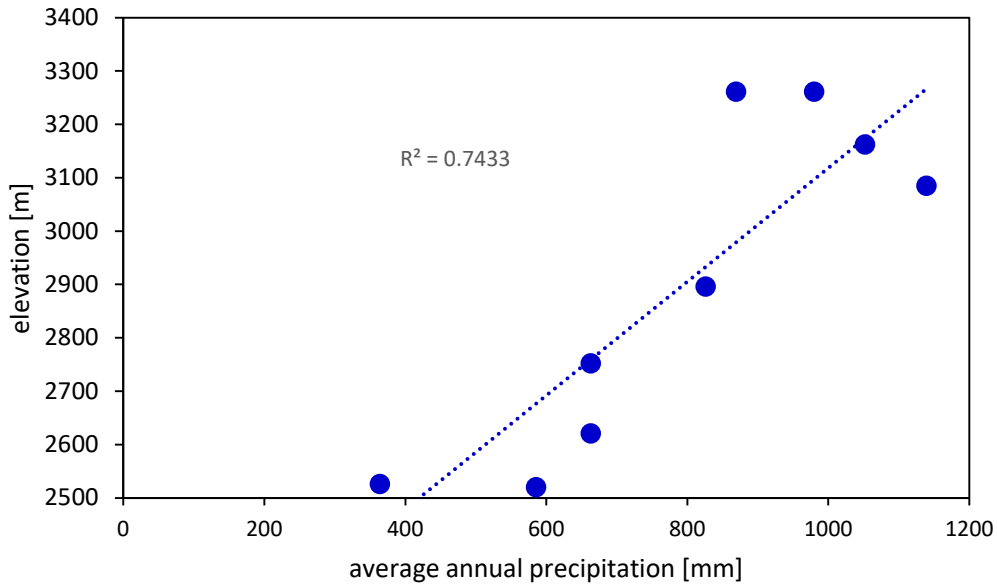


Figure A.20. Average annual precipitation, 1981-2015, at 6 SNOTEL and 3 weather stations, in relation to elevation.

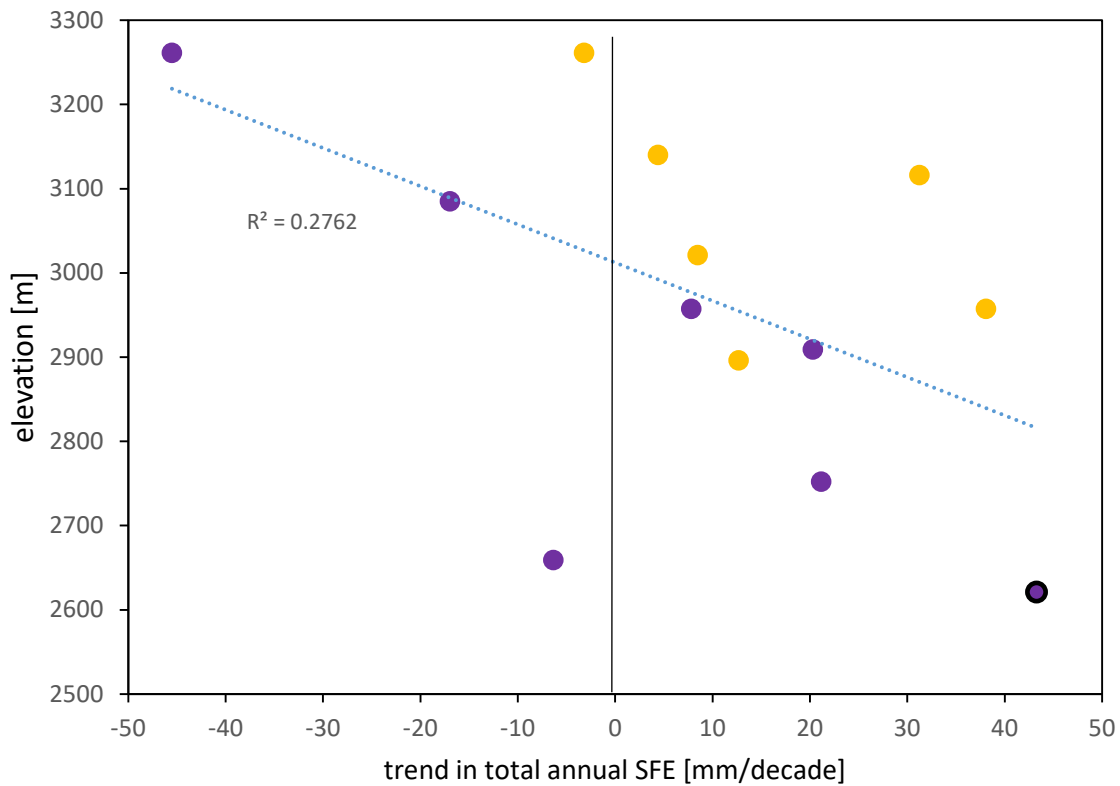


Figure A.21. Trends in total annual snowfall equivalent (total October-June SWE accumulation), 1981-2015, at 13 SNOTEL stations, in relation to elevation.

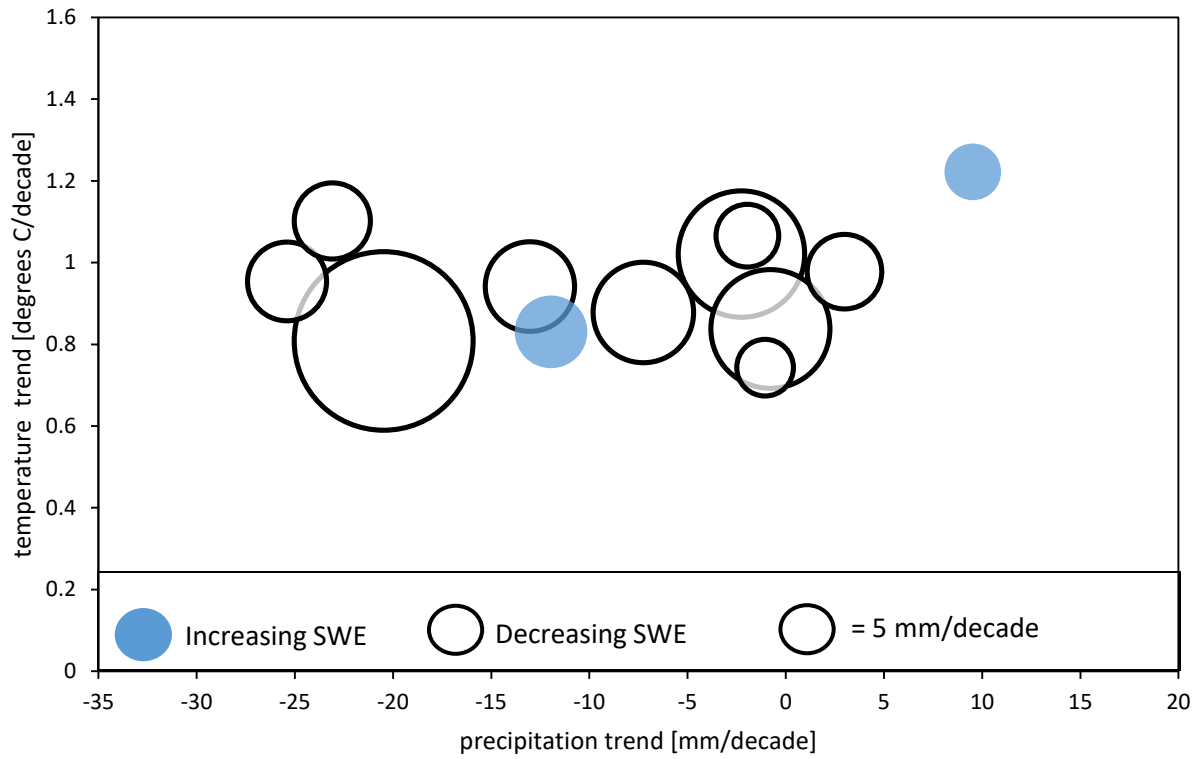


Figure A.22. Trends in April 1 SWE at SNOTELs in relation to trends in precipitation and temperature at the SNOTELs.

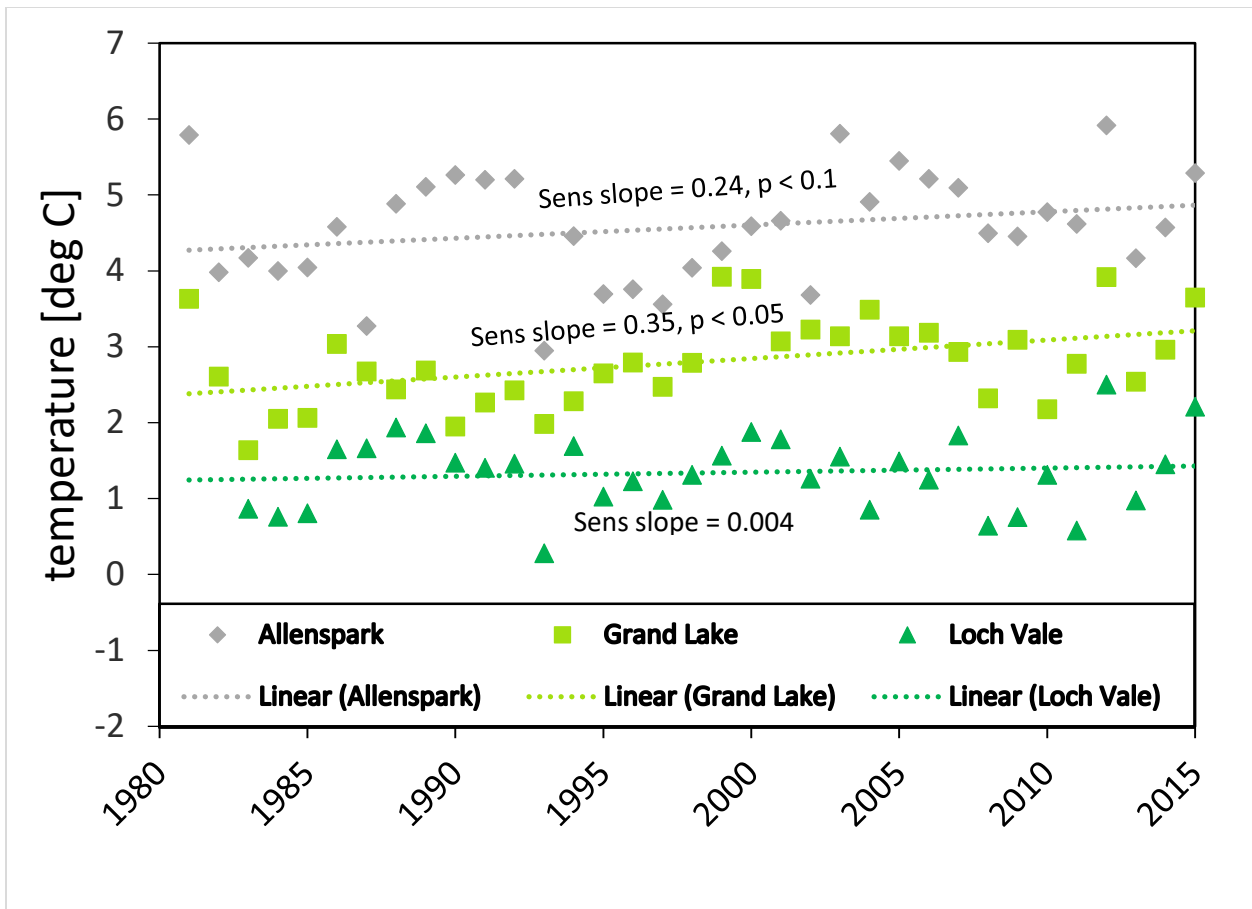


Figure A.23. Average annual temperature at three weather stations, 1981-2013. Dotted lines are linear trend lines (degrees C/decade), which closely match indicated Sens slope lines.

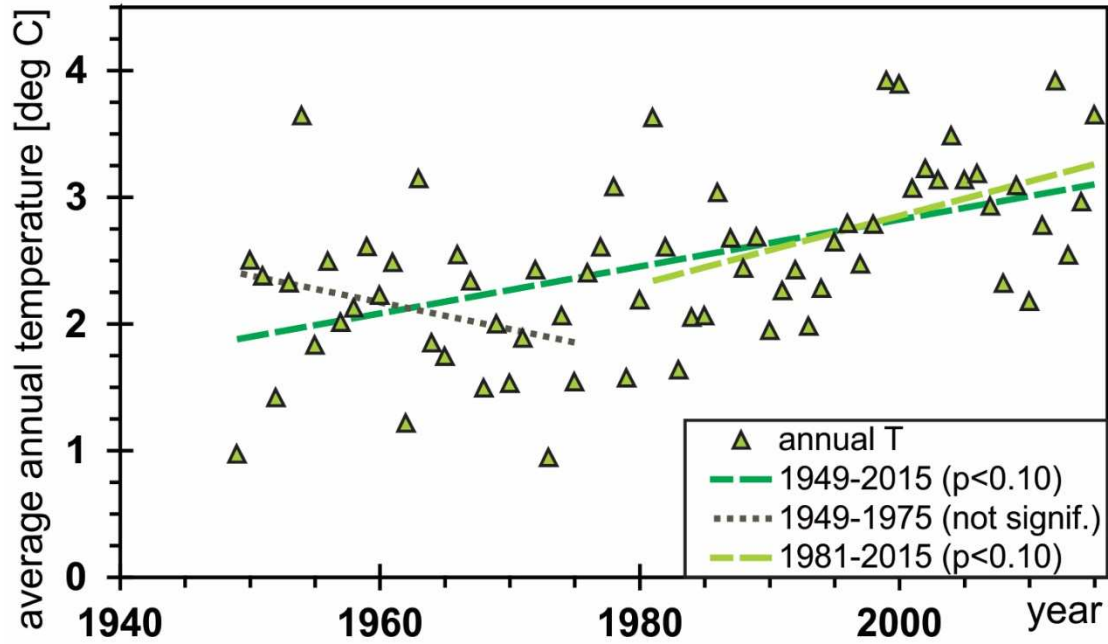


Figure A.24. Average annual temperature at Grand Lake, 1949-2015, with trends for entire and selected partial periods.

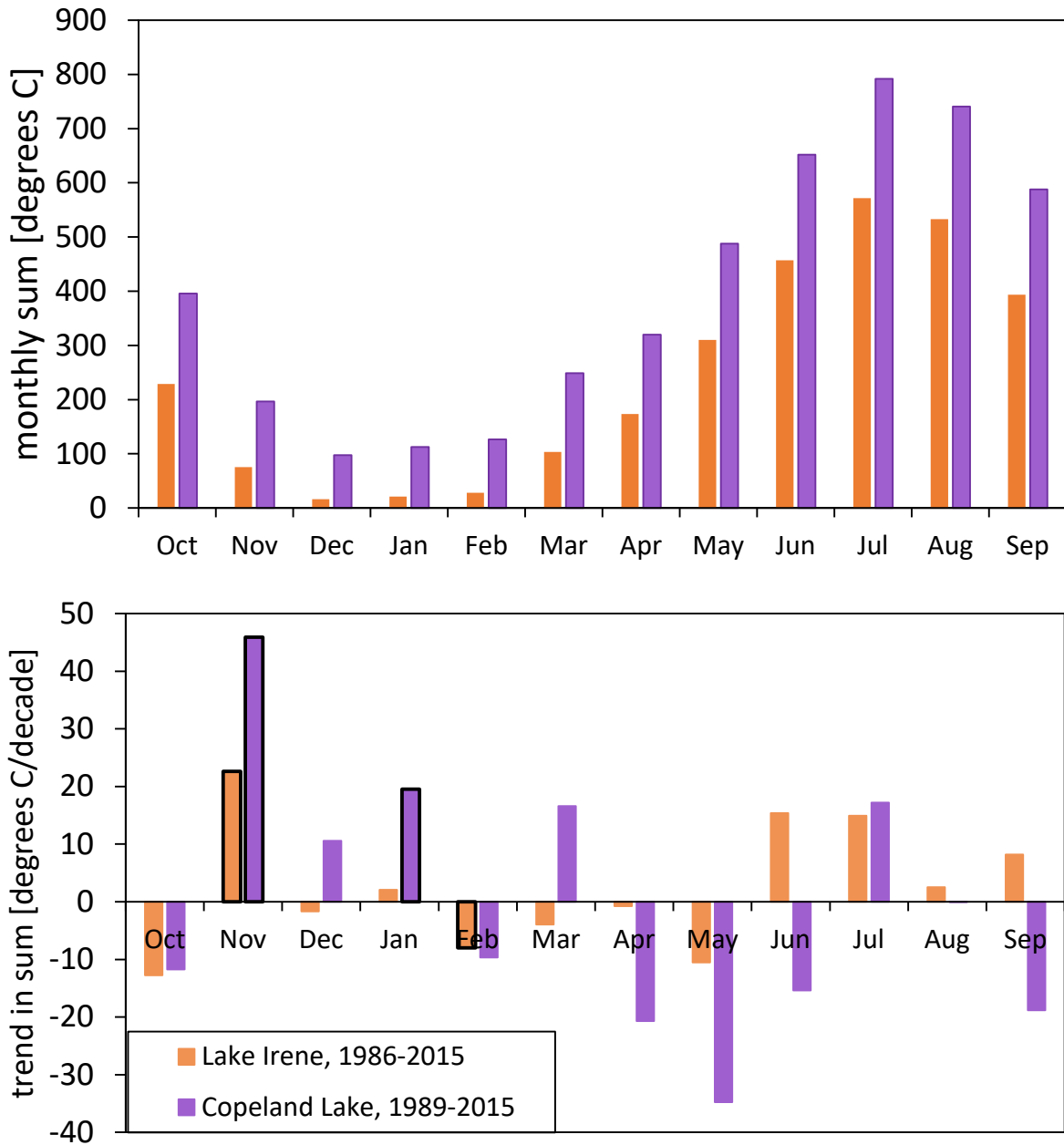


Figure A.25. a) Monthly sums of maximum daily temperatures warmer than zero for Lake Irene and Copeland Lake, and b) trends in these sums.

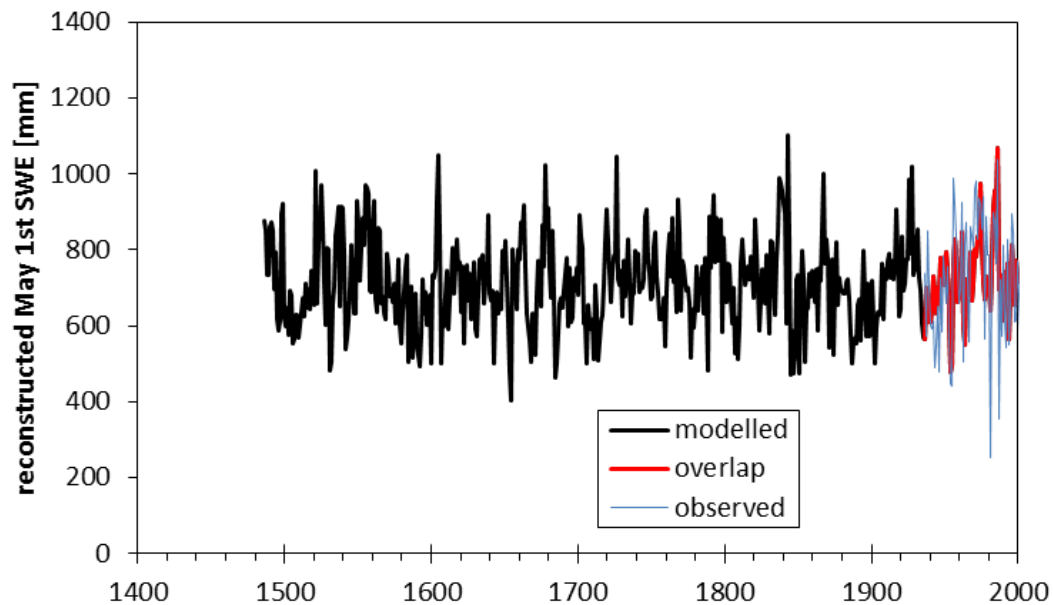


Figure A.26. Cameron Pass May 1st SWE reconstruction from 1486 to 2000.

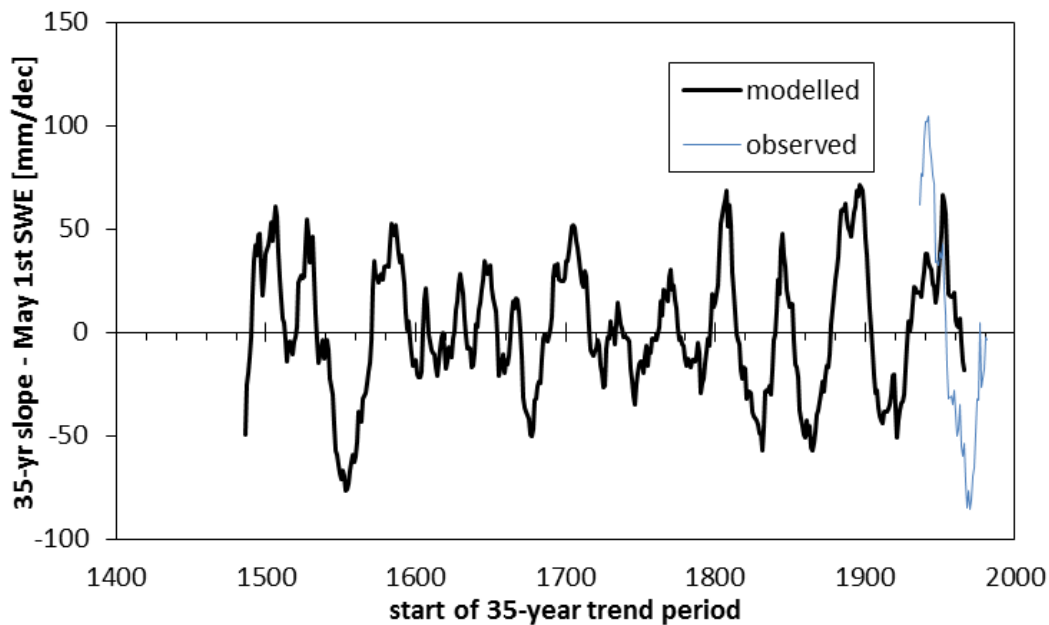


Figure A.27. Slope over 35-year time period for the reconstructed and observed (historical) May 1st SWE at Cameron Pass snow course.

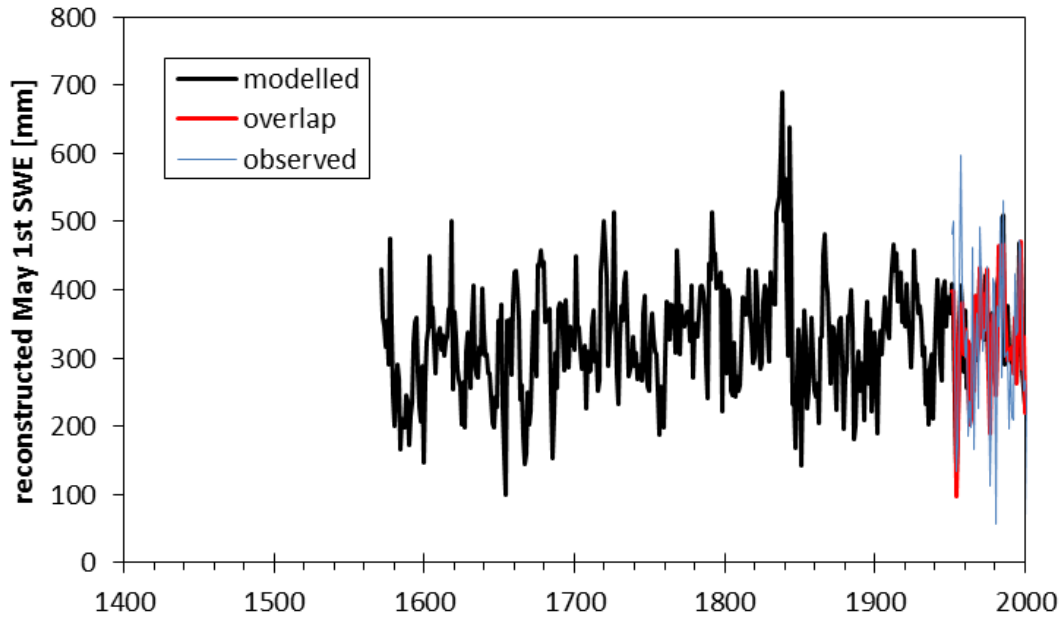


Figure A.28. Longs Peak May 1st SWE reconstruction from 1571 to 1999.

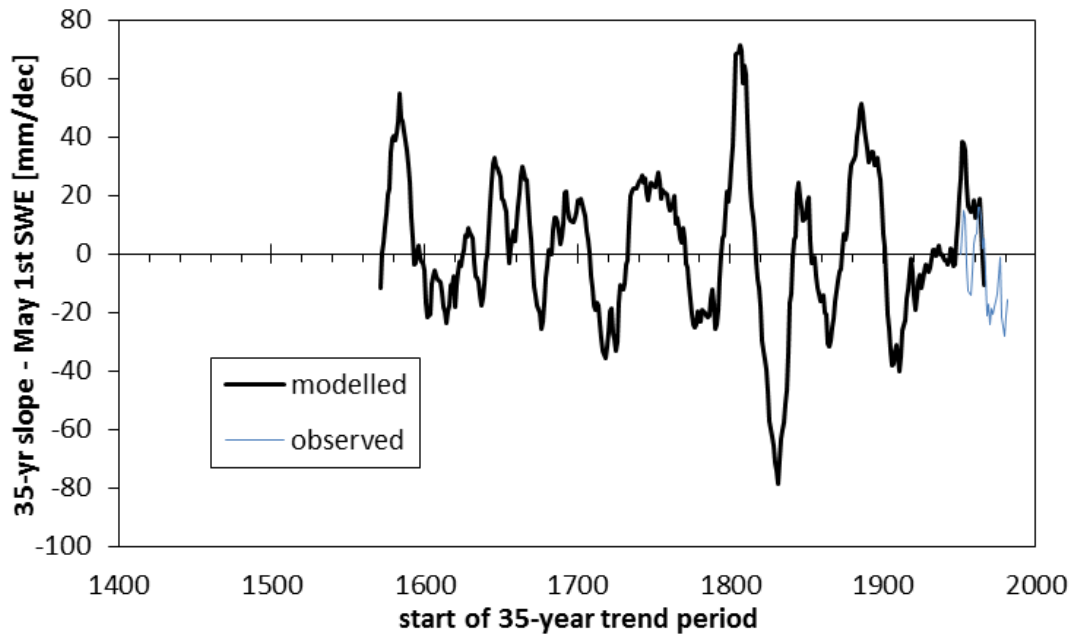


Figure A.29. Slope over 35-year time period for the reconstructed and observed (historical) May 1st SWE at Longs Peak snow course.

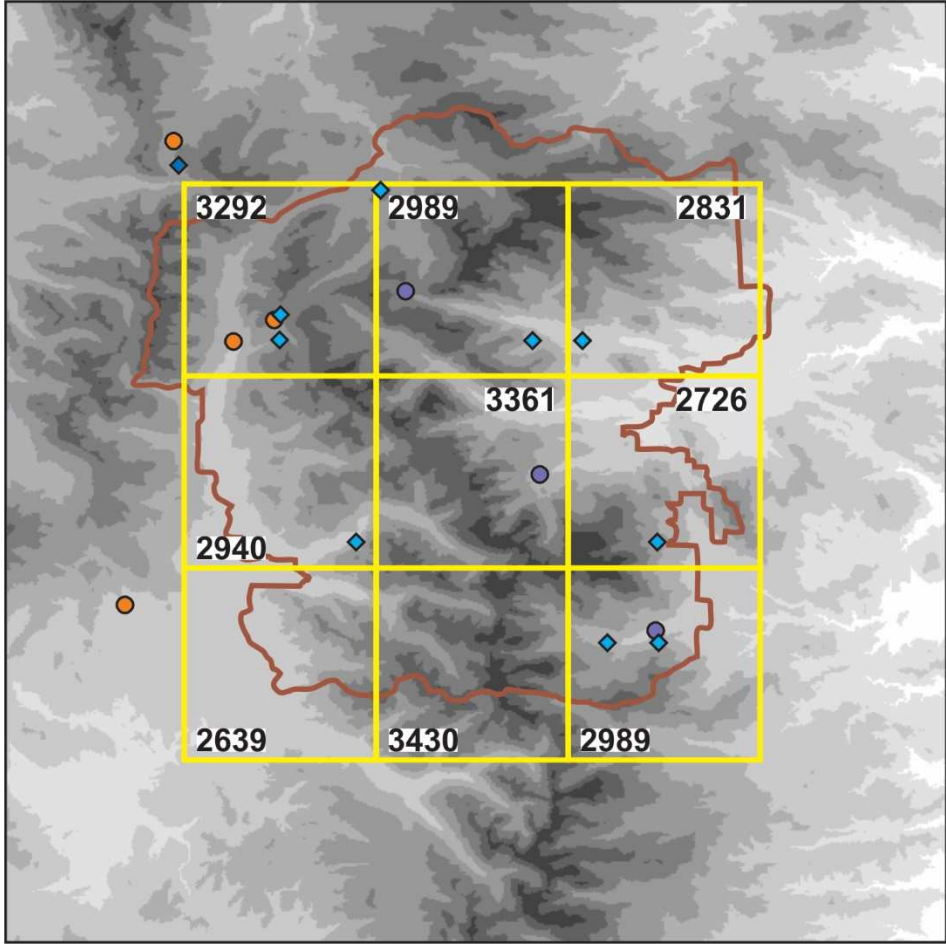


Figure A.30. Median elevations [m] for the nine 1/8 by 1/8 degree pixels of the CMIP5 climate model retrieval.

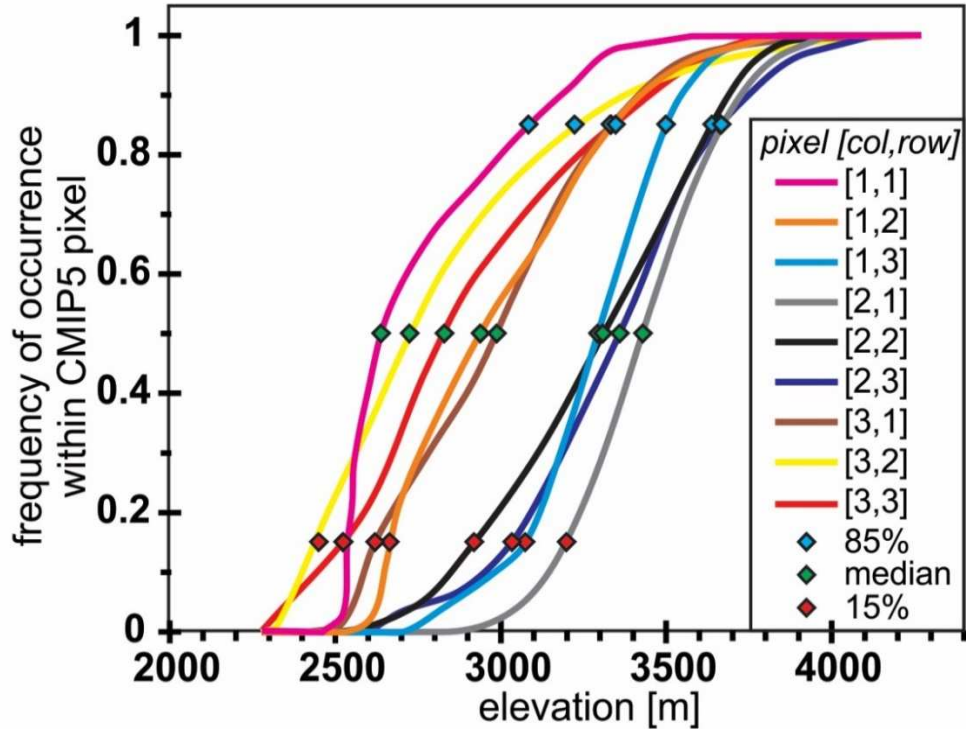


Figure A.31. Distribution of elevations within the nine pixels of the CMIP5 climate model retrieval.

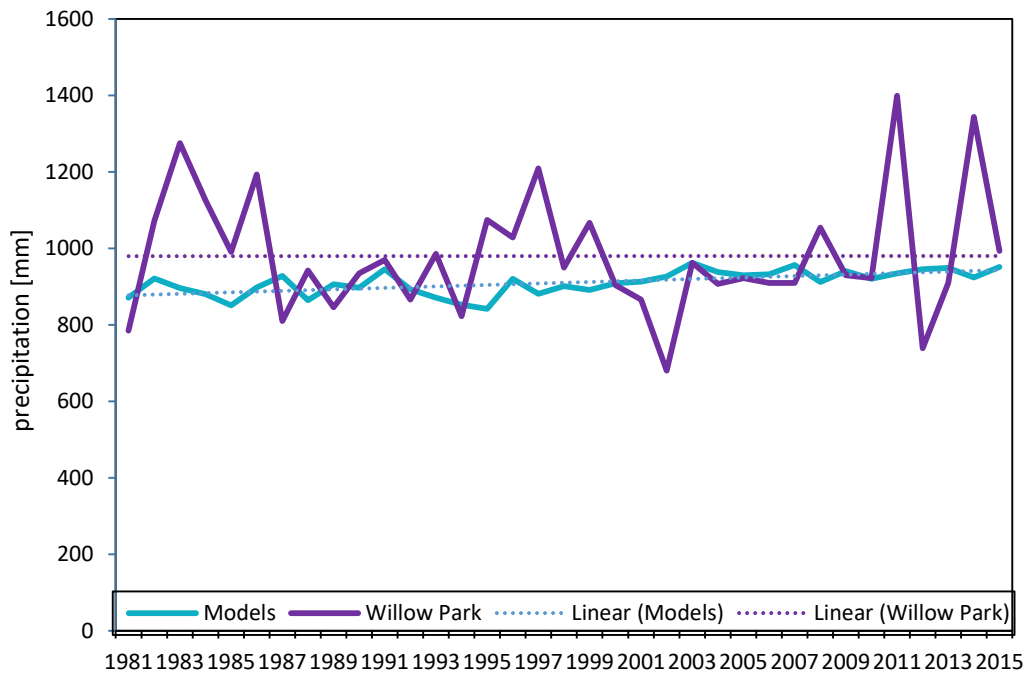


Figure A.32. Annual precipitation simulated by the CMIP5 model ensemble, and observed at Willow Park SNOTEL, 1981-2015.

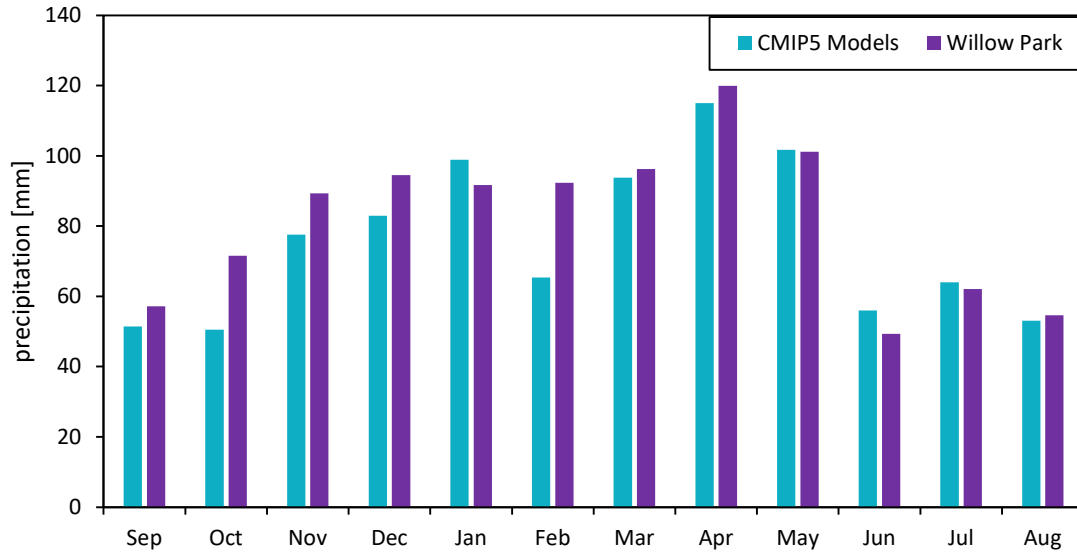


Figure A.33. Average monthly precipitation simulated by the CMIP5 model ensemble, and observed at Willow Park SNOTEL, 1981-2015.

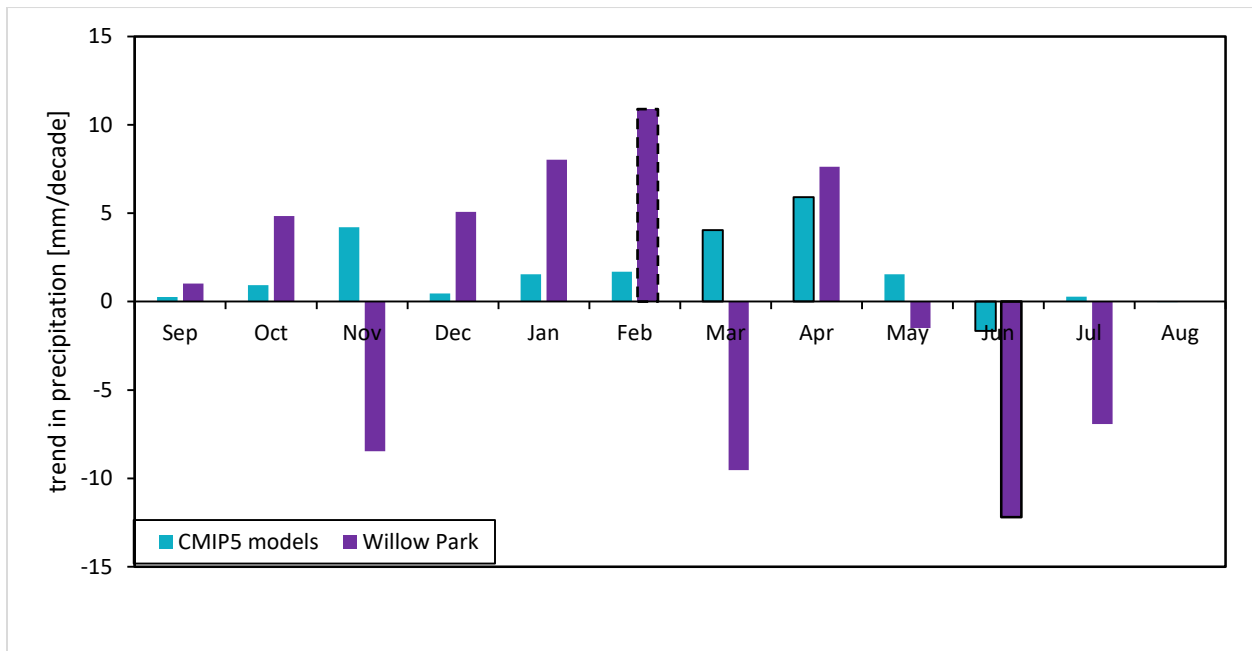


Figure A.34. Trends in monthly precipitation, 1981-2015, simulated by the CMIP5 model ensemble and observed at Willow Park.

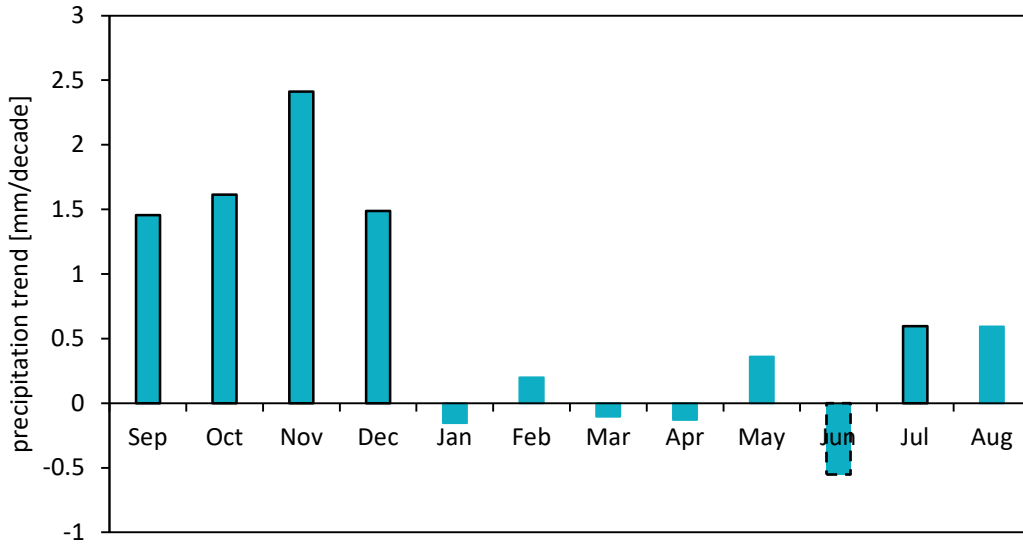


Figure A.35. Trends in monthly precipitation, 2015-2099, simulated by the CMIP5 model ensemble.

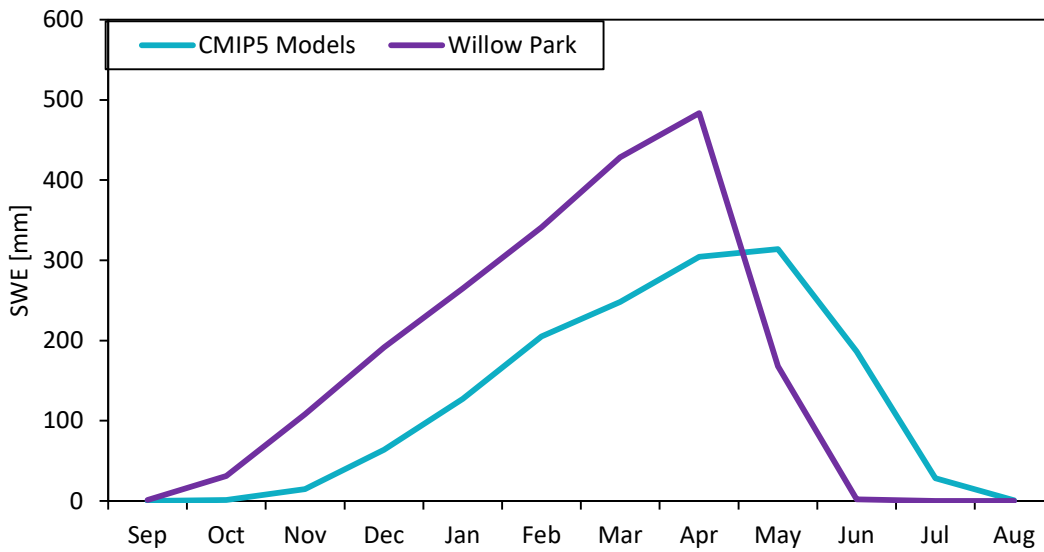


Figure A.36. Average first of month SWE, 1981-2015, simulated by the CMIP5 model ensemble and observed at Willow Park.

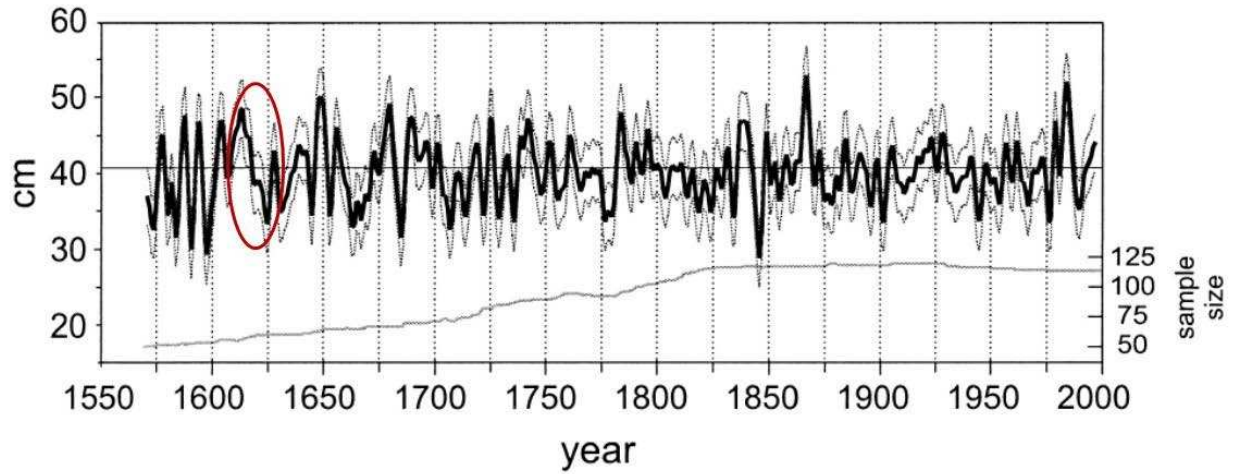


Figure A.37. 431-year SWE reconstruction for the Gunnison region, Colorado, smoothed with a 5-weight binomial filter (heavy line), and error bars (thin lines), 1571-1997. Thin line at bottom indicates number of tree-ring samples used over time. Oval indicates a period with a declining trend of about 13 years. From Woodhouse, 2003.